

AD-A135 863

DEFLOCCULANTS FOR TAPE CASTING BARIUM TITANATE
DIELECTRICS(U) RUTGERS - THE STATE UNIV NEW BRUNSWICK N
J DEPT OF CERAMICS W R CANNON FEB 88 N00014-82-K-0313

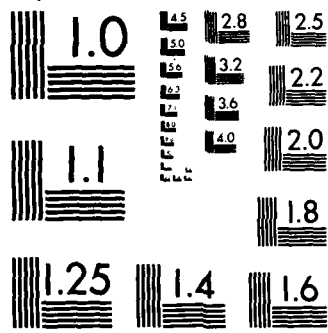
1/2

UNCLASSIFIED

F/G 11/9

NL





MICROCOPY RESOLUTION TEST CHART
NATIONAL BUREAU OF STANDARDS-1963-A

AD-A195 863

DTIC FILE COPY

4

ADVERTISERS

ADVERTISERS

ADVERTISERS FOR TAPE CASTING
ADVERTISERS FOR TAPE CASTING

ADVERTISERS FOR TAPE CASTING
ADVERTISERS FOR TAPE CASTING

DTIC
ELECTE
JUN 02 1988
S D

ADVERTISERS FOR TAPE CASTING
ADVERTISERS FOR TAPE CASTING

ADVERTISERS FOR TAPE CASTING
ADVERTISERS FOR TAPE CASTING

ADVERTISERS FOR TAPE CASTING
ADVERTISERS FOR TAPE CASTING

88 6 3 088



5200 SECURITY CLASSIFICATION OF THIS PAGE

REPORT DOCUMENTATION PAGE

1a. REPORT SECURITY CLASSIFICATION Unclassified		1b. RESTRICTIVE MARKINGS		
2a. SECURITY CLASSIFICATION AUTHORITY		3. DISTRIBUTION / AVAILABILITY OF REPORT		
2b. DECLASSIFICATION / DOWNGRADING SCHEDULE				
4. PERFORMING ORGANIZATION REPORT NUMBER(S)		5. MONITORING ORGANIZATION REPORT NUMBER(S) Distribution, etc.		
6a. NAME OF PERFORMING ORGANIZATION Department of Ceramics Rutgers, The State University	6b. OFFICE SYMBOL (If applicable)	7a. NAME OF MONITORING ORGANIZATION		
6c. ADDRESS (City, State, and ZIP Code) P. O. Box 909 Piscataway, NJ 08855-0909		7b. ADDRESS (City, State, and ZIP Code)		
8a. NAME OF FUNDING / SPONSORING ORGANIZATION Office of Naval Research	8b. OFFICE SYMBOL (If applicable)	9. PROCUREMENT INSTRUMENT IDENTIFICATION NUMBER N0014-82-K-0313		
8c. ADDRESS (City, State, and ZIP Code) Division of Materials Research Arlington, VA 22217		10. SOURCE OF FUNDING NUMBERS		
		PROGRAM ELEMENT NO	PROJECT NO	TASK NO
11. TITLE (Include Security Classification) Deflocculants for Tape Casting Barium Titanate Dielectrics				
12. PERSONAL AUTHOR(S) W. Roger Cannon				
13a. TYPE OF REPORT Final	13b. TIME COVERED FROM 3/15/82 TO 9/30/87	14. DATE OF REPORT (Year, Month, Day) February, 1988	15. PAGE COUNT	
16. SUPPLEMENTARY NOTATION				
17. COSATI CODES		18. SUBJECT TERMS (Continue on reverse if necessary and identify by block number) Dielectrics, Barium Titanate, Dispersants, ACRYLICS, Deflocculants, Tape Casting, Phosphate Ester. (JES)		
FIELD	GROUP			SUB-GROUP
19. ABSTRACT (Continue on reverse if necessary and identify by block number) The purpose of this study was to understand and improve the organic additives and processing used in nonaqueous tape casting of dielectrics. For this purpose a tape casting system, typical of those used in industry, was studied. The solvent system was MEK/ethanol, and the binder was an acrylic binder with two typical plasticizers, butyl benzyl phthalate and polyethylene glycol. A phosphate ester dispersant was used, which was not known to be used previously in tape casting but was found to be very effective.				
20. DISTRIBUTION / AVAILABILITY OF ABSTRACT <input checked="" type="checkbox"/> UNCLASSIFIED/UNLIMITED <input type="checkbox"/> SAME AS RPT. <input type="checkbox"/> DTIC USERS		21. ABSTRACT SECURITY CLASSIFICATION		
22a. NAME OF RESPONSIBLE INDIVIDUAL		22b. TELEPHONE (Include Area Code)	22c. OFFICE SYMBOL	

The first part of this study has been directed towards understanding the mechanisms of dispersion for barium titanate in an MEK-ethanol system using a commercial phosphate ester dispersant. The dispersant was found to be very effective in lowering the slip viscosity and in improving powder packing. The phosphate ester is thought to disperse barium titanate primarily by an electrostatic mechanism. This conclusion is based on three observations: (1) The zeta potential reaches a maximum at the same concentration of phosphate ester as the viscosity minimum. (2) The zeta potential also reaches a maximum at the solvent composition in the MEK-ethanol binary where the viscosity of the suspension is the lowest. (3) The conductivity of the solvent increases strongly with addition of the phosphate ester especially after being exposed to BaTiO_3 powder, indicating that the ionic strength is sufficiently high for electrostatic repulsion. Based on the measurements of zeta potential and ion concentration the potential energy barriers were calculated. The magnitude of the barrier heights could be used to explain both viscosity and settling volume.

Impurity water has a deleterious effect on the solvent-powder dispersion in that viscosity is increased and packing density of the powders is decreased. Although water increases the amount of dispersant adsorbed on the particle, it lowers its zeta potential which appears to be more important to the state of dispersion of the slip than the amount of dispersant adsorbed.

In the second part of the program the slip system with all the organic components was studied. The addition of binder, plasticizer and other organics to the solvent-powder system lowers the relative viscosity of the system and so it is assumed that these organics aid in dispersing the powder. It was found that the order of addition of the components was important both to the viscosity of the slip and the strength of the green tape. Dispersant added first resulted in the lowest slip viscosities, densest and strongest green tapes, whereas adding the powder to a mixture of all the organic components including the dispersant which had been allowed to age together resulted in the highest viscosities. The effect of each component relative viscosity was determined by measuring the relative viscosities for the slip when components were added one at a time. As a result PEG, used as a plasticizer, was found to be the only component which raises the relative viscosity. This increase in relative density was large only when the PEG contained water. It was proposed that water of hydration associated with the PEG lowers the effectiveness of the dispersant and so should not be allowed to age with the dispersant.

The ultimate tensile strength and ultimate tensile strain of cast tapes were studied under various conditions of drying and variations in the organic compositions. These results are reported here.

Table of Contents

Acknowledgment..... 1

I. INTRODUCTION..... 2

 A. Organic Additives..... 2

 B. Literature Survey..... 2

 C. Choice of the Slip Components..... 4

II. EXPERIMENTAL..... 6

 A. Materials..... 6

 1. Powder..... 6

 2. Organic Additives..... 7

 B. Measurements..... 8

 1. Rheology..... 8

 2. Electrical Conductance..... 8

 3. Electrokinetic Phenomena..... 8

 4. Absorption Isotherm..... 9

 5. Fourier Transform Infrared (FTIR) Spectroscopy..... 9

 6. Slip Preparation..... 9

 7. Tape Casting..... 9

 8. Green Density Measurement..... 10

 9. Tensile Strength of Green Tapes..... 10

 10. Sintering of Tapes..... 11

 11. Fracture Strength Measurements..... 11

III. RESULTS AND DISCUSSION..... 12

 A. Screening Tests for Dispersants..... 12

 1. Early screening test..... 12

 2. Recent Screening test..... 15

 B. The Phosphate Ester..... 16

 1. Nature of the Phosphate Ester..... 16

 2. Dispersion Characteristics..... 20

 a. Experimental..... 20

 b. Rheology and Settling Volume..... 21

 3. Mechanism of Dispersion..... 22

 a. Adsorption..... 22

 b. Electrophoresis..... 24

 c. Conductance Measurements..... 26

 d. Dissociation in the Solvent..... 28

 4. Effect of the MEK/Ethanol Ratio on Dispersion Properties... 30

 5. Application of the DVLO Theory..... 32

 C. Acrylic Binder..... 38

 D. Tape Casting Slips..... 43

 1. Order of Addition Sequence..... 43

 a. Batch Preparation..... 43

 b. Rheology Measurements..... 44

 c. Correlation between viscosity and other properties.... 47

 d. Green and Sintered Density..... 48

 e. Green and Fired Density..... 49

 f. Sintering of Tapes..... 50

 g. Flatness..... 52

 h. Sinter Tape Strength..... 53

 i. Electrical Properties..... 55

INSPECTED
4

per NP

Distribution/	
Availability Codes	
Dist	Avail and/or Special
A-1	

Table of Contents

2.	Role of Components in Dispersing the powder.....	56
a.	Rheological properties of slips.....	56
b.	Sedimentation Study.....	58
c.	Phosphate Ester Adsorption.....	59
d.	Electrophoretic Mobility.....	60
e.	Reaction Between Components of the Tape.....	61
f.	Assessment of Dispersibility of Individual Components.....	63
g.	The roll of water in the slip and the order of addition Sequence.....	67
h.	Electrical Conductivity.....	68
E.	<u>Casting Behavior and Tensile Strength of Cast BaTiO₃ Tape</u>	69
1.	Experimental.....	70
2.	The effect of the drying method on the strength.....	70
3.	Effects of binder to plasticizer ratio.....	72
4.	Effect of each plasticizer.....	74
5.	Effects of binder + plasticizer concentration.....	76
6.	Effects of dispersant Content.....	78
7.	Effect of homogenizer content.....	80
	Conclusions.....	81
	References.....	83
	Publications from this Work.....	86

Table of Contents

Table I.	Summary of Organic Additive for Tape Casting which have been Reported in the Literature.....	3
Table II.	Standard Tape Casting Composition.....	5
Table III.	Lot Analyses for HPB (lot 567) Barium Titanate Powder.....	6
Table IV.	Physical Properties of Solvents Used in this Study.....	7
Table V.	List of Various Commercial Dispersants Tested listed in order of their effectiveness.....	14
Table VI.	List of Effective Surfactants for Non-aqueous Slips and their Structure.....	17
Table VII.	Measured Minimum Apparent Viscosity of 45vol% Slips at Shear Rates.....	18
Table VIII.	Acrylic Solution Viscosities.....	41
Table IX.	Density of green and sintered tapes.....	48
Table X.	Yield Values and Shear Rate Exponents for Day One Slips.....	58
Table XI.	Sedimentation Study Observations.....	59
Table XII.	Viscosity of the Solution, Viscosity of the Slip and Relative Viscosity for Several Partial Slip Compositions.....	64
Table XIII.	Viscosity and Relative Viscosity Values Using the Simultaneous Addition Sequence. Before adding powder the solution was aged 24 hours. An old bottle of PEG was used. See Key of Table XII.....	65
Table XIV.	Viscosity and Relative Viscosity Values Using the Simultaneous Addition Sequence, using a new bottle of PEG. Dry: Solvent was taken from a new sealed bottle for each experiment, Wet: Solvent was exposed to the air for 2 hours to allow it to absorb moisture.....	66

Table of Contents

Figure 1.	Schematic of fixture used for biaxial flexure tests.....	11
Figure 2.	A Sketch of the Experimental Set-up for the Initial Screening test.....	12
Figure 3.	Apparent viscosity as a function of phosphate ester concentration for semi-dry and hydrated dispersions.....	21
Figure 4.	Packing fraction as a function of phosphate ester concentration for gravity settled semi-dry and hydrated dispersions.....	22
Figure 5.	Absorption isotherms for semi-dry and hydrated dispersions.....	23
Figure 6.	Viscosity, adsorption, and zeta potential as a function of phosphate ester concentration for semi-dry dispersions.....	25
Figure 7.	Conductivity as a function of phosphate ester concentration for semi-dry materials.....	27
Figure 8.	FTIR spectra of Emphos PS-21A scanned as a neat liquid and in MEK/ethanol. Solvent bands have been removed from the solution spectrum by spectral subtraction	29
Figure 9.	Proposed dissociation mechanism for the phosphate ester in MEK/ethanol.....	30
Figure 10.	Viscosity, adsorption, and zeta potential as a function of ethanol fraction for semi dry dispersions at 0.7 v/o phosphate ester.....	30
Figure 11.	Conductivity as a function of ethanol fraction for semi-dry materials at 0.7 v/o phosphate ester.....	31
Figure 12.	Total potential energy of interaction as a function of particle separation for phosphate ester concentrations varying from 0.0 vol% to 0.6 vol%.....	34
Figure 13.	Total potential energy of interaction as a function of particle separation for phosphate ester concentrations varying from 0.6 vol% to 1.6 vol%.....	34
Figure 14.	Total potential energy of interaction as a function of particle separation for hydrated materials.....	36
Figure 15.	Total potential energy of interaction as a function of particle separation for solvent fractions varying from 0.3 to 0.1 fractions of ethanol.....	37
Figure 16.	Total potential energy of interaction as a function of particle separation for solvent fractions varying from 1.0 to 0.3 fractions of ethanol.....	37
Figure 17.	Viscosity and relative viscosity versus acrylic concentration for slurries consisting of solvent, binder and powder.....	39
Figure 18.	Adsorption isotherm for the adsorption of Acryloid B7-MEK onto barium titanate powder from MEK/ethanol.....	40
Figure 19.	Langmuir plot for the adsorption of Acryloid B7-MEK onto barium titanate powder, from MEK/ethanol.....	40
Figure 20.	Plot of specific viscosity/concentration versus concentration used to determine intrinsic viscosity of Acryloid B7-MEK.....	42
Figure 21.	The processing and addition sequence used in preparation of samples.....	44
Figure 22.	Method of extrapolation from low shear rates to high shear rates.....	45
Figure 23.	Viscosity measured at 384 sec^{-1} as a function of aging time of the slip.....	46
Figure 24.	Viscosity measured at 9.8 sec^{-1} as a function of aging time of the slip.....	46
Figure 25.	Schematic drawing of the tape casting head.....	47

Table of Contents

Figure 26.	The ultimate tensile strength of green tapes.....	49
Figure 27.	Micrograph of as-sintered surface.....	51
Figure 28.	Micrograph of as-sintered surface.....	51
Figure 29.	Micrograph of as-sinter surface.....	51
Figure 30.	Flatness as a function of addition sequence and slip aging.....	52
Figure 31.	Surface profile as measured with a profilometer.....	53
Figure 32.	The biaxial flexure strength of sintered tapes as a function of addition sequence and aging time.....	54
Figure 33.	The surface of a sintered tape made from slips using the simultaneous addition sequence.....	54
Figure 34.	Dielectric constant as a function of frequency for tapes.....	55
Figure 35.	Viscosity versus shear rate for slurries prepared by adding dispersant first.....	56
Figure 36.	Viscosity versus shear rate for slurries prepared by adding the dispersant last.....	57
Figure 37.	Viscosity versus shear rate for slurries prepared by simultaneous addition.....	57
Figure 38.	Phosphate ester adsorption versus slurry aging time.....	60
Figure 39.	Zeta potential for particles in slips made by all component addition sequences and in the powder-solvent-dispersant systems.....	61
Figure 40.	FTIR spectra of cast Acryloid B7-MEK films.....	62
Figure 41.	FTIR spectra of Acryloid B7-MEK solutions.....	63
Figure 42.	Relative Viscosity Increase for Components. Results are taken from Table XII. The factor increase in relative viscosity as a result of addition of component shown on the abscissa.....	65
Figure 43.	Relative Viscosity Increase for Components. Results taken from Tables XIII and XIV.....	67
Figure 44.	Electrical conductivity of solutions.....	69
Figure 45.	The ultimate tensile strength of green tapes dried under various conditions. The three upper curve relate to tapes which were removed from the glass plate after 1 hour and dried under various conditions.....	71
Figure 46.	Effect of the binder to plasticizer ratio on the: (a) viscosity at 10 sec^{-1} and 300 sec^{-1} shear rate, (b) green density, (c) ultimate tensile strength, and (d) strain to failure. The total binder + plasticizer content was kept constant.....	73
Figure 47.	The ratio PEG/Butylbenzyl Phthalate is varied and the following properties measured: (1) slip viscosity, (2) tape green density, (3) ultimate tensile strength and (3) strain to failure.....	75
Figure 48.	Effect of binder + plasticizer content on the: (a) viscosity at 10 sec^{-1} and 300 sec^{-1} shear rate, (b) green density, (c) ultimate tensile strength, and (d) strain to failure. The solvent, binder, plasticizer, homogenizer and dispersant concentration were kept constant while the powder content was varied. In (c) "constant viscosity" the solvent content was varied to maintain a constant viscosity independent of binder + plasticizer content.....	77
Figure 49.	Effect of dispersant concentration on the: (a) viscosity at 10 sec^{-1} and 300 sec^{-1} shear rate, (b) green density, (c) ultimate tensile strength, and (d) strain to failure.....	79
Figure 50.	Effect of homogenizer content on the: (a) green density, and (b) ultimate tensile strength.....	80

Final Report - 1988

Acknowledgment

The major portion of the research described in this report was performed by Kurt Mikeska and John R. Morris, Jr. in partial fulfillment of the research requirement for a Ph.D. James Rydzak, a graduate student in Chemistry and Ceramics advised John R. Morris on the FTIR study. Undergraduate students who have contributed considerably to this report are Angela Karas, Richard Hill, Robert McNivan, Michael Fiori, Joselyn Kowalski, David Eng, and Joseph Saltarelli.

1. INTRODUCTION

A. Organic Additives

Organic additives are added to tape casting slips to impart a variety of properties to the slip and green tape. The function of each of these has been reviewed several times [1-3]. Binders/plasticizers impart some degree of strength and hardness yet must allow the tape to be flexible for handling in subsequent processing steps. Other additives include release agents, wetting agents and homogenizers. A dispersant may be added to lower the viscosity of the slip and to insure a dense green tape but is not always added. Never-the-less proper dispersion of the powders is important and becoming increasingly important for multilayer capacitors where some manufacturers are seeking to achieve 10 to 15 μm thick tapes with high reliability. An important part of this research has been to examine the a typical dispersant, its interaction with the other organic components of tape casting slips and the ability of other components to disperse the powder.

B. Literature Survey

The organics used in commercial tape casting remain mostly proprietary but some have been published in the open literature. Table I summarizes the organic compositions for nonaqueous systems contained in the open literature, listing complete systems found in patents and publications and alternate ingredients suggested by various authors (Other Possibilities). According to Table I binary solvent systems, generally employing an alcohol and a more volatile solvent, are most often used. The proportion of each may be adjusted to achieve the proper vaporization rate or the azeotrope may be chosen so that the solvent composition is constant during evaporation. The presence of alcohols or ketones in the solvents gives most systems a high dielectric constant. Of the binders currently in use, polyvinyl butyral (PVB) is the most popular binder published in patent and the technical literature; however, acrylic binders are also widely used. The acrylic binder depolymerizes (or unzips) at low burn-off temperatures and burns out completely while the polyvinyl butyral burns out more slowly. [4,5] This may, in fact, offer an advantage in providing strength during the burnout period. The most widely used plasticizers are either phthalates or glycols such as polyethylene glycol (PEG).

Final Report - 1988

Table I. Summary of Organic Additive for Tape Casting which have been Reported in the Literature.

SOLVENT	BINDER	PLASTICIZER	DISPERSANT	OTHER COMPONENTS	REF.
toluol	ethyl cellulose methyl abietate	diethyl oxalate triethylene glycol dihydro- abietate			(11,12)
toluene	polyvinyl butyral	triethylene glycol hexoate		polyethylene glycol alkyl ether- a	(13,14)
acetone	cellulose acetate butyrate resin	dimethyl phthalate tricresyl phosphate			(15)
	polyethylene	butyl stearate			(15)
	polyvinyl alcohol	glycerine			(15)
	polyvinylchloride acetate	butyl benzyl phthalate			(15)
ethanol toluene	polyvinyl butyral	dibutyl phthalate		polyethylene glycol ethyl ether- a	(16)
ethanol trichloroethylene	polyvinyl butyral	polyethylene glycol octyl phthalate	merhaden oil		(17,18)
toluene	polyvinyl butyral	polyethylene glycol	merhaden oil		(28)
ethanol (8) trichloroethylene (8,9) tetrachloroethylene (9)	polyvinyl butyral	polyalkylene glycol derivatives (triethylene glycol hexoate) mixed phosphate esters (hexyl, octyl, decyl alcohols)	merhaden oil		(19,20,22)
ethanol toluene cyclohexanone	polyvinyl butyral	dibutyl phthalate		polyethylene glycol alkyl ether- a	(5)
methyl ethyl ketone	vinyl chloride acetate	butyl benzyl phthalate			(1)
toluene	polyvinyl butyral	polyethylene glycol			(1)
ethanol methyl ethyl ketone	ethyl methacrylate methyl acrylate methyl methacrylate	polyethylene glycol butyl benzyl phthalate	phosphate ester	cyclohexanone- b	(21)
methanol toluene	polyvinyl butyral	dioctyl phthalate		cyclohexanone- b	(8)
OTHER POSSIBILITIES					
benzene (13,14) butanol (13) diacetone (13) isopropanol (13) methyl isobutyl ketone (13) xylene (21) bromochloromethane (17,18)	petroleum resins (13) polymacrylate ester (13) nitrocellulose (14,24) polyvinylchloride (15)	methyl abietate (13,23) ethyl oxalate (14) glycoate (13)	glycerol trioleate (19,20) benzene sulfonic acid (19,20)	alkylaryl polyether alcohols (13)- a polyethylene ester (13)- a polyoxyethylene acetate (13)- a	
				a- wetting agent b- homogenizer	

Only a few dispersants are listed in Table I. Fish oil, a very effective dispersant, was suggested for early tape casting formulations[1] and is widely used commercially. Although it is a very good universal dispersant, as a naturally occurring product it is subject to variability and availability. A synthetic dispersant which is more reliable is preferred by many manufacturers.

Several additives are given generic names such as wetting agents and homogenizers but it is not quite clear what the actual function of these ingredients is. The wetting agent has, for instance, been described as allowing the binder to wet the powder. [3] It is unclear what this means. The homogenizer has been described merely as improving the homogeneity of the slip, though it apparently acts as a dispersant and prevents skin formation.[6,7] Cyclohexanone has been used for this purpose.[8]

C. Choice of the Slip Components

In choosing the organic composition for the slip, the binder is often chosen first. We chose to use an acrylic binder obtained from Rohm and Haas, Acryloid B-7. Since the time the program began other acrylic binders specifically designed for tape casting have been developed.

Many formulations also do not use a separate dispersant (see Table I) since the binder acts as a dispersant itself. There are two advantages of the single binder system. First, there are no burn-out problems with a dispersant and second, no dispersant is present to interfere with the binder. Usala [9] presented some results on a commercial binder developed for tape casting of multilayer capacitors in nonaqueous systems. The acrylic binder, which are random copolymers that contain optimally 0.6 % polyacrylic acid (PAA) functional groups, are very similar to the one used in this study except that it has a narrower molecular weight distribution. The narrower molecular weight distribution should provide higher green tape strength without excessively high slip viscosity. This binder was designed to disperse the powder without an additional dispersant added, however, in the work presented by Usala, the commercial acrylic binder did not fully disperse the powder without the addition of acetic acid or a dispersant with a high acid number. Usala concluded that viscosity is high because of "bridging" of binder molecules between particles. The presence of acetic acid adsorbed on the surface reduced the bridging. If the bridging mechanism is important then a block copolymer might be developed whose functional groups anchor the polymer to the particle but do not easily bridge to other particles. This may, however, reduce its effectiveness as a binder. One of the challenges is to develop a binder which is strong but during the dispersion stage does not bridge the particles.

Besides the capability of dispersing the powder, the binder should provide strength for the tape. A second challenge for binder development is to develop binders specific for a given powder. Fowkes[10] proposes that a strong bond between a polymer and a powder is made when there is a strong Lewis acid/Lewis base interaction. Thus optimization of tape casting systems may require development of other binders which are basic and interact more strongly with acid powders. Both PVB and the acrylic binders (containing acid groups) are acidic and should attach strongly to $BaTiO_3$ and Al_2O_3 but other functional groups could be attached for use with a more acidic surface.

Final Report - 1988

The entire composition of the slip studied during this program is shown in Table II. Variations to this composition were made occasionally to better understand their function. The choice of MEK-ethanol as a solvent was based on the fact that the acrylic binder is very soluble in MEK and, in fact, premixed in MEK. The ethanol was added as a second solvent to correspond to compositions shown in Table I. Butyl benzyl phthalate and polyethylene glycol (PEG) were added as plasticizers which according to Table I are typical plasticizers. Cyclohexanone was also added. The functions of these components was more clearly defined as a result of this research and is reported herein. The choice of the phosphate ester as a dispersant was based on a series of screening tests and is reported in the experimental part of the report.

Table II. Standard Tape Casting Composition.

<u>COMPONENT</u>	<u>VOLUME PERCENTAGE</u>	<u>WEIGHT PERCENTAGE</u>
Barium Titanate Powder ¹	35.0	77.2
MEK ² /Ethanol ³ Solvent	33.25	10.6
Acrylic Binder ⁴	20.0	7.1
Butyl Benzyl Phthalate ⁵	5.0	2.2
Polyethylene Glycol 400 ⁶	5.0	2.2
Phosphate Ester ⁷	0.75	0.3
Cyclohexanone ⁸	<u>1.0</u>	<u>0.4</u>
TOTAL	100.0	100.0

- ¹Type HPB, Tam Ceramics
- ²Reagent Grade, Fisher Scientific
- ³Absolute Ethanol, Florida Distilleries
- ⁴Acryloid B7-MEK, Rohm and Haas
- ⁵Santicizer 160, Monsanto Corporation
- ⁶Carbowax 400, Fisher Scientific
- ⁷Emphos PS-21A, Witco Chemical
- ⁸Reagent Grade, Fisher Scientific

II. **EXPERIMENTAL**

A. **Materials**

1. Powder

High purity barium titanate* powder was used for this study. The barium titanate is manufactured by an oxalate co-precipitate process, calcined at 850°C, and subsequently spray dried.

A typical lot analysis is shown below.

Table III. Lot Analyses for HPB (lot 567) Barium Titanate Powder

Loss on Ignition (TAM)	0.33%
+325 Mesh (TAM)	.01%
B.E.T. specific surface (TAM)	3.56 m ² /g
B.E.T. specific surface (this study)	3.5 m ² /g
Density (TAM)	5.5 g/cm ³
Density (this study)	5.9 g/cm ³
BaO/TiO ₂ mole ratio (TAM)	0.997
Fisher number (TAM)	1.19

* Manufactured by Tam Ceramics Inc, Niagra Fall, N.Y.

2. Organic Additives

Fisher Scientific reagent grade methyl ethyl ketone and absolute ethanol from Florida Distilleries were used as solvents. The properties of MEK and ethanol are summarized in Table IV. The azeotrope, which consists of sixty-six volume percent MEK and thirty-four volume percent ethyl alcohol, was chosen on the basis of evaporation at constant composition, but subsequent work showed that for our system the best dispersion in the MEK-Ethanol binary occurred at the azeotrope.

Table IV. Physical Properties of Solvents Used in this Study.

	<u>METHYL ETHYL KETONE</u>	<u>ETHYL ALCOHOL</u>
Structural Formula	$\text{CH}_3\text{CH}_2\text{COCH}_3$	$\text{C}_2\text{H}_5\text{OH}$
Molecular Weight	72.11	46.07
Density (25°C)	0.7996 g/cm ³	0.80363 g/cm ³
Viscosity (25°C)	0.20 cps	1.2 cps

The binder, Acryloid B-7 from Rohm and Haas, is a thirty weight percent solution of acrylic resin in methyl ethyl ketone. According to other sources [25] is a copolymer consisting of 62% ethylmethacrylate (EMA), 37% methylacrylate (MA), and 0.6% methyl acrylic acid (MAA). The number average molecular weight is 68,000 and the weight average molecular weight is 445,000 giving a polydispersity of 6.7.

Santicizer 160TM, a butyl benzyl phthalate from Monsanto Corp. and Carbowax 400TM, a polyethylene glycol of molecular weight 400 from Fisher Scientific were selected as plasticizers. These plasticizers are commonly used in the multilayer capacitor industry and were recommended by the manufacturer of the binder. Cyclohexanone, reagent grade from Fisher Scientific, was added to reduce skin formation during drying. The dispersant, Emphos PS-21A from Witco Chemicals was chosen on the basis of screening tests described below.

The relative amounts of each component which are shown in Table II were determined by starting with the proportions given by Mistler et al. [1] and making adjustments to optimize rheology. The amount of dispersant, a critical parameter, was optimized for this system as part of this study. Thirty-five volume percent powder was selected to allow easy casting, although loading up to approximately forty-five percent was possible with this system. Amount of binder and binder plasticizer ratio were determined by manufacturers recommendation and subsequent empirical testing.

B. Measurements

1. Rheology

Two types of rheometers were used., the 2x HAT Brookfield* cone-plate microviscometer utilizing a CP-42 cone-plate arrangement and the Haake** rotoviscometer utilizing a Haake Rotovisco RV/CV/LV 100 with a ZA 30 coaxial cylinder. The Rotovisco was interfaced with a Hewlett-Packard HP 86B computer.

2. Electrical Conductance

AC conductivity of suspensions were used to provide an indication of ionic concentrations. They were prepared and processed at 25.0 vol% solids.

All conductance measurements were performed with a YSI 32 conductance meter+ using a sample cell with a cell constant of 1.068 cm^{-1} at $24.0 \text{ }^{\circ}\text{C}$ as determined by KCl solution standards.

3. Electrokinetic Phenomena

In this study microelectrophoresis measurements were made using a Rank Bros. Mark II Electrophoresis apparatus# equipped with a rotating prism. A closed flat rectangular cell fabricated of fused silica was used. The high cell resistivity of silica is preferable when using low conductivity (i.e., low dielectric constant) media. The cell geometry included a two electrode set-up. Electrodes were constructed of platinum and blacked with in a 0.2% solution of chlorplatinic acid containing 0.02% lead acetate.

The calculation of zeta potentials, ζ , from electrophoretic mobilities, μ , was taken as [26,27]

$$\mu = \epsilon \zeta / 1.5 \eta \quad (1)$$

where $\epsilon = \epsilon_r + \epsilon_0$ is the dielectric constant, η is the viscosity of the liquid.

* Brookfield Engineering Laboratories, Inc..
 ** HAAKE MessTechnik Gmb H V. Co..
 + Yellow Springs Chemical Co., Yellow Springs, OH
 # Rank Brothers, Cambridge, England

4. Absorption Isotherm

Adsorption isotherms were determined for both the phosphate ester and the acrylic binder on the barium titanate powder. Samples containing 25 vol% powder, MEK/ethanol and various amounts of either phosphate ester or acrylic binder were mixed and agitated for twenty-four hours to allow complete adsorption. Powder was consolidated by centrifuge and the supernatant was analyzed. The phosphate ester content was determined by analyzing aliquots of the supernatant for phosphorus by a Perkin-Elmer ICP/6500 inductively couple argon plasma atomic emission spectrometer. The phosphate ester concentrations were subsequently calculated based on the theoretical ester molecular weights discussed in the previous section. Analysis of the acrylic binder in the supernatant was carried out by two techniques, simple gravimetric analysis and FTIR quantitative analysis using a cylindrical internal reflectance accessory. The gravimetric analysis consisted of drying a known volume of solution and weighing the residue. A standard calibration curve was determined for two milliliter samples of known acrylic concentration and unknown solution concentrations were obtained by plotting weights of two milliliter samples on this calibrating curve.

5. Fourier Transform Infrared (FTIR) Spectroscopy

Fourier Transform Infrared (FTIR) Spectroscopy was utilized for several types of analysis in the study. In all cases a Perkin-Elmer Model 1750 FTIR with Model 7300 professional computer was used. A dry air purge was employed to minimize the effects of atmospheric moisture.

6. Slip Preparation

Slips containing all the components were prepared with several order of addition sequences. For instance in the dispersant first case, the solvent, dispersant, and powder were premixed, ultrasonically agitated for two minutes, and allowed to age for twenty-four hours before the remaining components were added. In the dispersant last case, all components except the dispersant were premixed, ultrasonically agitated, and aged for twenty-four hours before the dispersant was added. In the simultaneous addition slurry, all of the liquid components were premixed, ultrasonically agitated, and aged prior to addition of the powder. After the final components were added, all batches were again ultrasonically agitated for two minutes and the slurries were placed on a slow roller mill for the duration of the study. There were no grinding media added to the slurries as the purpose of the slow rolling action was to simply keep the components from separating during the aging study. The slurries were removed from the slow roller mill only for viscosity measurement and tape casting which occurred at twenty-four hour intervals.

7. Tape Casting

After preparing the slip as described above the slip was stirred with a glass stirring rod. The slip was next magnetically mixed for thirty minutes. The beaker was sealed during mixing to prevent solvent evaporation. After magnetic mixing, the slip was filtered by passing it

through a nylon filter situated in the bottom of a large syringe. Before casting, the slip was deaired in a vacuum for five minutes.

Tapes were cast onto clean glass using a Cladan laboratory scale caster, Model 133A. Prior to casting, the carrier glass was cleaned with absolute alcohol to remove surface contaminants. An inlet air pressure of 80 psi was applied which resulted in a casting head speed of 10.97 cm/sec (0.36 ft/sec). The blade height was 0.152 mm (0.006 in) hence the slurry was subjected to an average shear rate of 720 reciprocal seconds.

The cast tapes were stripped from the glass after twenty-four hours and allowed to dry on a porous foam rubber surface to permit evaporation from both surfaces. Seventy-two hours after casting, the tapes were cut into appropriate shapes for property measurement.

8. Green Density Measurement

Green density was determined from geometrical measurements and sample weights. Weights were measured before and after binder burnout on a Mettler analytical balance accurate to 0.00001 grams. Volume was determined by cutting 6.45 cm² (1 in²) samples, and by measuring the thickness using a Mitutoyo Model 7326 thickness gage accurate to 0.0025 mm (0.0001 in). To eliminate variation in measured thickness due to deformation under the load of the measuring platens, the samples were placed between two pieces of precision machined glass (variation of less than 0.0013 mm (0.00005 in) in a square inch sample). Five measurements were taken per sample and a values used in the calculation. This technique was found to give very consistent and reproducible data although there may be some overestimation of volume since the volume of the binder but not the weight of the binder was included in the calculation. Density was calculated using the relation:

$$\rho = w(1 - \text{LOI})/l^2t$$

where: ρ - green density

w - sample weight

l - length (1 inch)

t - thickness

LOI - fractional loss of ignition.

Loss on ignition was determined thermogravimetrically.

9. Tensile Strength of Green Tapes

Green tensile strength was measured by the technique described in reference [28]. Briefly, this method involves cutting dog-bone shaped testing samples from the green tape using a scalpel, and testing them on an Instron universal testing machine. Air pressure actuated grips were used to minimize tearing which occurred when standard mechanical grips were used, and the standard loading rate was 2.5 cm/min.

10. Sintering of Tapes

The tapes were sintered using the following heating schedule. Slow heating (1 °C. per minute) to 500 °C. followed by a one hour hold was employed to facilitate complete burnout of all organics. Rapid heating to the firing temperature was followed by a one hour soak and cooling to room temperature. The ultimate firing temperature ranged from 1325 to 1375 °C.

Fired density was measured by a geometrical technique similar to that used to evaluate the green tapes. In this instance, however, there was no need to place the samples between glass plates in order to measure the thickness since the sintered tapes did not deform under the load applied by the thickness gage. Geometrical measurement was found to give much more reproducible results than immersion techniques for measuring the density of these thin samples.

11. Fracture Strength Measurements

Fired strength was measured using a biaxial flexure technique described by Wachtman et al. (28). The fixture, shown in Figure 1, consists of an aluminum cup on the inside surface of which are machined three holes. Ball bearings are placed in the holes to act as sample supports. The disc shaped sample is placed on the bearings and a fourth ball bearing in which a flat surface has been machined is placed flat surface down in the center of the disc. The assembly is then placed on the load cell of an Instron universal testing machine and the load is applied to the upper ball.

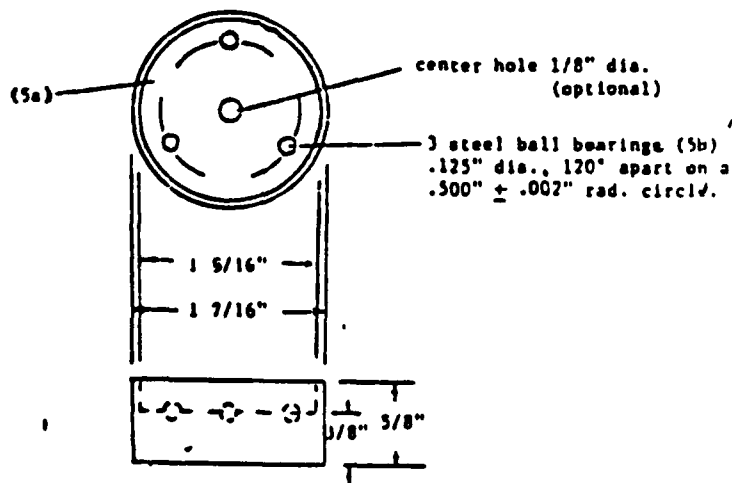


Figure 1. Schematic of fixture used for biaxial flexure tests.

III. RESULTS AND DISCUSSION

A. Screening Tests for Dispersants

1. Early screening test

In the early stages of the program, about 70 commercial dispersants were screened. They were collected from as many suppliers as possible for preliminary evaluation. To do this several surface-agent manufacturers were contacted and asked to send samples of their non-aqueous dispersants which may be compatible with our system. Other dispersants were available in our laboratory. A list of most of these dispersants is contained in reference (5) along with an evaluation of their solubility in MEK-ethanol. The solubility test was performed by mixing a small amount of dispersant with MEK-ethanol azeotrope and checking for cloudiness.

From the initial screening tests, 29 dispersants were chosen for further evaluation. These are listed in Table V by both their commercial name and generic name where possible.

The second screening test was a rheological test. The basis of the test is that those dispersions with the lowest minimum viscosity are the ones with the least agglomerates and the most stable dispersion. Viscosity was determined using a rotating disc viscometer in the experimental set-up shown in Figure 2.

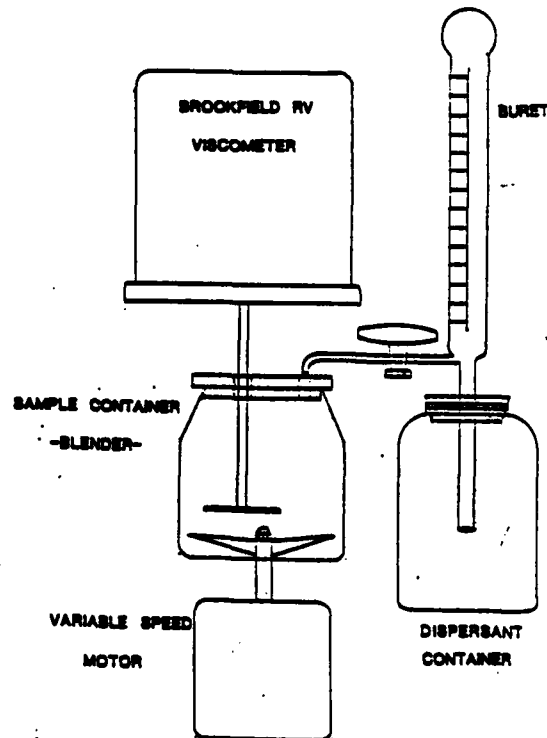


Figure 2. A Sketch of the Experimental Set-up for the Initial Screening test.

Final Report - 1988

A dispersion of 70 wt % solids was placed in a sample container and subjected to shear mixing forces by a variable speed blender. The initial barium titanate MEK-ethanol dispersion was blended until homogeneous. Known amounts of dilute dispersant were added through a graduated buret and stirred until the slurry appeared uniform. The blender was subsequently stopped and the viscosity was determined using a Brookfield rotating disk viscometer. This procedure was carried out for each addition of dispersant until a minimum viscosity was achieved or until it was qualitatively determined that further addition of dispersant would have minor effects on the overall dispersion of the slurry.

These are ordered according to their effectiveness in lowering the viscosity in Table V, starting with the least effective. Of all the dispersants only the last three dispersants were very effective and the viscosity decreased most steeply for the Emphos 21A. Unfortunately the minimum viscosities of the last three could not be compared because they were below the sensitivity of the viscometer.

Table V. List of Various Commercial Dispersants Tested listed in order of their effectiveness.

Trade Name	Manufacturer	Identity
Monazoline-T	Mana Industries	Substituted imidazoline (1-hydroxyethyl 2-alkyl-imidazonlines) from tall oil acids
Monazoline-C	Mona Industries	Substituted imidazoline (1-hydroxyethyl 2-alkyl-imidazonlines) from coconut acids
Sedisperse-D	Micromeritics	Saturated aliphatic hydrocarbons
Zonyl-FSN	E. I. DuPont	Fluorinated surfactant
Monazoline-O	Mana Industried	Substituted imidazoline (1-hydroxyethyl 2-alkyl-imidazonlines) from oleic acids)
AMP-95	International Minerals & Chem.	2-amino 2-methyl 1-propanol
Sedisperse-F	Micromeritics	Saturated aliphatic hydrocarbons
Witconol H31A	Witco Chem. Co.	Polyethylene glycol 400 monostearate
Alkazine-TO	Alkaril Chemicals	Tall Oil hydroxyethyl imidazoline
Fluorad FC-170-C	3M Company	fluorinated surfactant

Final Report - 1988

Table V. List of Various Commercial Dispersants Tested listed in order of their effectiveness. (Continued)

Alkazine O	Alkaril Chemicals	Oleic hydroxyethyl imidozoline
Emerest 24	Emery Industries	Glycerol trioleate
Dispersionol HP	Arkansas Co.	Proprietary
Duponol-G	E. I. DuPont	Proprietary
Amerlate WFA	Amerchol Corp.	Lanolin fatty acids
Poly Vinyl Buterol	Rohm and Haas	Poly Vinyl Buterol
Aerosol TR-70	American Cyanamid	Sodium bistridecyl sulfosuccinate
Witcamine PA-78B	Witco Chemical Co.	Salt of fatty imidazoline
Monawet MB-45	Mona Industries	Diisobutyl sodium sulfosuccinate
Dispersional-C	Arkansas Co.	Proprietary
Aerosol-OT-75	American Cyanamid	Sodium dioctyl sulfosuccinate
Monawet MO-70	Mona Industries	Dioctyl sodium sulfosuccinate
Drewfax 007	Drew Chemical	Sodium dioctylsulfosuccinate
Aerosol C-61	American Cyanamid	Ethanolated alkylguanidine amine
Monawet MM80	Mona Industries	Dihexyl sodium sulfosuccinate
Aerosol AY-100	American Cyanamid	Sodium diisobutyl sulfosuccinate
Zonyl-A	E. I. DuPont	Ethoxylate
Fish Oil	Spencer Kellogg	Fatty acid
Emphos PS-21A	Witco Chem. Co.	Phosphate Ester

2. Recent screen test

The second series of screening tests attempted to categorize dispersants and to determine whether one category was more effective than another. The most general categories are surfactants and steric stabilizers. Surfactants are classified here as macromolecular dispersants with molecular weight usually under 1000 and with a polar functional group or groups. Steric stabilizers may either be natural or synthetic. The synthetic steric stabilizers are not yet commonly used for tape casting but have high potential for dispersing oxide powders in a nonaqueous slip. These steric stabilizing polymer dispersants are higher molecular weight and usually block copolymers with a stabilizing and an anchor moiety. Block copolymers have been specifically developed for tape casting by at least one manufacturer who have shown that it provides better dispersion of BaTiO_3 than fish oil.[29] A number of natural dispersants including fish oil operate at least partially by the steric stabilizing mechanism but are not block copolymers. For instance, Shanefield has reported that no measurable zeta potential can be detected on alumina particles dispersed with fish oil [1] and so it likely operates by a steric mechanism.

Table VI is a list of surfactants (by commercial name as well as generic name), compiled from recommendations of a number of commercial manufacturers, considered the most potent types of dispersants in solvent systems. These are divided into anionic, cationic and nonionic, terms which are generally used for aqueous systems, but they are also applicable to nonaqueous systems because they are indicators of the acidity or basicity (in the Lewis sense) of the surface. It has been noted, for instance, that anionic surfactants best disperse basic powders and cationic surfactant powders disperse acidic powders in solvent systems.[30].

All the surfactants listed in Table VI were tested for dispersing BaTiO_3 in MEK-ethanol. Table VII shows the minimum viscosity measured with a concentric cylinder viscometer, as well as, the per cent added to achieve the minimum viscosity.. Viscosity was measured as a function of concentration of the surfactant at 10 sec^{-1} and 300 sec^{-1} with each surfactant tested in 45 vol% suspensions of BaTiO_3 powder in 66 % MEK-34 % ethanol solvent system.

Results indicate that the phosphate esters are most effective in dispersing the powder, although the nonionic ethoxylate of castor oil was somewhat effective. This may indicate that the ethoxylate groups, also present in the phosphate ester are of importance. $BaTiO_3$ is slightly basic in nature. Thus it is expected that an anionic surfactant may be effective. It may also be noted, however, that the other anionic surfactants, the sulfosuccinates, were not effective in dispersing the powder. In the discussion below we consider the dispersion mechanism of the phosphate ester, PS-21A and its interaction with other components.

B. The Phosphate Ester

1. Nature of the Phosphate Ester

The chemical structure of the phosphate ester, Emphos PS-21A, manufactured by Witco Corp. is proprietary. Information supplied by the manufacturer and subsequent characterization by FTIR were used to determine the structure proposed below. Attempts to characterize the molecular weight and molecular weight distributions by HPLC, during this study, were imprecise due long retention times caused by the high boiling point of the ester. The molecular weights stated below were supplied by the manufacture and determined from the proposed molecular structures. For the purpose of this report, the polymer structures described below will be used throughout. It is important to note that the actual material may contain some unknown species (there is some unreacted phosphoric acid present in the composition) and that the phosphate ester may undergo further reactions when mixed with the MEK-ethanol solvents.

Table VI. List of Effective Surfactants for Non-aqueous Slips and their Structure.

DISPERSANTS

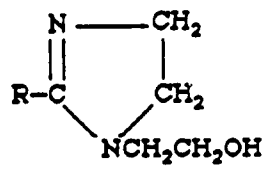
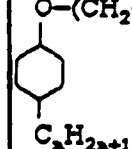
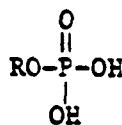
DISPERSANT	TYPE	IDENTITY	FUNCTIONAL GROUP
Emphos PS-21A Monafax 831 Monafax 939 Forsterge LFS Forsterge LF Acid	Anionic	Phosphate Ester	$\begin{array}{cc} \text{O} & \text{O} \\ & \\ \text{R}'\text{-P-OH} & \text{R-P-OH} \\ & \\ \text{R}'' & \text{OH} \end{array}$
Monawet MO65-150 Emcol 4500 Aerosol TR-70 Aerosol OT-75 Witconate P10-59 Drewfax 007	Anionic	Sulfosuccinate	$\begin{array}{c} \text{R}'\text{OOCCH}_2 \\ \\ \text{R}''\text{OCCSO}_3^- \end{array} \quad \text{A}^+$
Emcol CC36 Emcol CC55 Emcol CC57	Cationic	Quaternary Ammonium	$\left[\begin{array}{cc} \text{R}' & \text{R}''' \\ & \diagdown \quad / \\ & \text{N} \\ & / \quad \diagdown \\ \text{R} & \text{R}'' \end{array} \right]^+ \quad \text{A}^-$
Monazoline CY	Cationic	Imidazoline	
Aerosol C81 Surfactol 318 Surfactol 365	Cationic Non-ionic	Ethoxylated Amine Complex Ethoxylate of Castor Oil	$\begin{array}{c} \text{O} \\ \\ \text{CH}_2\text{-C-OR} \\ \\ \text{CH-C-OR}' \\ \\ \text{CH}_2\text{-C-OR}'' \\ \\ \text{O} \end{array}$
Igepal CO530 Igepal CO610 Igepal CA620 Igepal RC520 Triton X-100	Non-ionic	Polyethyleneoxyethanol	$\text{O}-(\text{CH}_2\text{CH}_2\text{O})_{n-1}-\text{CH}_2\text{CH}_2\text{OH}$ 
Witcamide 5138	Non-ionic	Alkanolamide	$\begin{array}{c} \text{O} \\ \\ \text{R-C-N} \\ \quad \diagdown \quad / \\ \quad \quad \text{R}'' \quad \text{R}' \end{array}$

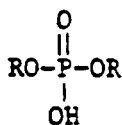
Table VII. Measured Minimum Apparent Viscosity of 45 vol% Slips at Shear Rates

DISPERSANT	VISCOSITY (Pa-sec) (300 sec ⁻¹)	VISCOSITY (Pa-sec) (300 sec ⁻¹)	CONC. AT MIN. VISCOSITY (%)
Emphos PS-21A	39 ± 22	12 ± 1	0.75
Monafax 831	15 ± 1	11 ± 0	1.00
Monafax 93C	*	*	*
Forsterge LFS	21 ± 13	18 ± 0	1.00
Forsterge LFacid	17 ± 2	13 ± 1	1.50
Monavet MO65-150	6235 ± 762	663 ± 7	3.00
Emcol 4500	4626 ± 328	573 ± 6	1.00
Aerosol TR-70	*	*	*
Aerosol OT-75	9028 ± 82	685 ± 10	3.00
Witconate P10-59	*	*	*
Emcol CC36	5627 ± 639	445 ± 3	4.00
Emcol CC55	350 ± 14	57 ± 1	3.00
Emcol CC57	1051 ± 141	85 ± 2	2.00
Monazoline CY	*	*	*
Surfactol 318	77 ± 0	20 ± 1	3.00
Surfactol 365	*	*	*
Igepal CO530	1159 ± 522	180 ± 0	4.00
Igepal CO610	3351 ± 552	306 ± 2	4.00
Igepal CA620	284 ± 139	294 ± 1	4.00
Igepal RC520	3218 ± 1691	87 ± 3	4.00
Triton X-100	187 ± 91	87 ± 2	4.00
Witcamide 5138	5561 ± 224	593 ± 20	1.00
Drewfax 007	7525 ± 797	600 ± 29	2.00

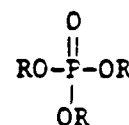
Emphos PS21A is the corresponding ester of phosphoric acid [31]. Phosphoric acid contains three hydroxyl groups and can form esters in which one, two, or three of the P-OH hydroxyl groups have been replaced by alkoxy groups to form mono-, di-, and trialkyl esters [32,33]. In this study the specific R group is an ethoxylate [31]. The corresponding esters may take the form:



ethoxyl phosphate
ester

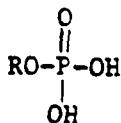


diethoxyl phosphate
ester

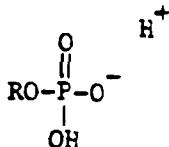


triethoxyl phosphate
ester

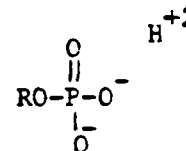
The P-OH groups of the monoethoxyl and diethoxyl phosphate esters contain acidic hydrogens which undergo ionization in aqueous and polar liquids (8-12). A monoethoxyl ester, for example, could exist as a dianion, monoanion, or neutral ester (8,9).



neutral ethoxyl
phosphate ester



monoanionic ethoxyl
phosphate ester



dianionic ethoxyl
phosphate ester

The ionization of the esters in polar liquids allows the polymer to act as an anionic surfactant.

The proposed structure of the alkoxy functional (R) group is an ethoxylate structure ($R = (\text{CH}_2\text{CH}_2\text{O})_7(\text{CH}_2)_9\text{CH}_3$ (polyoxyethylene)) derived from a straight chain C_{10} primary alcohol and seven ethylene oxide groups ($\text{C}_{10}\text{H}_{21}[\text{OCH}_2\text{CH}_2]_7\text{OH}$ decylheptaoxyethylene glycol monoether). Phosphoric acid is subsequently reacted with the ethoxylate to form the corresponding ethoxylated phosphate esters shown above. The theoretical molecular weights of the mono and diethoxylated structures are 546 and 994, respectively.

Emphos PS21A is a equal mixture of mono and dialkyl phosphate esters. The chemical structure discussed above is based on an ethoxylation process and approximate molecular of 540 and 950 for the mono and diethoxylated esters, respectively, as supplied by the manufacturer [31].

The phosphate ester has a density of 0.925g/cm^3 and acid numbers of 130 and 200 at pH 5.5 and 9.5, respectively.

2. Dispersion Characteristics

A series of experiments were designed to consider more closely the dispersion capabilities of the phosphate ester and to determine the effect of moisture content on viscosity in dispersions containing solvent, powder and dispersant only.

a. Experimental

For the dry condition the solvents used to make the azeotrope solution of MEK-ethanol were dried statically over Linde* molecular sieves M.S. type 3A (1/6" pellets) prior to use. The molecular sieves were dried at 200°C for twenty four hours in a circulating air oven before use. The sieve loading was 5:1 (g M.S./g solvent). The solvents were left in contact with the sieves for twenty four hours. After drying over the sieve, the solvent was filtered with common filter paper into a clean, dry glass jar prior to use. Residual moisture, as determined by Karl Fischer reagent methods, is 0.0059%.

The HPB barium titanate powder was dried at 200°C in a vacuum drying oven for twenty four hours prior to use. The powder was allowed to cool at room temperature inside a desiccator containing calcium sulfate desiccant before use. Residual moisture is measured by Karl Fischer method was 0.112%.

The "hydrated" samples were prepared using absolute ethanol and Fisher reagent grade MEK with known additions of distilled deionized water. The "semi-dry" samples were prepared using absolute ethanol and Fisher reagent grade MEK without the water additions. Water content measured by Karl Fischer technique is 3.79%. In these experiments the absolute ethanol and MEK were used as received and not dried over molecular sieve as was the case in the earlier "dry" experiment. Therefore, a distinction is made between the "dry" samples and the "semi-dry" samples. The barium titanate used in the hydrated and semi-dry experiments was vacuum dried for twenty four hours at 200°C.

For each of the above conditions, a series of dispersion samples for each concentration of phosphate ester were prepared. Concentrations ranged from 0.2 vol% to 2.0 vol% phosphate ester. The dispersant was first added to the solvent and mixed by shaking. A known quantity of powder was then added to the solution of dispersant and solvent. The total sample volume was 16.35 ml. Samples were agitated ultrasonically for 2.0 minutes at 40 W/cm² and cooled in an ice bath during sonification. Each sample was subjected to the full range of its shear rates in order to determine dispersion rheology. Rheology measurements were taken immediately after agitation to avoid possible internal structure formation within the suspension which may occur with time.

* Alfa Products Inc..

b. Rheology and Settling Volume

Figure 3 shows measured apparent viscosity as a function of phosphate ester concentration under semi-dry and hydrated conditions at 25.0 v/o solids. The semi-dry dispersions indicate a minimum viscosity at 0.6 v/o to 0.8 v/o phosphate ester. The hydrated dispersion had a higher viscosity than the semi-dry dispersion which suggests that water decreases the degree of dispersion. Also, an apparent inflection is seen in the viscosity curve of the hydrated dispersion. Gravity settled dispersions, as shown in Figure 4, indicate the inflection in the flocculation curve is real and is associated with water additions. Also the gravity settling results indicate a higher settled volume for the hydrated suspensions which again suggests that water decreases the degree of dispersion. There is ample evidence in the literature that molecular water and hydroxyl groups at solid/liquid interfaces affect adsorption of stabilizing materials at the interface (13-18). In addition, dispersant/liquid interaction can be affected by the presence of water (i.e., solvency, electrical double layer interactions, zeta potential and polymer conformational states). Each interaction has the potential to affect dispersion stability.

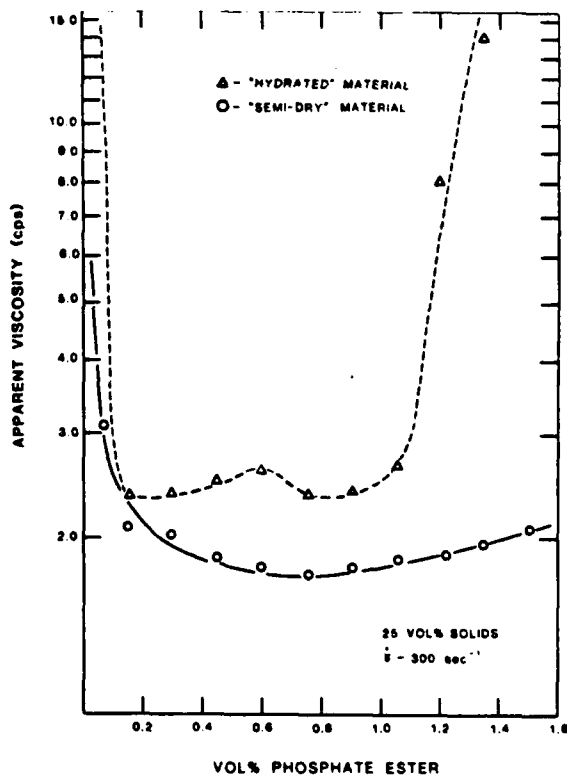


Figure 3. Apparent viscosity as a function of phosphate ester concentration for semi-dry and hydrated dispersions.

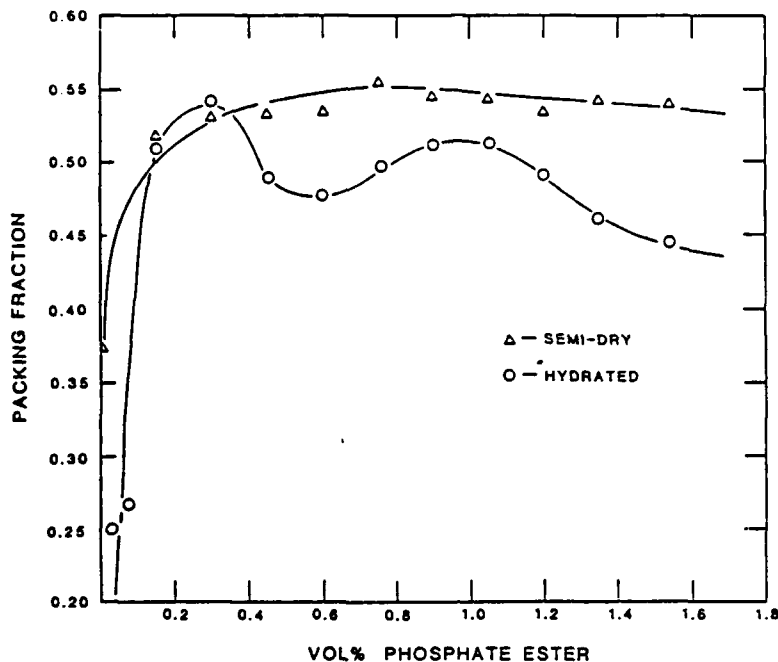


Figure 4. Packing fraction as a function of phosphate ester concentration for gravity settled semi-dry and hydrated dispersions

3. Mechanism of Dispersion

a. Adsorption

To better understand the mechanism by which the phosphate ester disperses the barium titanate particles, adsorption of the phosphate ester on the barium titanate surface was studied. Composite adsorption isotherms for the adsorption of the phosphate ester onto the barium titanate surface for the semi-dry and the hydrated dispersions are shown in Figure 5. An adsorption plateau initially occurs for the semi-dry dispersions at an equilibrium concentration of approximately 3.7×10^{-4} mole fractions of phosphate ester and an adsorption surface excess of approximately 1.36×10^{-6} moles/m² of phosphate ester. The adsorption plateau for the semi-dry samples indicates there was no further adsorption of the phosphate ester beyond monolayer coverage in the measured initial concentration range.

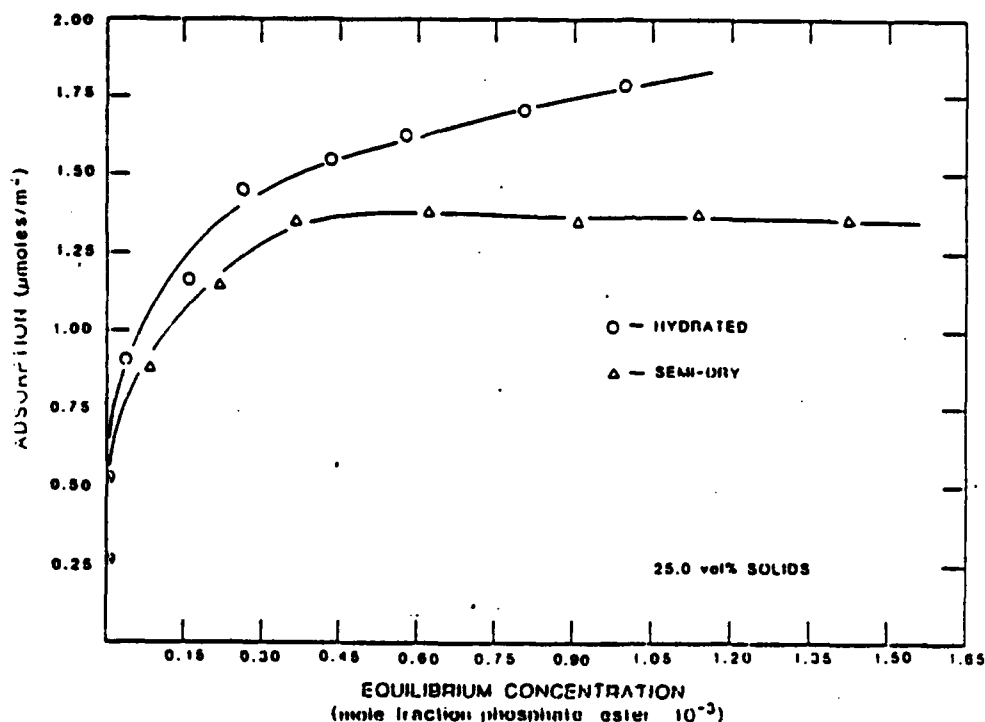


Figure 5. Absorption isotherms for semi-dry and hydrated dispersions.

The plateau for the hydrated samples is less well defined. The initial onset of a plateau occurs at an equilibrium concentration of approximately 2.6×10^{-4} and a surface excess of approximately 1.45×10^{-6} moles/m², followed by a continued increase in adsorption as the initial concentration of phosphate ester was increased. Apparently, the presence of water in the system caused the phosphate ester to continue to adsorb at the interface as the initial concentration of the phosphate ester was increased. The ill defined plateau may be caused by weakly adsorbed molecular water held at the interface, where the weakly held water is constantly displaced at the surface along with the phosphate ester in a adsorption-desorption process. In addition, the presence of water may alter the properties of the liquid phase and solid surface (e.g., increases dielectric constant, increases dissociation of the phosphate ester, increases electrolyte concentration, makes the phosphate ester more lyophobic) and cause continued adsorption of the hydrocarbon tail.

From monolayer adsorption values of the phosphate ester for the semi-dry dispersions, it is determined that the phosphate ester occupies an average of 122 Å²/molecule on the particle surface. Molecular models and characteristic bond lengths show that this value is between the surface coverage values predicted for a closed packed horizontal surface orientation, where all the molecules lie flat on the surface, and a closed packed vertical surface orientation, where all the molecules extend out into the bulk liquid. This suggests that the molecules are oriented to form

"loops" or "tails" which extend out from the surface into the liquid in an open arrangement. This seems reasonable considering the ionic nature of the phosphate ester, the mono- and diethoxylated chemical structure, and that phosphate esters have tetragonal bond angles [34]. The active adsorbing portion of the molecule consists of the ionic phosphoryl group and the polar ether groups. In non-aqueous media these groups are lyophobic and will interact strongly at the solid surface. The lyophilic hydrocarbon polymer "tail" portion of the molecule will be repelled from the surface and extend into the bulk liquid.

b. Electrophoresis

Electrophoretic mobilities were measured as a function of phosphate ester solution concentration under semi-dry conditions. In order to determine electrophoretic mobility under similar conditions to those in which rheology, settling volume, adsorption and conductivity experiments were made, samples were prepared and processed at 25.0 vol% solids and prepared simultaneously along with the adsorption and conductivity samples from identical batches of materials. Aliquots of the resulting supernatants containing a very dilute suspension of barium titanate particles were extracted with a syringe and injected into to the flat sample cell for analysis. This made it possible to compare rheology, adsorption and zeta potential.

Figure 6 compares zeta potential, adsorption, and viscosity as a function of phosphate ester concentration. A comparison of the viscosity curve with the adsorption curve shows that monolayer coverage and minimum viscosity both occur at approximately the same concentration of phosphate ester. The initial monolayer coverage occurring at an equilibrium concentration of approximately 3.7×10^{-4} mole fractions of phosphate ester corresponds to an initial dispersion concentration of 0.8 v/o phosphate ester which is the approximate concentration where a minimum in viscosity was established.

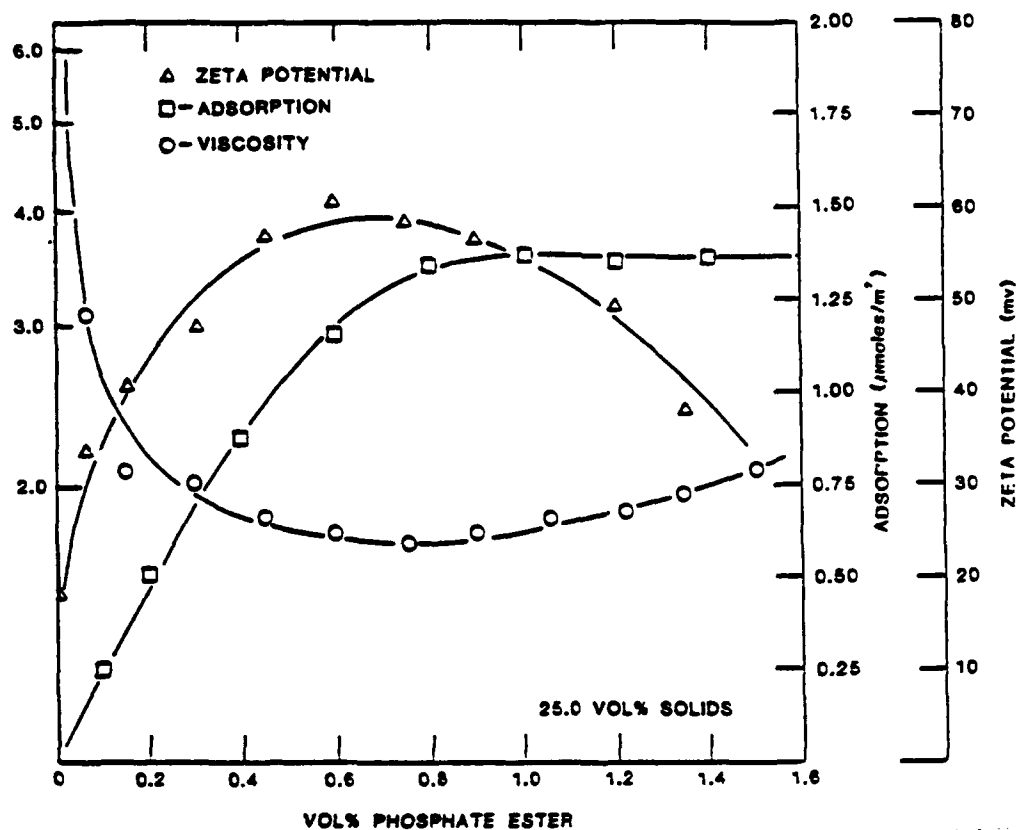


Figure 6. Viscosity, adsorption, and zeta potential as a function of phosphate ester concentration for semi-dry dispersions.

The results of Figure 6 may give some indication of the stabilizing mechanism since sterically stabilization should be strongly affected surface adsorption whereas, electrostatic repulsion is more directly related to zeta potential. Unfortunately, both the onset of monolayer coverage and the maximum zeta potential occur at approximately the same concentration as the minimum viscosity. If steric stabilization is considered to be the mechanism, however, then viscosity would not normally increase beyond the concentration at which the monolayer forms. Viscosity behavior on the other hand is consistent with electrostatic stabilization where the viscosity increases with further addition of dispersant (electrolyte) because of double layer shrinkage and in this case decrease of zeta potential. Possible mechanisms are also available for an increase in viscosity beyond the monolayer coverage due to co-adsorption of solvent [35], reorientation of adsorbed material [36].

A number investigators have observed charging of powders resulting from addition of surfactants. Kitahara [37] reviewed the electrokinetic behavior of oxide powder in hydrocarbon solvents and both Fowkes [38] and Kitahara [37] observed that anionic surfactants charge particles positively as we observed in these experiments. Kitahara [37] also observed that the zeta-potential generally passed through a maximum, as shown in Figure 6. This can be explained by considerations of equilibrium between surfactant in solution and on the surface.

Fowkes [38] noted that the same anionic surfactants which charge the oxide particles positively in a hydrocarbon charge the particle negatively in water. We made this same observation for phosphate ester comparing our more polar solvent system with water and observed similar results. A simple electrophoresis test was performed in which a dilute suspension was placed between two graphite electrodes and the relative amount of powder collecting on the electrodes was observed. For BaTiO_3 in neutral water there was a slight collection at the cathode indicating a slight positive charge indicating the pH was just below the zero point of charge. When the phosphate ester was added the pH dropped and a large amount collected on the anode indicating that the anionic surfactant reversed the charge on the surface. In the nonaqueous suspension with the phosphate ester a large amount of powder collected on the cathode due to its positive charge. Charge reversal in an aqueous suspension has been explained by the formation of a hemi-micelles by Somasundaran and Fuerstenau [39]. Whether the phosphate ester polymers form a strict "hemi-micelles" on the particle surface in our aqueous system or not, the hydrophobic molecules adsorbed to a greater extent in the water than did the more lyophilic molecules in the solvent. This led to the formation of the negative charge in the aqueous media. Adsorption data indicated more phosphate ester adsorption in the aqueous system (2.45×10^{-6} moles/ m^2) when compared to the nonaqueous system (1.35×10^{-6} moles/ m^2).

c. Conductance Measurements

Conductance measurements were performed in order to provide an indication of ion concentrations and to gain some insight on the phosphate ester dissociation mechanism.

AC conductance measurements were performed on the following semi-dry solutions and dispersions and are indicated in Figure 7: (1) a solution of pure solvent (MEK-ethanol azeotrope) and phosphate ester, (2) a dispersion consisting of solvent, phosphate ester, and barium titanate, (3) a supernatant of the dispersion in number 2, i.e., solutions of solvent and phosphate ester with the barium titanate centrifuged out.

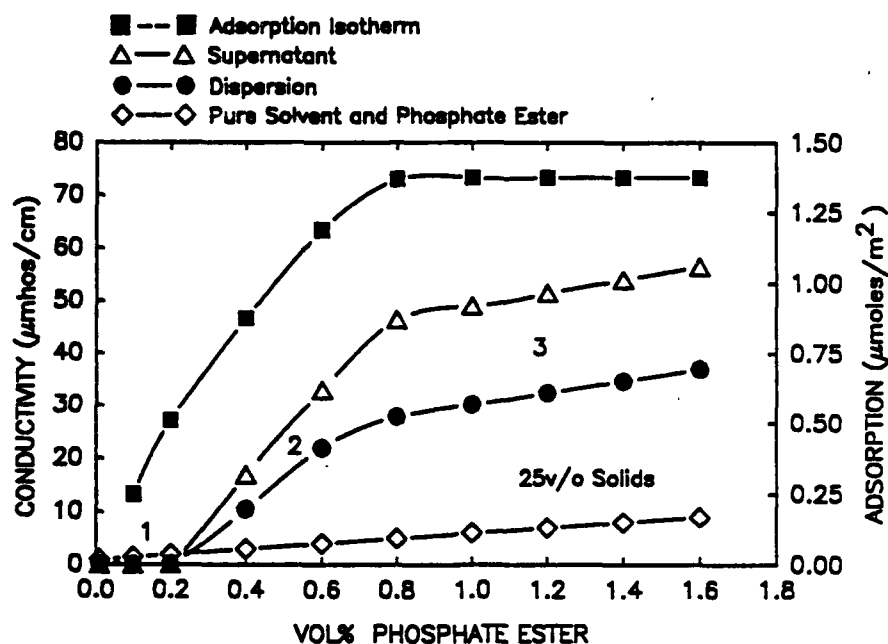


Figure 7. Conductivity as a function of phosphate ester concentration for semi-dry materials.

The figure shows conductivity increases for all samples as phosphate ester concentration was increased. The solution of pure solvent and phosphate ester showed only a slight increase in conductivity as phosphate ester concentration was increased. The conductivities of the dispersions and supernatants are substantial higher than the conductivities of the solution of pure solvent and phosphate ester. The conductivities of the supernatants are higher than the conductivities of the dispersions due to the insulating properties of the barium titanate.

The conductivity results suggest that proton dissociation (ionization) of the phosphate ester is relatively slight in the pure solvent while ionization is appreciable in the presence of the powder. The powder appears to promote surfactant dissociation.

These results are in good agreement with a mechanism proposed by Fowkes et al. [38]. In aqueous solutions, surfactants typically ionize in the liquid medium. Once ionized, the charged surfactants adsorb onto the powder surface by electrostatic forces. It is proposed that this does not occur in our nonaqueous system (the solution of pure solvent and phosphate ester shows only slight conductance). Fowkes et al. [38] suggests that the charging mechanism in nonaqueous systems is the reverse of aqueous systems. In non-aqueous systems, the surfactant adsorbs as a neutral molecule onto the solid surface. After adsorption, the surfactant dissociates and transfers a proton to the solid surface creating a charged surface. They reported some results with isotope tagged ions which supported this model. It is suggested, for our system, that the phosphate ester adsorbs as a neutral molecule onto the surface of the barium titanate. Once adsorbed

onto the surface, the acidic phosphate ester ionizes, transfers a proton to the surface of the solid and creates a positively charged surface. When the concentration of phosphate ester is sufficiently high, an adsorption-desorption process occurs. The negatively charged phosphate ester desorbs from the surface into the solvent where it acts as a counterion to the positively charged surface, thus forming an electrical double layer along with the co-ionic protons.

The three regions shown in Figure 7 can be explained in terms of the above non-aqueous charging mechanism. They also correlate with the adsorption data which is included in Figure 7 (from Figure 5). In region 1, many adsorption sites are available on the solid surface and subsequently all the phosphate ester is adsorbed on to the surface, as indicated by the steep slope in the initial portion of the adsorption isotherm. In region 1, the concentration of surfactant is insufficient for the adsorption-desorption process to occur (i.e., all the polymer is adsorbed onto the surface), dissociation of the phosphate ester is minimal, the conductivity of the dispersion is slight, and charging is minimal (zeta potential is low). Note that the slope of the conductivity line for the dispersion is the same as the slope of the conductivity line for the solution of pure solvent and phosphate ester suggesting minimal dissociation of the phosphate ester in both cases.

In region 2 the concentration of phosphate ester is sufficient to promote adsorption-desorption and dissociation of the phosphate ester. The adsorption isotherm indicates phosphate ester in the bulk liquid in this region, however, monolayer coverage has not yet been obtained. This is a region of active adsorption and desorption and of rapidly increasing conductivity and zeta potential as noted by the increase in the slope of the conductivity curve in this region.

In region 3 the concentration of phosphate ester is such that monolayer coverage has been reached. In this region no more phosphate ester can adsorb onto the surface; thus, dissociation of additional surfactant increases at a slower rate than in region two. The zeta potential has now reached a maximum and starts to decrease. The slope of the conductivity line for the dispersions is now near that of the solution of pure solvent and phosphate ester where minimal dissociation is occurring.

d. Dissociation in the Solvent

In order to determine the mechanism for phosphate ester dissociation in MEK/ethanol, FTIR spectra of pure phosphate ester as a neat liquid and phosphate ester in MEK/ethanol solution were compared. Spectral subtraction by the Perkin-Elmer DIFF subroutine was utilized to eliminate the solvent from the solution spectrum. As shown in Figure 8, there are two major differences in the two spectra. The broad band at 1640 cm^{-1} due to O-H bending is present in the pure liquid but not in the solution, and a non-gaussian band at 1710 cm^{-1} is present only in the solution spectrum. A non-gaussian band usually indicates an interaction between components which shifts or broadens a particular band, making complete spectral subtraction impossible. The position of this band corresponds to that of the carbonyl (C=O) stretch in methyl ethyl ketone. Thus, the dissociation-reaction involves an O-H bond in the phosphate ester and the C=O bond in MEK. A reaction, such as Figure 9 depicts is therefore proposed. As a phosphate ester molecule and a MEK molecule approach, and O-H bond between them is formed which stretches the C=O bond in MEK and stretches or breaks

an O-H bond in the phosphate ester. If this bond is broken, the hydronium ion is liberated to the solution leaving a negative charge on the phosphoryl group. Based on the conductivity measurements the degree of dissociation is probably limited. It is only in the presence of a polar surface such as the surface of the powder or water that dissociation is extensive. Unfortunately, work was not completed on the FTIR spectroscopy of the phosphate ester in the supernatant solution for comparison.

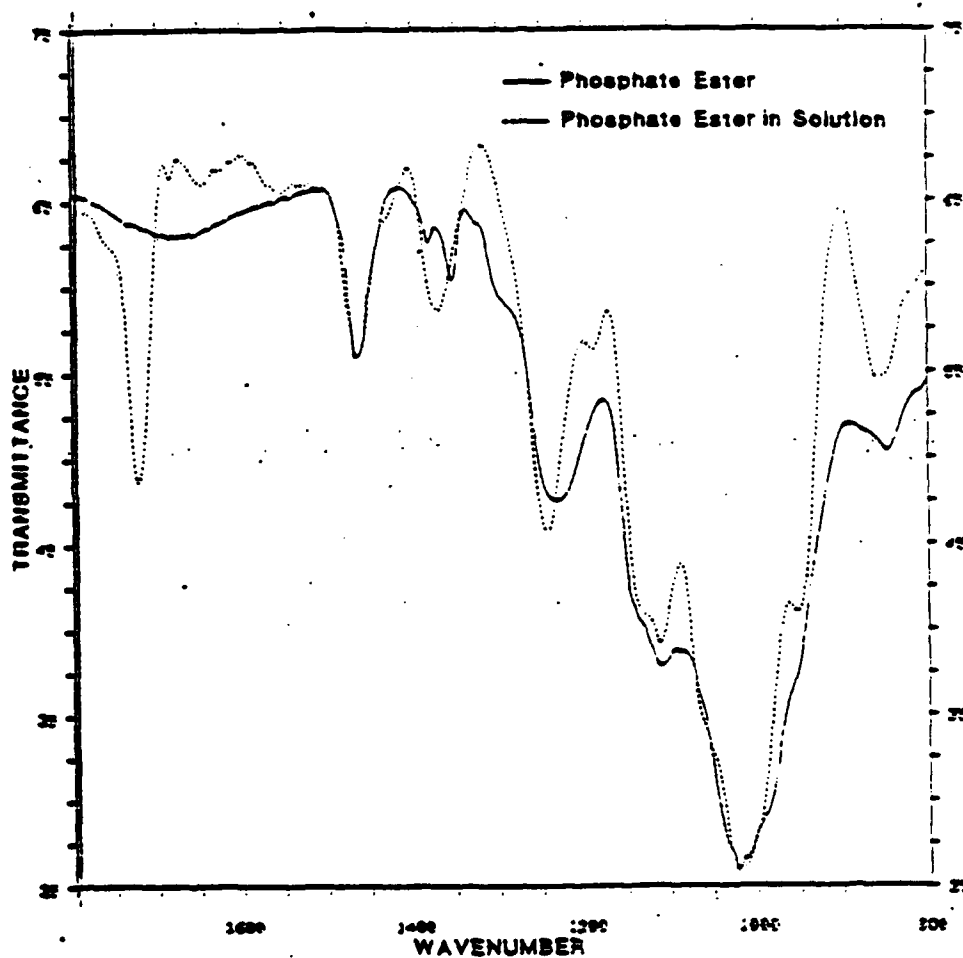


Figure 8. FTIR spectra of Emphos PS-21A scanned as a neat liquid and in MEK/ethanol. Solvent bands have been removed from the solution spectrum by spectral subtraction.

The adsorption curve in Figure 10 indicates approximately a constant surface excess concentration at 1.36×10^{-6} moles/m² as a function of MEK/ethanol fraction. The figure indicates a slight increase in adsorption at the extreme fraction. Since the scatter of points shown in the curve is within the experimental error of ± 10 g/ml, a linear relationship is assumed. The 1.36×10^{-6} moles/m² adsorption value determined here is the same value determined from the original adsorption isotherm in Figure 5 for monolayer coverage. Therefore, the phosphate ester adsorbed to approximately a monolayer at all fractions of MEK/ethanol. It can be concluded that adsorption of the phosphate ester onto the barium titanate surface is not affected by varying the MEK/ethanol ratio. The increased flocculation shown on either side of the azeotrope solution by the rheology measurements cannot be attributed to changes in the amount of phosphate ester adsorbed. Zeta potential again was found to be maximum under the same conditions that the viscosity is at a minimum.

AC conductance as a function of solvent fraction is shown in Figure 11 for the same type sample described above: (1) pure solvent and phosphate ester, (2) dispersions consisting of solvent, phosphate ester, and barium titanate, (3) supernatants of the dispersions in number 2. The conductivities of solvent plus phosphate ester samples are small relative to the dispersions and supernatants, as before. The conductivities of the pure solvent increased slightly at the ethanol end member, as expected, due to its higher dielectric constant. This is in agreement with the previous results.

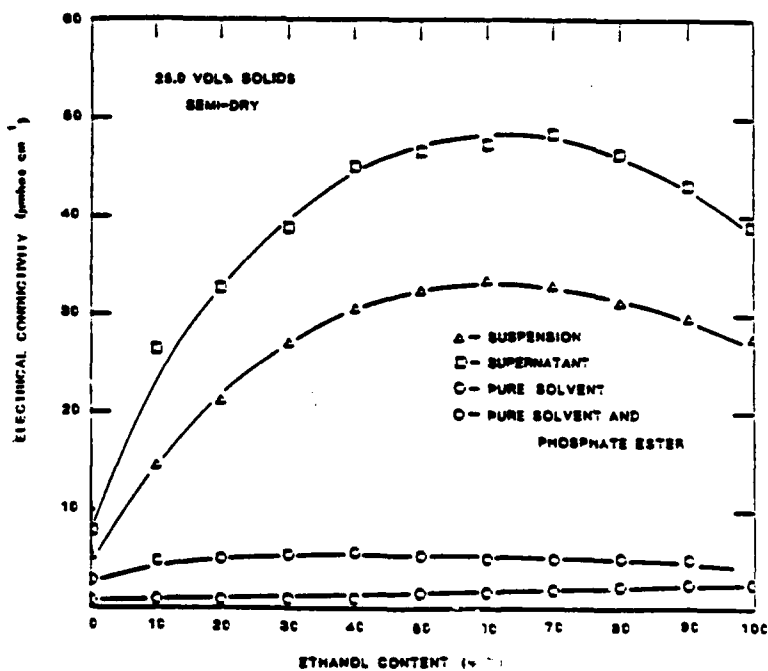


Figure 11. Conductivity as a function of ethanol fraction for semi-dry materials at 0.7 v/o phosphate ester.

Conductivities for the dispersion and supernatants increased and reached a maximum on approach to the ethanol end member. The increase in conductivity was again expected at high fractions of ethanol, since its dielectric constant (24.3) is higher than the MEK's dielectric constant (18.5). Thus, the ionic strength of the dispersions and supernatants increased due to increased dissociation of the phosphate ester with increasing ethanol fraction.

A comparison of the zeta potential and viscosity data, as a function of ethanol fraction (Figure 10), shows that the maximum zeta potential again coincides with the minimum in viscosity. The decrease in the zeta potential at high ethanol fractions coincides with increased conductivity. It is suggested that the increase in ionic strength at high ethanol fractions leads to a compression of the electrical double layer resulting in a decrease in zeta potential, and thus, a decrease in dispersibility. On the MEK side the increased zeta potential with increasing ethanol must be attributed to increased charging of the surface.

5. Application of the DVLO Theory

Additional insight on the steric and electrostatic contributions to the overall dispersion mechanism can be obtained by using the adsorption, zeta potential, and conductance data to plot potential energy of interaction diagrams for two approaching particles according to DVLO theory.

For a combined electrostatic and steric mechanism (electrosteric) the total potential energy of interaction is the sum of the attractive energy V_A due to van der Waals forces and the repulsive energies due to the electrostatic contribution V_R and the steric contribution.

The van der Waals attractive force was estimated for two spheres with radii of 0.5 microns using the a form of the Hamaker expression for spheres of equal radii:

$$V_A = - \frac{A'}{12} \left\{ \frac{1}{x(x+2)} + \frac{1}{(x+1)^2} + 2 \ln \left[\frac{x(x+2)}{(x+1)^2} \right] \right\} \quad (9)$$

where a is the particle radius, H is the particle separation, $x = H/2a$, and A' is the effective Hamaker constant which takes the form;

$$A' = (A_{11}^{1/2} - A_{22}^{1/2})^2 \quad (10)$$

A' was estimated as 4.09×10^{-20} J using approximation that barium titanate is similar to titania.

The Makor equation was used to estimate the steric repulsive energy between two approaching particles of radius r , with and an adsorbed layer thickness of δ , according to (18);

$$V_R(\text{steric}) = N_s k T \theta_\infty \pi (\delta - d)^2 \left[\frac{2r + \delta + d}{\delta} \right] \quad (11)$$

where N_s is the number of adsorbed molecules per unit area, θ_∞ is the fractional surface coverage and is considered to be approximately 0.2., and d is the distance from the surface of the particle to the point of adsorbed film contact. N_s was estimated from monolayer coverage values of 122 \AA^2 per molecule. δ was estimated as 25 \AA .

The electrostatic repulsive potential energy due to the interaction of the diffuse parts or the electrical double layer can be approximated by:

$$V_R(\text{electrostatic}) = 2\pi\epsilon_r\epsilon_0 r \psi_d^2 \ln(1 + \exp[-\kappa H]) \quad (12)$$

where the relative dielectric constant was estimated as 20.4 and the potential at the shear plane was estimated by the zeta potential. The thickness of the diffuse layer was estimated from the conductivity data by:

$$1/\kappa = (\epsilon_r\epsilon_0 D/2\sigma)^{1/2}$$

where D is the diffusion constant and σ the conductance. The diffusion constant was estimated from the Stokes Einstein equation assuming the phosphate ester was the charge carrying species and a friction coefficient of 1.2.

The length of the diffuse layer created by the dissociation of the phosphate ester at the maximum degree of dispersion (0.8 vol%) assuming a molecular weight of 750, a density of 0.925 g/cm^3 , one electronic charge per molecule, $D = 5.7 \times 10^{-10} \text{ m}^2/\text{sec}$, and a conductance of $3.6 \times 10^{-5} \text{ coul}^2/\text{sec/Kg m}^3$, is approximately 43 \AA . This Debye length is about the same as those calculated for some aqueous systems and can be attributed to the high ionic strength of the suspension caused by dissociation of the highly acidic phosphate ester.

Figure 12 and 13 shows the sum of the combination of the electrostatic and steric contributions to the dispersion force as a function of separation distance for two approaching particles for semi-dry suspensions dispersed with the phosphate ester. The Makor equation takes into consideration the steric contribution.

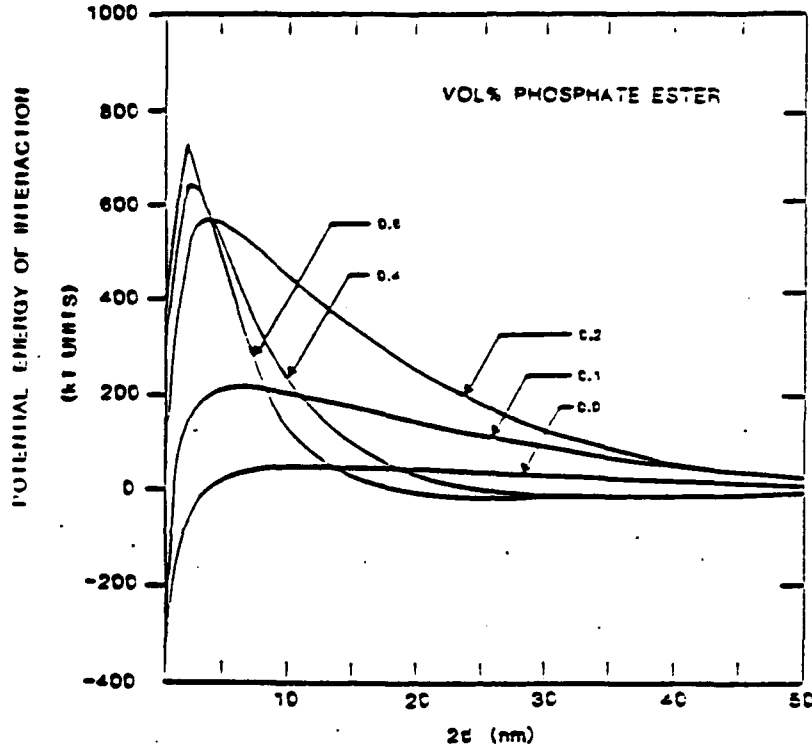


Figure 12. Total potential energy of interaction as a function of particle separation for phosphate ester concentrations varying from 0.0 vol% to 0.6 vol%.

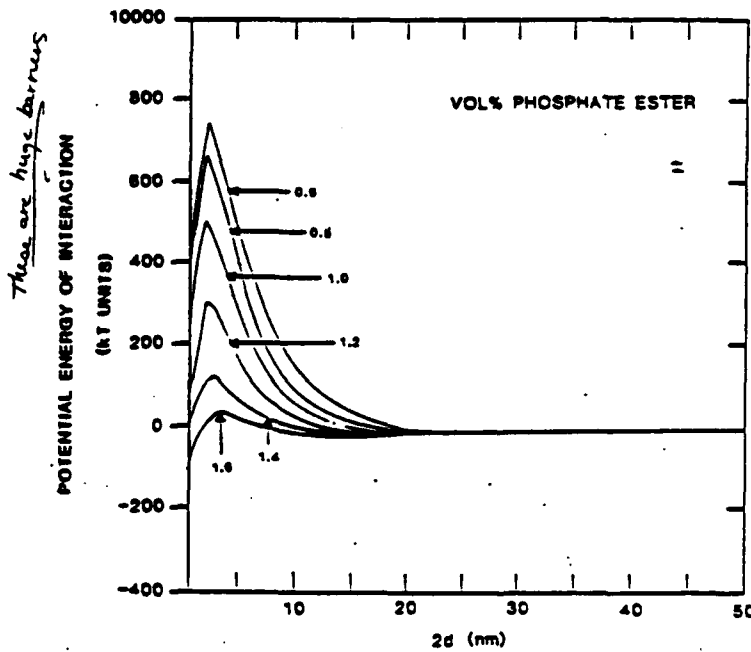


Figure 13. Total potential energy of interaction as a function of particle separation for phosphate ester concentrations varying from 0.6 vol% to 1.6 vol%.

Figure 12 shows the potential energy curves for suspensions with concentration of phosphate ester increasing from 0.1 vol% to 0.6 vol%. Figure 13 shows the potential energy curves for concentrations of phosphate ester increasing from 0.6 vol% to 1.6 vol%. Although the barrier height is much higher than would be expected, qualitatively they help explain the results. (Possibly the wrong Hamacker constant resulted in the high energy barriers.) In the first curve the potential increases as the concentration of phosphate ester increases and reaches a maximum at 0.6 vol%. This is the concentration of phosphate ester at which the maximum degree of dispersion occurred according to the rheometry measurements. At concentrations below 0.6 vol% the potential decreases and flocculation was shown to increase. At concentrations above 0.6 vol% the potential decreases as the concentration of phosphate ester increased and this coincided with an over-deflocculated condition according to rheometry measurements. The heights of the barriers to flocculation coincide with the degree of dispersion.

The energy curves also shows that the length of the diffuse layer decreases (i.e., double layer is compressed) as the concentration of phosphate ester is increased due to an increase in ionic strength as shown in the conductivity data. The length of the diffuse region in addition to the height of potential barrier can help to explain the viscosity data.

Figure 14 shows the potential diagrams for hydrated suspensions. Data for only three concentrations was available. Nevertheless, the heights of the energy barriers are less than at corresponding concentrations of phosphate ester for the semi-dry suspensions due to decreased zeta potentials and higher ionic strengths in the hydrated suspensions. The degree of dispersion was found to be less for the hydrated suspensions than for the semi-dry suspensions according to rheometry measurements. This is predicted by the energy interaction diagrams.

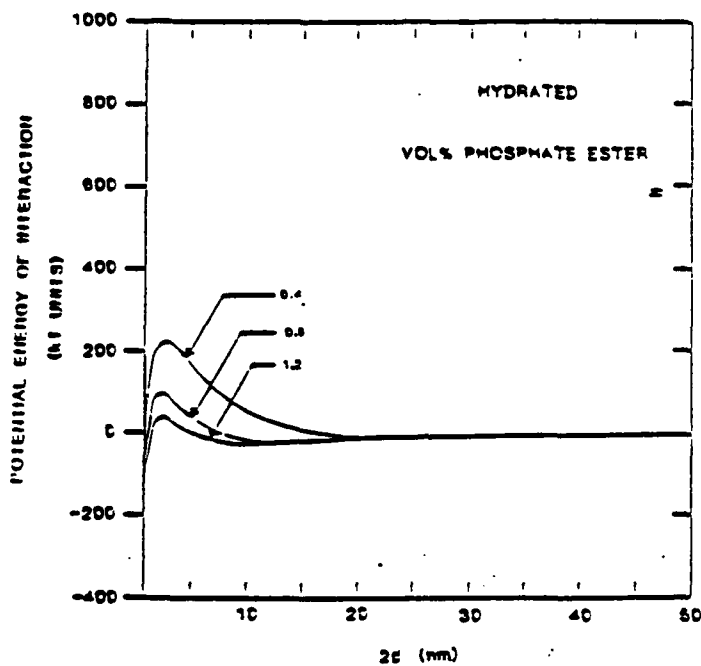


Figure 14. Total potential energy of interaction as a function of particle separation for hydrated materials.

Potential energy diagrams for varying solvent composition are shown in Figures 15 and 16. Again, the degree of dispersion coincides with the heights of the potential barriers.

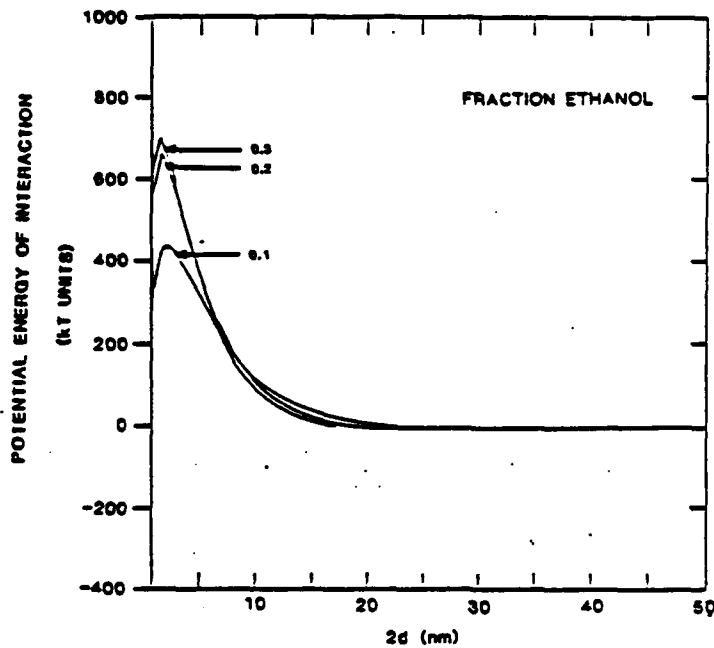


Figure 15. Total potential energy of interaction as a function of particle separation for solvent fractions varying from 0.3 to 0.1 fractions of ethanol

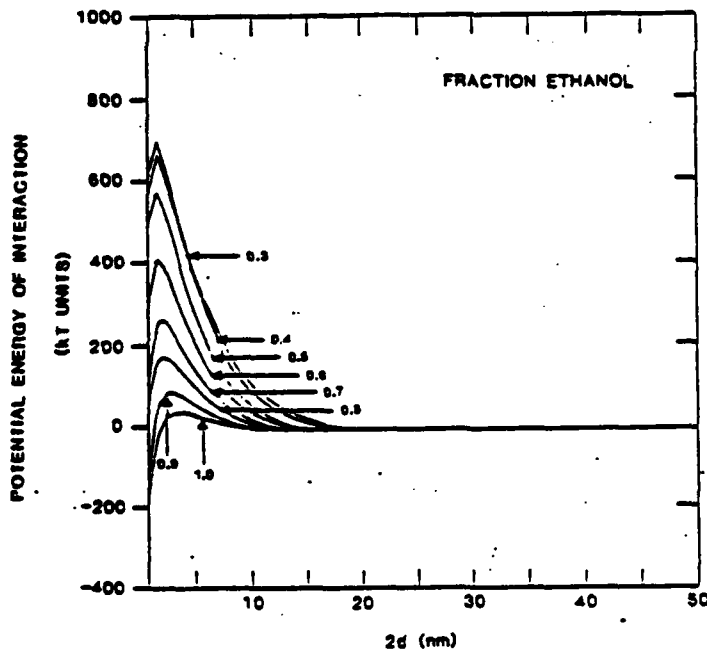


Figure 16. Total potential energy of interaction as a function of particle separation for solvent fractions varying from 1.0 to 0.3 fractions of ethanol.

C. Acrylic Binder

Since the commercial acrylic binder is so important component in the slip, some basic information was obtained regarding its ability to disperse the powder. As discussed in section II, the acrylic binder has a number average molecular weight of 68,000 and contains 0.6% methyl acrylic acid (MAA). According the Usala[9] the MAA is very important to the ability of the acrylic binder to disperse the powder. If too little is present, the powder is not well dispersed, presumably because the binder does not anchor well to the powder. If too much MAA is present, the viscosity is high presumably because the binder bridges between particles. Because of the high molecular weight the binder likely acts as a steric stabilizer in dispersing the powder. To investigate dispersion characteristics of the acrylic binder, viscosity versus concentration behavior, electrophoretic properties and adsorption were studied for the system consisting of barium titanate powder, MEK/ethanol solvent and acrylic binder.

Viscosity and relative viscosity versus concentration of acrylic binder additions are plotted in Figure 17. Viscosity decreases sharply with acrylic addition indicating that the acrylic binder is a good dispersant. A minimum point is reached between 0.5 and 1.0 volume percent acrylic. Further addition results in an increase in viscosity, presumably a result of higher solution viscosity due to higher concentration of acrylic polymer. Relative viscosity decreases with acrylic addition until the point of minimum viscosity is reached, and remains constant with any further addition. Thus the viscosity does not follow the characteristic U-shaped curve for electrostatic stabilization as did the curve for the phosphate ester. Although Figure 3 was not plotted as relative viscosity as Figure 17 is, that is not important since the phosphate ester did not affect the viscosity of the solution significantly. In the Acryloid B7-MEK case, the viscosity does increase but the relative viscosity remains constant, indicating that the viscosity increase is entirely due to increased solution viscosity. This result provides some evidence for a steric stabilization mechanism. To verify this hypothesis, electrophoretic mobility of particles stabilized by acryloid B7-MEK were measured and found to be very low.

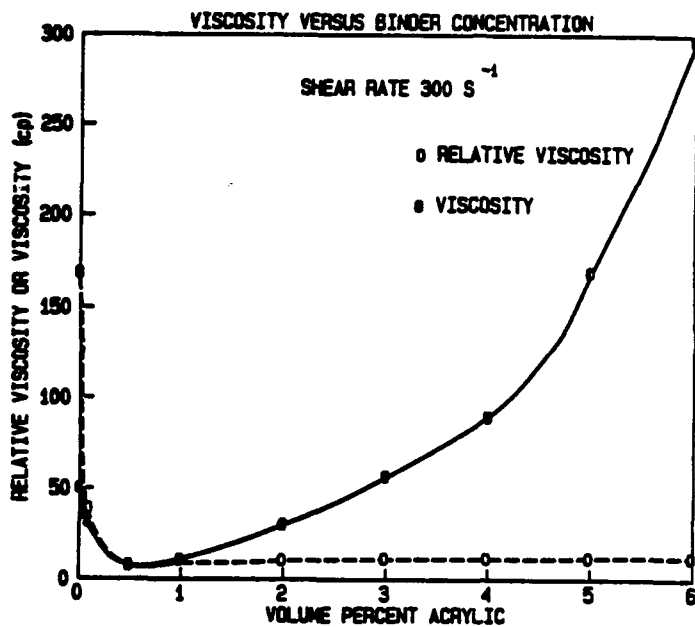


Figure 17. Viscosity and relative viscosity versus acrylic concentration for slurries consisting of solvent, binder and powder.

An adsorption isotherm plotting surface excess concentration versus equilibrium concentration is given in Figure 18. Adsorption increases rapidly with concentration up to a plateau value, where only slightly more acrylic is adsorbed upon addition. The isotherm is again a high affinity type with a level plateau indicating strong adsorbent-adsorbate interaction with little competition from solvent [40]. The shape of the isotherm agrees well with those of Eirich [41] for the adsorption of PMMA onto various surfaces from hydrocarbon solvents. The concentration corresponding to a monolayer coverage is near the that required to achieve a minimum viscosity, as expected.

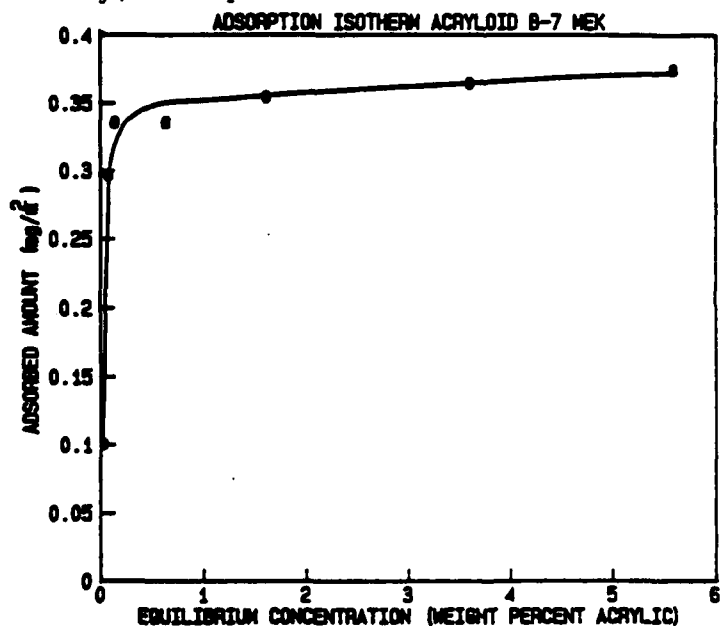


Figure 18. Adsorption isotherm for the adsorption of Acryloid B7-MEK onto barium titanate powder, from MEK/ethanol

The adsorption isotherm was fitted to a modified form of the Langmuir equation as described for the phosphate ester in the previous report. In linearized form this is:

$$1/\Gamma^S [C_2 + 1/(k-1)] = C_1 C_2 / W_0 \Delta C_2 / MA \quad (3)$$

where Γ^S - adsorption (mg/m^2)

- k - equilibrium constant
- W_0 - initial weight of solution
- M - mass of barium titanate powder
- A - specific surface area of powder
- C_1 - solution concentration of solute
- C_2 - solution concentration of solvent

Since adsorption experiments were carried out in dilute solutions where $C_1 \sim 1$, $C_1 C_2 \sim C_2$. Also, the term $W_0 C_2 / MA$ can be approximated as Γ^S_2 , therefore Equation (3) becomes:

$$1/\Gamma^S [C_2 + 1/(k-1)] = C_2 / \Gamma^S_2 \quad (4)$$

When the adsorption data are plotted as C_2 / Γ^S_2 versus C_2 , as shown in Figure 19, the slope (m) can be used to determine the adsorption at monolayer coverage, since $m = 1/\Gamma^S$. Similarly, the ratio of the slope to intercept can be used to estimate the equilibrium constant, k, since $k = (m/b) + 1$ where b is the intercept. Knowing the equilibrium constant, the energy of adsorption can be calculated by the equation:

$$\Delta G^\circ = -RT \ln(k) \quad (5)$$

where ΔG° - free energy of adsorption
 R - universal gas constant
 T - absolute temperature.

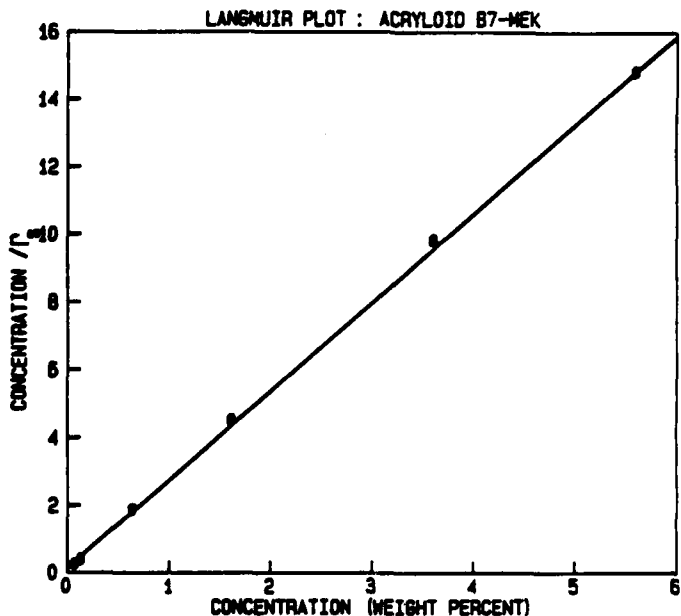


Figure 19. Langmuir plot for the adsorption of Acryloid B7-MEK onto barium titanate powder, from MEK/ethanol.

Final Report - 1988

A free energy of adsorption of -1.06 kJ/mole (-4.45 kcal/mole) was calculated for the acrylic binder. The negative value indicates a strong thermodynamic driving force for adsorption. The magnitude of this value is slightly lower than the value of -1.54 kJ/mole (-6.49 kcal/mole) for phosphate ester adsorption in the same system, indicating that phosphate ester adsorption is favored thermodynamically. The area per adsorbed acrylic molecule (a_2) was calculated from the monolayer adsorption (Γ^S) using the following equation:

$$a_2 = M/\Gamma^S N_a \quad (5)$$

where M = molecular weight of acrylic
 N_a = Avagadro's number.

An area of 5400 Å² per molecule was arrived at by this calculation. This area is not large enough for a molecule of molecular weight of 68,000 to lie flat on the surface and so we can assume that loops and tails of the molecules extend out from the surface.

The configurational state of an adsorbed polymer is an important factor determining its effectiveness as a steric barrier. Eirich [42] has shown by comparing intrinsic viscosities and flow characteristics of liquids through capillary tubes coated with adsorbed polymers that the conformational states of adsorbed polymers and polymers in solution are very similar. Thus, the adsorbed layer thickness, δ , can be approximated by the root mean square length of the polymer in solution, $(r^2)^{0.5}$. In an effort to determine this length, intrinsic viscosity was calculated from the capillary tube viscometer data shown in Table VIII. Viscosity, in centipoise, was measured using a Cannon-Fenske viscometer. Specific viscosity was determined using the relation:

$$\eta_{sp} = \eta_{rel} - 1. \quad (6)$$

To calculate the intrinsic viscosity, η_{sp}/C was plotted versus C as shown in Figure 20, where C = concentration.

Table VIII. Acrylic Solution Viscosities

X_1 (Vol. % Acrylic)	η (cp)	η_{rel}	η_{sp}	$\frac{\eta_{sp}}{X_1}$
0.0	0.7728	1.0	-	-
0.1	0.8598	1.1126	0.1126	1.126
0.5	1.3218	1.7104	0.7104	1.421
1.0	2.1028	2.7210	1.7210	1.721
2.0	4.4289	5.7310	4.7310	2.365

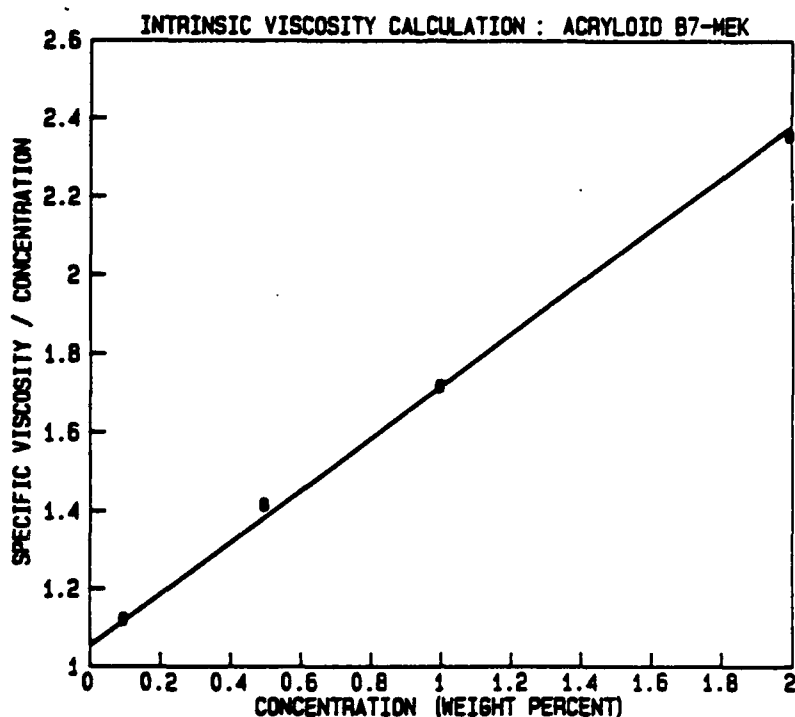


Figure 20. Plot of specific viscosity/concentration versus concentration used to determine intrinsic viscosity of Acryloid B7-MEK.

Flory [43] determined the relationship between intrinsic viscosity, $[\eta]$, and the root mean square length of the polymer chain to be:

$$[\eta] = \Phi[(r^2)M]^{3/2} \quad (7)$$

where Φ - a constant
 M - molecular weight.

Using this relation, the root mean square length was calculated to be 40.4 Å. Hence, the adsorbed layer thickness can be approximated at 40 Å. The acrylic polymer can be assumed to form random coils with some segments being in contact with the powder surface, but most of them extending into the liquid.

Thus, the acrylic binder is an effective dispersant in terms of producing slurries with low relative viscosities. The acrylic adsorbs strongly on the powder surface as indicated by a free energy of adsorption of -4.4 kcal/mole. The strong adsorption likely results from the acrylic acid functional portion of the polymer. Results in this section support the hypothesis that the acrylic binder acts as a steric stabilizer for barium titanate particle in MEK/ethanol.

D. Tape Casting Slips

The goal of this portion of the program was to examine the tape casting slip in detail. We considered the role of each organic component added in dispersing the tape and the manner in which they interact. One of the early questions asked was: "Do the other components in the slip lead to increased agglomeration or do they help disperse the powder." Relative viscosity was used to as one measure of this. Relative viscosity, η_r , is defined as

$$\eta_r = \eta_{slip} / \eta_{fluid\ part}$$

Early work in this program [21] showed that addition of all slip components listed in Table II did, in fact, lead to a lower relative viscosity than that of the solvent, powder and phosphate ester only. It was thus concluded that the other organic components aided in dispersing the powder. Further work was performed as part of this program to determine which of the components was most effective in lowering the relative viscosity.

During this study it was also noted that the order of addition of the components was also important and affected the relative viscosity. A study was, therefore, undertaken to determine the affect of order of addition on the properties of the slip and the resulting tape. This problem is also of technological importance since various manufacturers add their components in different orders.

To determine the effect of order of addition we have prepared slurries of identical composition using three component addition sequences, dispersant first, dispersant last, and simultaneous addition. The slurries were also aged for several days to determine if the effects of component addition sequence vary with slurry aging time.

The rheological properties of the slip, green density, and green tensile strength were measured and samples were sintered to determine sintered density, sintered strength, flatness, and electrical properties .

1. Order of Addition Sequence
 - a. Batch Preparation

Three batches of identical composition were prepared as outlined in Figure 21, using three different component addition sequences: dispersant first; dispersant last; and simultaneous addition. In the dispersant first case, the solvent, dispersant, and powder were premixed, ultrasonically agitated for 2 minutes, and allowed to age for 24 hours before the remaining components were added. In the dispersant last case, all components except the dispersant were premixed, ultrasonically agitated, and aged for 24 hours before the dispersant was added. In the simultaneous addition slurry, all of the liquid components were premixed, ultrasonically agitated, and aged before addition of the powder. After the final components were added, all batches were again ultrasonically agitated for 2 minutes and the slurries were placed on a slow roller mill for the duration

of the study. There were no grinding media added to the slurries as the purpose of the slow rolling action was to simply keep the components from separating during the aging study. The slurries were removed from the slow roller mill only for sample taking.

BATCH A (DISPERSANT FIRST)	BATCH B (DISPERSANT LAST)	BATCH C (SIMULTANEOUS ADDITION)
36% BARIUM TITANATE 33.6% MEK/ETHANOL 0.76% PHOSPHATE ESTER	36% BARIUM TITANATE 33.6% MEK/ETHANOL 20% ACRYLIC BINDER 6% PEG 400 6% BUTYL BENZYL PHTHLATE 1% CYCLOHEXANONE	33.6% MEK/ETHANOL 20% ACRYLIC BINDER 6% PEG 400 6% BUTYL BENZYL PHTHLATE 0.76% PHOSPHATE ESTER 1% CYCLOHEXANONE
SONICATE 2 MIN. AGE 24 HR.	SONICATE 2 MIN. AGE 24 HR.	SONICATE 2 MIN. AGE 24 HR.
ADD: 20% ACRYLIC BINDER 6% PEG 400 6% BUTYL BENZYL PHTHLATE 1% CYCLOHEXANONE	ADD: 0.76% PHOSPHATE ESTER	ADD: 36% BARIUM TITANATE

Figure 21. The processing and addition sequence used in preparation of samples.

At twenty-four hour intervals slurry viscosity was measured and tapes from each batch were cast onto glass. A Cladan laboratory scale caster was used. The tapes were stripped from the casting glass after a twenty-four hour drying period and samples of the appropriate shapes for property measurements were cut.

b. Rheology Measurements

Viscosity was measured using the Brookfield cone-plate viscometer at shear rates ranging from 3.84 to 384 reciprocal seconds. In some cases the slurry was too viscous to be measured at the highest shear rates, so the value was extrapolated from data at lower shear rates. This was done by plotting shear stress versus shear rate as shown in Figure 22, extrapolating the least squares line through the data out to 384 reciprocal seconds and determining the corresponding shear stress. Multiplying this value by the appropriate viscometer constants gives the viscosity.

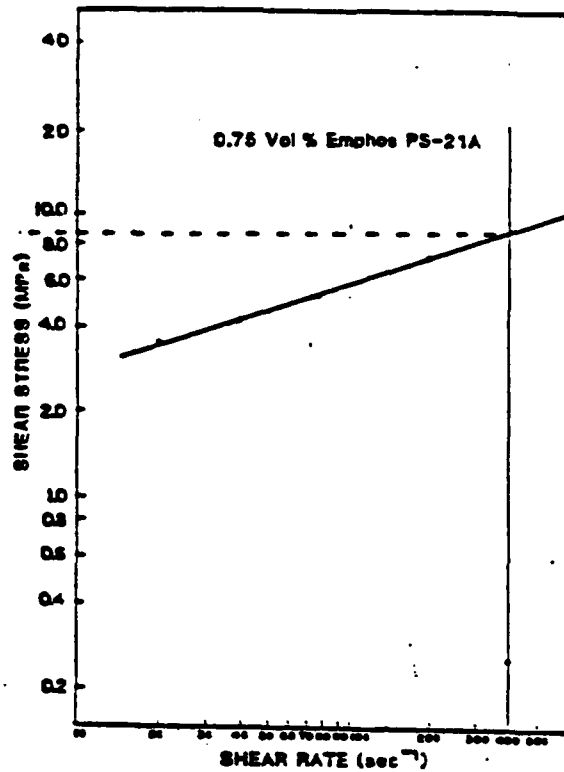


Figure 22. Method of extrapolation from low shear rates to high shear rates.

In Figures 23 and 24 results are compiled for viscosity in two different shear rate ranges as a function of aging time of the slip for the three orders of addition. In the dispersant first case at the high shear rate (Figure 23), viscosity is initially low, but with slurry aging time it increases to a constant value of approximately 300 centipoise. In the dispersant last case the trend is the opposite. On the first day the viscosity is high, and with slurry aging time it decreases to a constant value of approximately 500 centipoise. In the simultaneous addition case, the viscosity remained virtually constant at 410 centipoise.

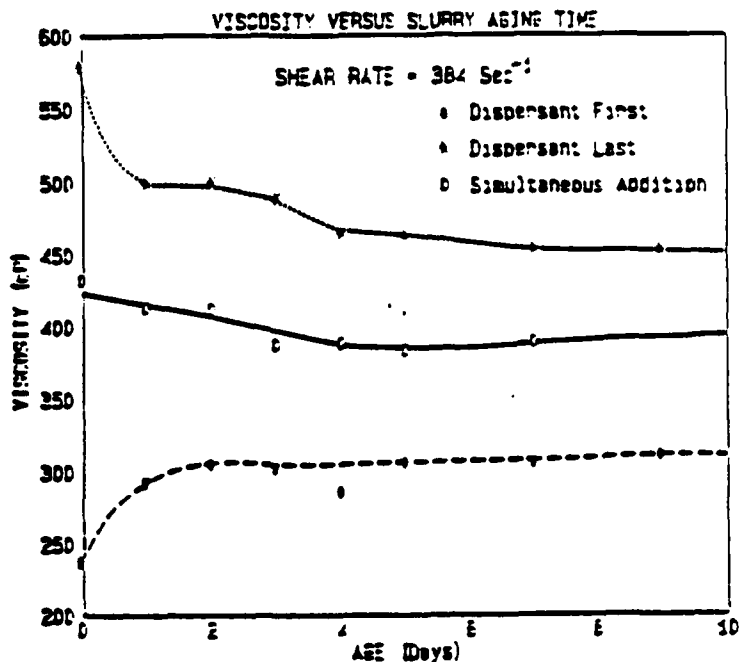


Figure 23. Viscosity measured at 384 sec⁻¹ as a function of aging time of the slip.

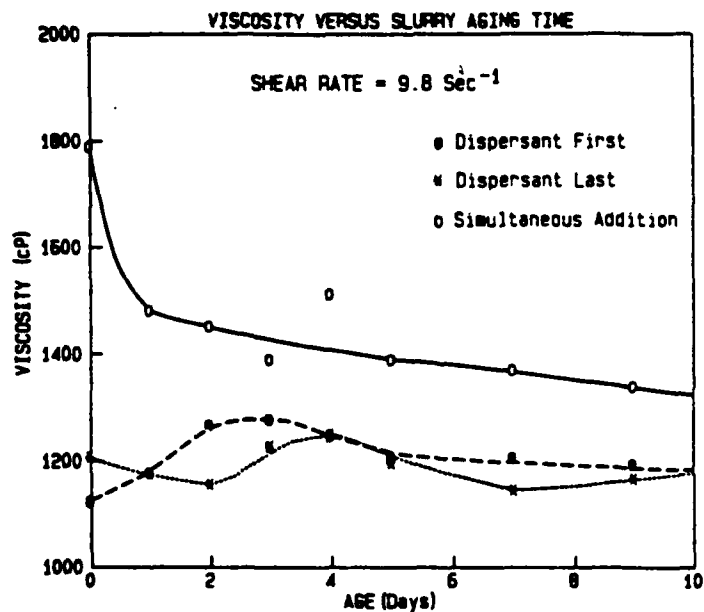


Figure 24. Viscosity measured at 9.8 sec⁻¹ as a function of aging time of the slip.

In Figure 24 viscosity is plotted versus slurry aging time for all three component addition sequences at a low shear rate, 9.8 sec^{-1} . As can be seen in Figure 24, these results are very different from the high shear rate data. At this low shear rate the floc structure of the slurry and the strength of these flocs play important roles in determining the slurry viscosity. At the low shear rate, slurries made by simultaneous addition of the components have the highest viscosities, with the first day value being by far the largest. This can be interpreted to mean that these slurries have the greatest concentration of flocs or agglomerates, and that these are most prevalent in the first day of the aging study. Dispersant first and dispersant last slurries appear to have nearly the same viscosities throughout the aging study with a mean value of approximately 1200 centipoise.

c. Correlation between viscosity and other properties

In order to correlate these viscosities to other properties such as tape density, green strength, etc., it is necessary to consider the tape casting process more closely to determine at which tape is formed.

The tape casting process can be thought of as two extreme rheological conditions. During casting, the blade shears the slurry at rates estimated to be as high as several thousand reciprocal seconds and after application, a shear rate of less than one reciprocal second results in spreading and leveling [44]. In the particular tape casting head used for this study, shown schematically in Figure 25, the average shear rate can be estimated at 720 reciprocal seconds by dividing the head velocity by the blade gap clearance. This high shear condition lasts for a very short time, about 0.05 seconds for the head used in this study.



Figure 25. Schematic drawing of the tape casting head

As a result of the flow conditions under the blade, striations inevitably are formed, the magnitude of which are a function of blade geometry and gap clearance. Trailing knife edge blades produce the smallest striations, while flat or round edge spreaders have more pronounced effects. Smaller gap clearance results in larger striations. The elimination of these striations, along with final particle packing in the tape is determined by flow at a very low shear rate. Surface tension and the downward pull of gravity are the driving forces for leveling and settling. Smith et al. [45] derived mathematical relationships which describe these flow conditions. The time to eliminate a striation of linear dimension, L, was given as:

$$\tau = \gamma L / \eta$$

where γ = surface tension of slurry
 η = viscosity of slurry.

Whether a striation is eliminated or not, thus depends on a competition between the rate of solvent evaporation and this leveling process.

It can then be argued that the state of agglomeration at the time the powders settle into their final packed state is most important and that this is toward the end of the tape casting process where the shear rate is low. Naturally the slip has just undergone a high shear rate and so the powder may not have had a chance to reach their equilibrium state for the slower shear rate. This all depends on time expired before the packing actually occurs. The resolution of the question may best be determined by correlating these viscosity measurements with properties of the green tape.

d. Green and Sintered Density

Green and sintered densities were measured for day one tapes of all three component addition sequences. First day tapes were measured because the largest difference in measured properties is expected on the first day, and because the majority of commercial operations cast tapes without aging the slurry. As can be seen in Table IX, dispersant first tapes have the highest densities, dispersant last tapes have intermediate values, and simultaneous addition tapes are the least dense. This trend holds true for both the green and the sintered state. These results agree with the low shear rate viscosity measurements, as the least viscous and presumably best dispersed system produces the tapes with the most efficient packing and the most viscous slurry produces the least dense tapes.

DAY ONE DENSITY COMPARISON

ADDITION SEQUENCE	GREEN DENSITY		FIRED DENSITY	
	³ g/cm	% Th.	³ g/cm	% Th.
DISPERSANT FIRST	2.873	52.0	5.132	93.3
DISPERSANT LAST	2.764	50.2	5.076	92.2
SIMULTANEOUS ADD	2.694	48.9	4.821	87.6

Table IX. Density of green and sintered tapes

e. Green Tensile Strength

Green tensile strength was measured as a function of slurry aging time for the three component addition sequences. As can be seen in Figure 26, the simultaneous addition tapes show the lowest strengths in all cases. In fact these tapes were so fragile that strength measurement was not possible for the first three days of the study, the tapes broke under their own weight as they were placed in the testing fixture. Dispersant first and dispersant last tapes were both significantly stronger than the simultaneous addition tapes, with dispersant first tapes being slightly stronger than dispersant last tapes. Figure 26 correlates quite well with Figure 24 for viscosity measured at a low shear rate in that higher viscosities are usually an indication of agglomeration. Agglomerated slip do not form high density green compacts and so are expected to be weaker. The shapes of the curves of Figure 26 and Figure 24 are quite similar if one considers high viscosity correlates with low strength. In contrast, Figures 26 and 23 do not correlate well. These results support the hypothesis that the final packing density of the powder in the tape is related to the viscosity measured at low shear rates.

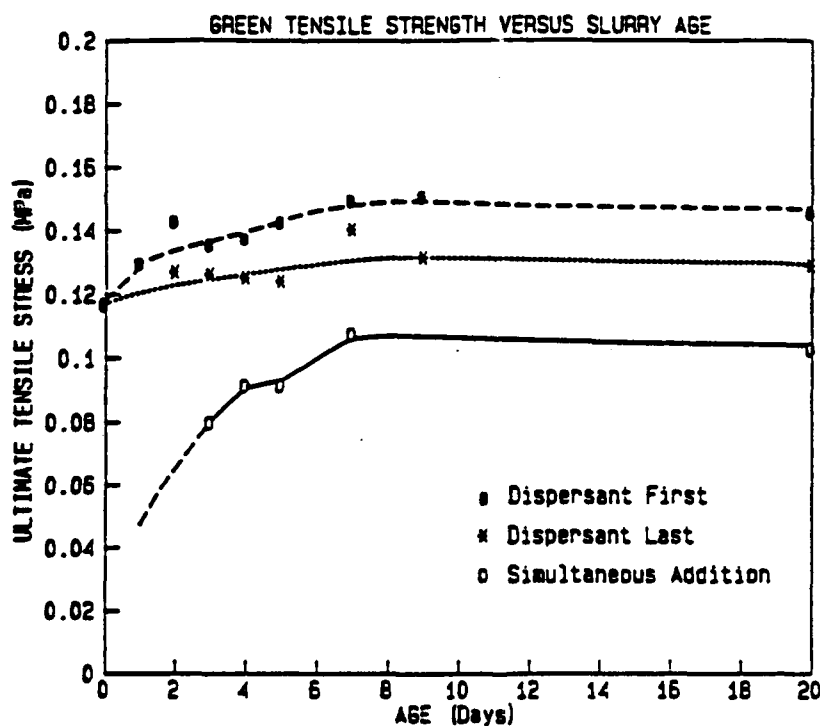


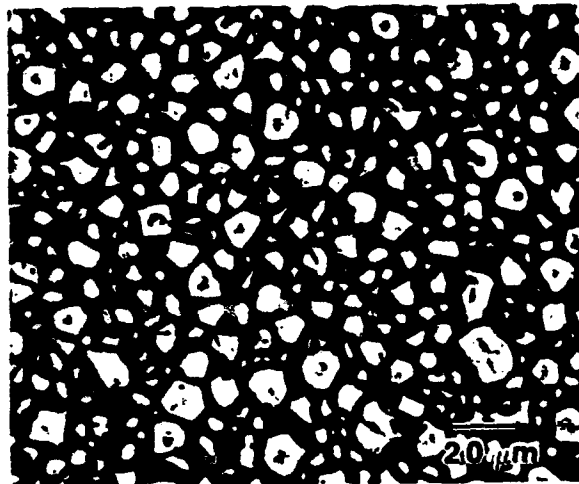
Figure 26. The ultimate tensile strength of green tapes.

SEM micrographs of the as cast surfaces of first day tapes for the simultaneous addition tapes reveal pores, uncoated particles, and clumps of binder, whereas the surface of the dispersant first and dispersant last tapes are quite uniform. These inhomogeneities are the most probable cause of the low strength of these tapes. After six days, the dispersant first and dispersant last tapes again appear to be uniform, with only a few small flaws. The simultaneous addition tape has areas of uniform well bonded tape but contains large voids which limit the strength. Finally, after ten days, the dispersant first and dispersant last tapes begin to show some evidence of agglomeration, while the simultaneous addition tapes appear to be more uniform than the earlier tapes.

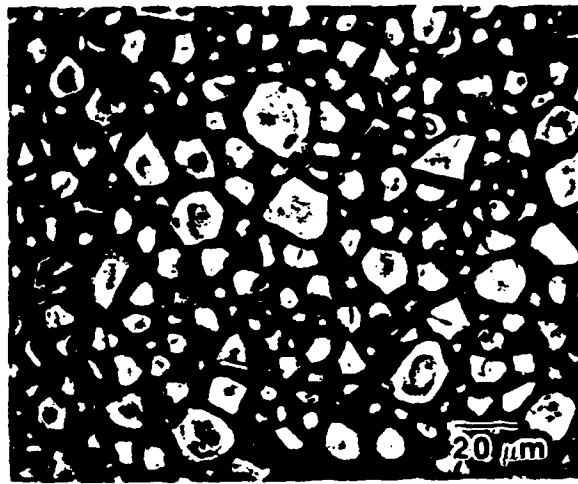
slips aged 6 days.

f. Sintering of Tapes

The tapes were sintered according to the schedule described in section II with soak times for one hour at temperatures ranging from 1325 to 1375 degrees C. The surfaces of the as-sintered tapes were then observed using optical microscopy, at a magnification of 400x. Optical microscopy was found to be a useful technique because of the relatively large size of the grains and the large degree to which the grain boundaries are decorated by thermal etching. As can be seen in Figures 27, 28, and 29 this material exhibits a very short firing range. At 1325 °C. (Figure 27A) the material is undersintered and immature, and by 1375 °C. (Figure 29B) the microstructure is dominated by exaggerated grain growth. For the remainder of the study a firing temperature of 1365 °C. was chosen as a temperature at which the microstructure appears to be mature, but exaggerated grain growth is not observed.

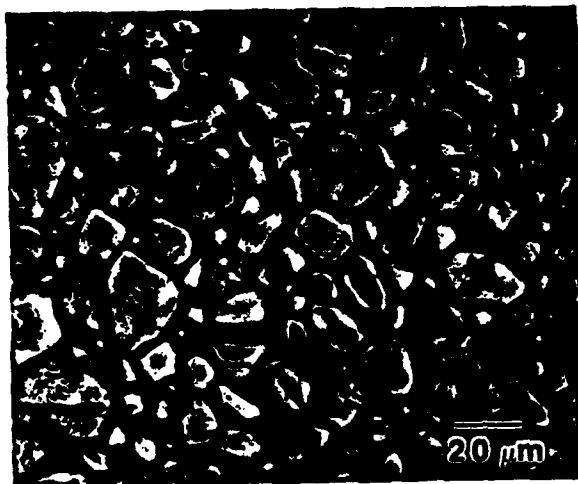


A. 1350°C

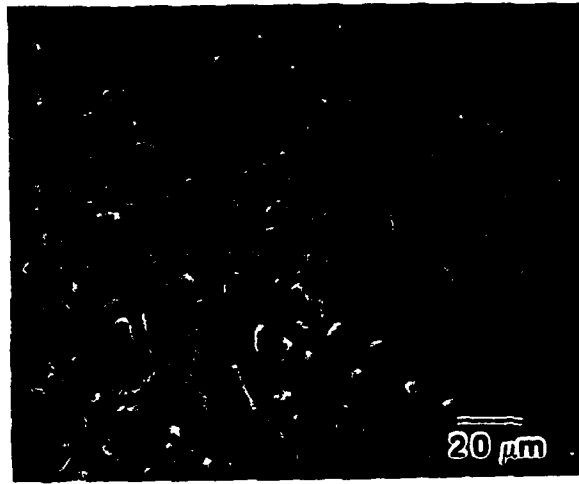


B. 1355 °C

Figure 27. Micrograph of as-sintered surface.

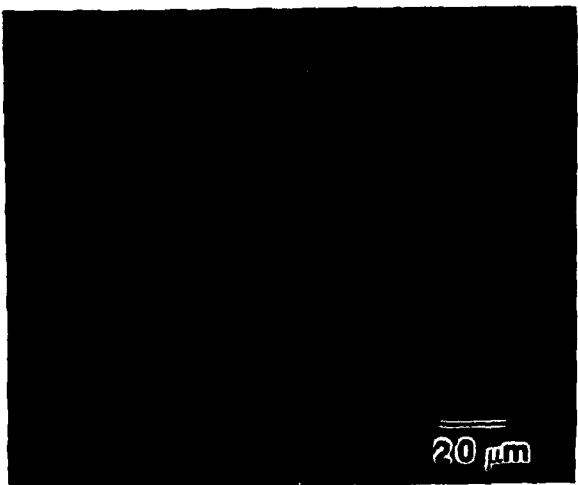


A. 1360 °C

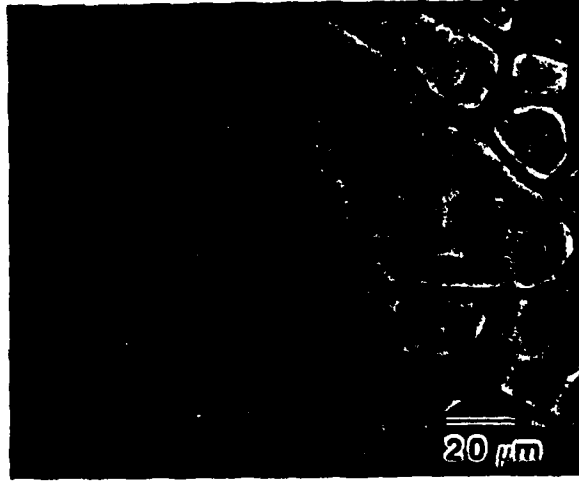


B. 1365 °C

Figure 28. Micrograph of as-sintered surface.



A. 1370 °C



B. 1375 °C

Figure 29. Micrograph of as-sinter surface.

g. Flatness

Flatness of the sintered tapes was evaluated in a semi-quantitative way by observing the camber of the biaxial flexure discs before breaking them, and rating the flatness on the scale from one to four. Flatness data for all three component addition sequences is plotted in Figure 30. In all cases the dispersant first tapes are the flattest, dispersant last tapes have intermediate values, and simultaneous addition tapes are the least flat. These results follow directly from the low shear rate viscosity data, and the density measurements. That is, tapes made from low viscosity slurries have more uniform packing, as evidenced by higher green density, and consequently less warpage during firing is observed. Figure 31 shows the flatness as measured by a profilometer on first day tapes. Results agree with the less quantitative results of Figure 31.

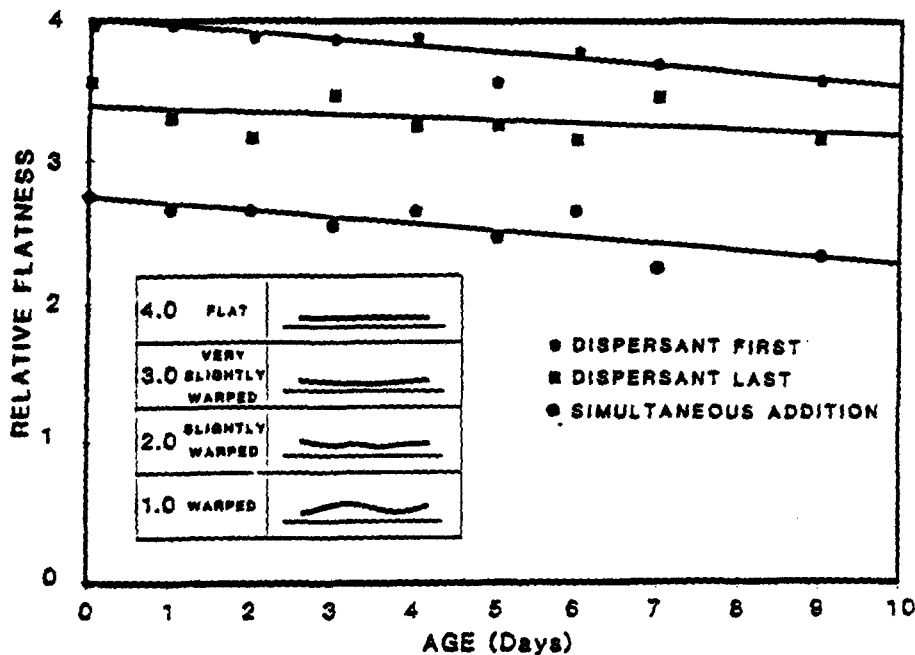


Figure 30. Flatness as a function of addition sequence and slip aging.

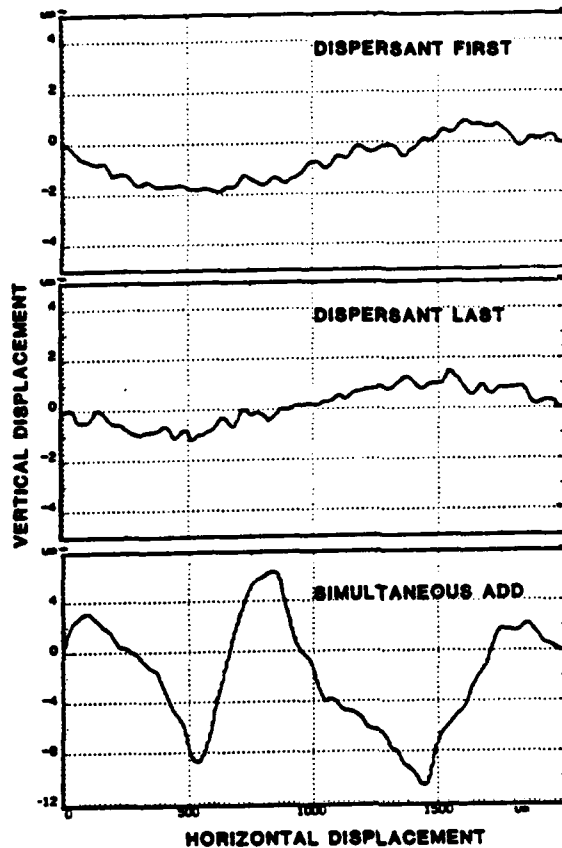


Figure 31. Surface profile as measured with a profilometer.

Another trend which can be seen in Figure 30, is a decrease in flatness with slurry aging time for tapes made by all component addition sequences. This behavior is not easily explained in terms of any of the other measurements made in this study, and is simply presented as an empirical observation.

h. Sinter Tape Strength

The strength of sintered tapes, as measured by biaxial flexure, is plotted in Figure 32. There appears to be very little difference between the three component addition sequences after the second day of the aging study, but there appears to be a significant difference in the first day. The simultaneous addition tapes are much weaker than either dispersant first or dispersant last tapes in this case. This is an important result because on the first day the affects of adding the components in different sequences should be most pronounced, and because most commercial tapes are made from unaged slurries. The low strength of the day one simultaneous addition tapes can be traced to large (100 to 200 micron) flaws which have been observed only in these tapes. Figure 33 shows these flaws in a SEM micrograph of the as sintered surface. The diameter of the flaws is sufficiently large that they appear to have resulted from binder agglomerates. This, however, may also be related to poor packing.

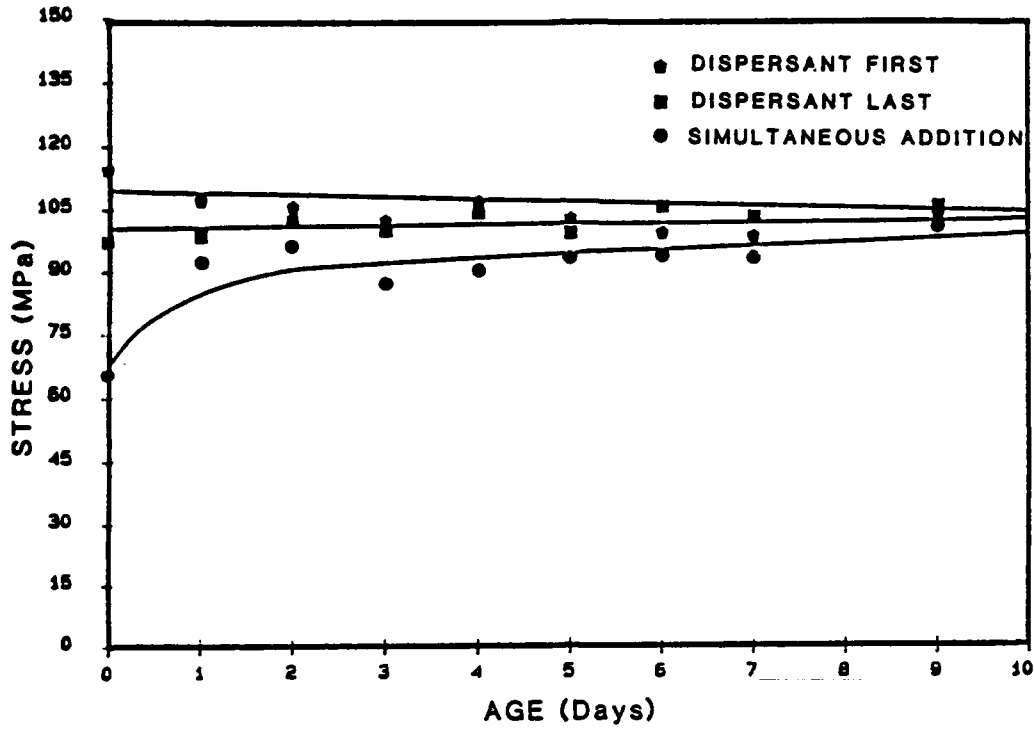


Figure 32. The biaxial flexure strength of sintered tapes as a function of addition sequence and aging time.

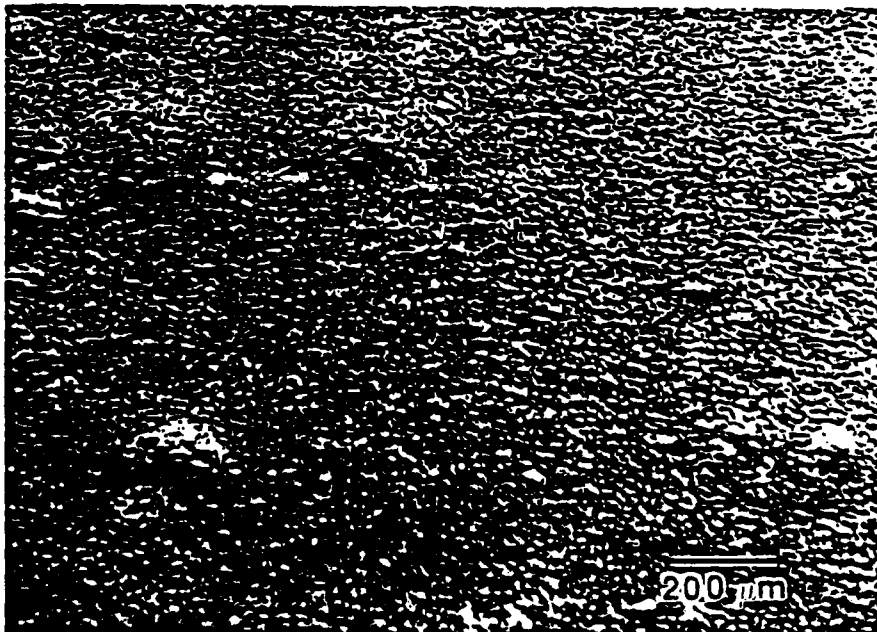


Figure 33. The surface of a sintered tape made from slips using the simultaneous addition sequence.

i. Electrical Properties

Dielectric constant and dielectric loss were measured over a large range of frequencies (1 khz to 10 Mhz). The early results indicated that dielectric constant varied with thickness. For tapes with thicknesses of 0.125 mm to 0.150 mm the dielectric constant is approximately 800 whereas thicker tapes made by multilaying the thinner tapes had a dielectric constant of 1600. These values are shown in Figure 34. Differences in the dielectric constants arise from their thickness differences but the standard deviation we feel depends on the addition sequence. On the few measurements made on the thicker samples this trend of higher standard deviation is reinforced. The standard deviation is higher when for the simultaneous addition sequence.

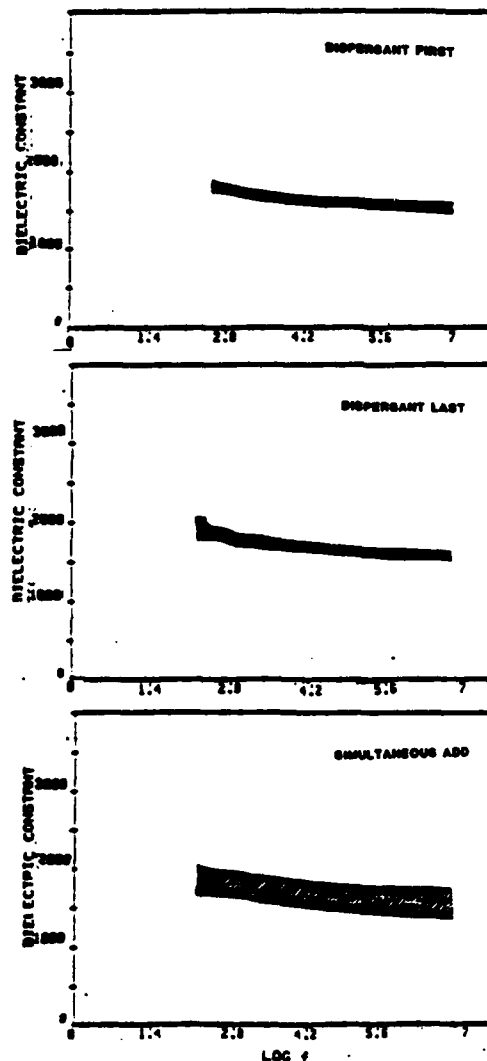


Figure 34. Dielectric constant as a function of frequency for tapes

2. Role of Components in Dispersing the powder.

a. Rheological properties of slips

A number of experiments were designed to determine the role each organic plays in the process of dispersion and why the order of addition is important. In this first set of experiments the shear stress shear rate properties of the slip were considered. By examining these results a better understanding of the floc structure of the slip can be obtained. The degree of shear thinning is related to the volume fraction of flocs in the slip [46] which break up by shearing. The Bingham yield a good measure of the strength of flocs. [46]

For these measurements the concentric cylinder viscometer was used. It is capable of accurate measurements at low shear rates. Using this more sensitive instrument, shear stress versus shear rate curves were run for day one slurries made by all three component addition sequences. The behavior of day one slurries is of interest because the greatest difference in viscosity occurs on the first day.

Figures 35, 36 and 37 plot this data for the dispersant first, dispersant last and simultaneous addition cases, respectively. From these curves, it is evident that the low shear rate rheological behavior is drastically different for the three cases. All curves, however, show a yield stress, below which no flow is observed, with some degree of shear thinning. Dispersant first and dispersant last slurries show little or no hysteresis, while simultaneous addition slurries exhibit marked hysteresis. This result appears to be indicative of flocculation in cast simultaneous addition tapes.

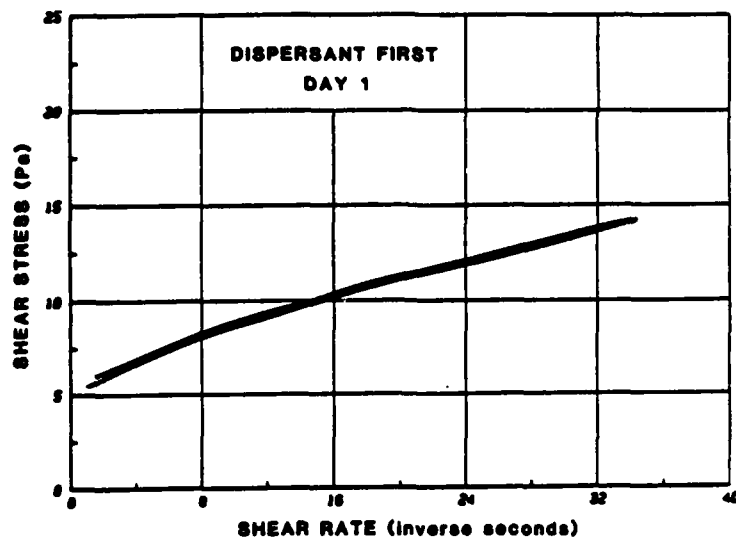


Figure 35. Viscosity versus shear rate for slurries prepared by adding dispersant first.

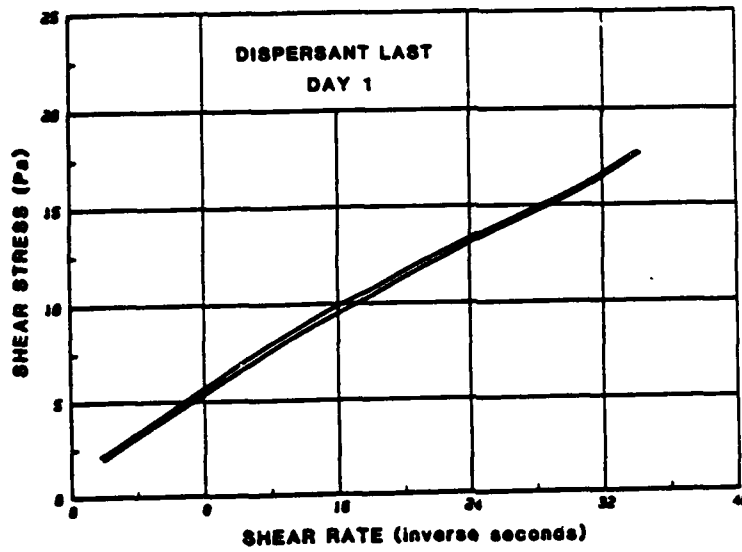


Figure 36. Viscosity versus shear rate for slurries prepared by adding the dispersant last.

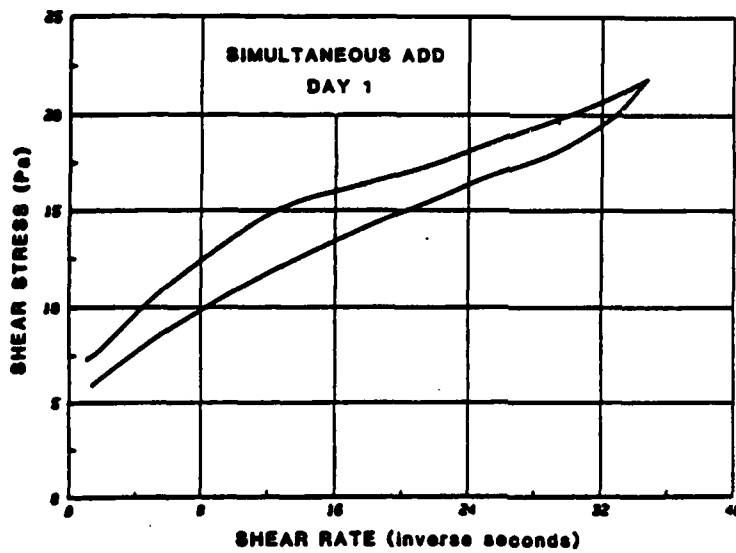


Figure 37. Viscosity versus shear rate for slurries prepared by simultaneous addition

To obtain a better understanding of these low shear rate curves, yield values and shear rate exponents were calculated. A least squares line through the initial portion of the shear stress versus shear rate curve was extrapolated to a shear rate of zero to determine the yield point. The data were then fit to the Ostwald equation:

$$\tau = kD^n + \tau_B$$

where τ = shear stress
 D = shear rate
 k = a constant
 n = the shear rate exponent
 τ_B = the Bingham yield stress.

A shear rate exponent of unity describes a Newtonian system. Shear thickening slurries exhibit higher values, and lower values indicate shear thinning behavior. The yield values and shear rate exponents are computed in Table X.

Table X. Yield Values and Shear Rate Exponents for Day One Slips

<u>ADDITION SEQUENCE</u>	<u>YIELD VALUE</u>	<u>SHEAR RATE EXPONENT</u>
Dispersant First	6.07 Pa	0.275
Dispersant Last	1.97 Pa	0.675
Simultaneous Add.	8.99 Pa	0.318

Dispersant first slips exhibit a high yield but little shear thinning characteristics. The small degree of shear thinning and the low viscosity are typical of well dispersed systems. The low shear rate exponent in this case means that there are a small volume fraction of flocs present. In the dispersant last case the yield value is very low, probably because of increased adsorption of the polymer binder on the surface which prevents particles from agglomerating the their primary minimum. On the other hand the shear rate exponent is quite high indicating a large volume fraction of flocs were initially present which break up during the test. In the simultaneous addition sequence the yield stress is particularly high and the shear rate exponent is still somewhat higher than the dispersant first case.

b. Sedimentation Study

In order to better understand the behavior of the slurries described above, a sedimentation study was undertaken. The observations from this study are listed in Table XI.

Simultaneous addition slurries settled rapidly (several days) resulting in a high sediment volume which was readily redispersible. The sediment cake was soft and loose with the resultant supernatant clear which is typical of flocculated suspensions.

Table XI. Sedimentation Study Observations

	<u>DISPERSANT</u> <u>FIRST</u>	<u>DISPERSANT</u> <u>LAST</u>	<u>SIMULTANEOUS</u> <u>ADDITION</u>
SEDIMENTATION RATE	moderate	slow	rapid
SEDIMENT VOLUME	low	low	high
SEDIMENT CAKE	hard	moderate	soft
REDISPERSIBILITY	difficult	yes	yes
SUPERNATANT	slightly cloudy	cloudy	clear

Dispersant first slurries settle at an intermediate rate (one to two weeks) forming a hard dense sediment which required ultrasonic agitation to redisperse which is typical of well dispersed systems. The slightly cloudy supernatant indicates that there were very fine well dispersed particles which did not settle. Softer cakes and more rapid settling is an indication of a large volume of flocs.

c. Phosphate Ester Adsorption

A first approach to understanding the effect of order of addition sequence is to assume the first species to be introduced to the slip to adsorb on the surface of the powder. Any subsequent additives could only adsorb on the surface if they could either crowd onto the surface or if the first component would desorb from the surface allowing the second component to adsorb on the surface. To better understand the adsorption and desorption from the surface, the surface concentration of phosphate ester as a function of aging time was measured for the three order of addition sequences.

The results of this study are plotted for the three addition sequences in Figure 38. In the dispersant first case the level of phosphate ester adsorption is highest on the initial day of the study, and decreases with aging time until a constant value is reached after three days. The surface concentration decrease with time indicates strong competition for adsorption sites between the dispersant and one of the other components. The leveling off to a constant value represents an equilibrium or steady state condition where adsorption and desorption rates are equal.

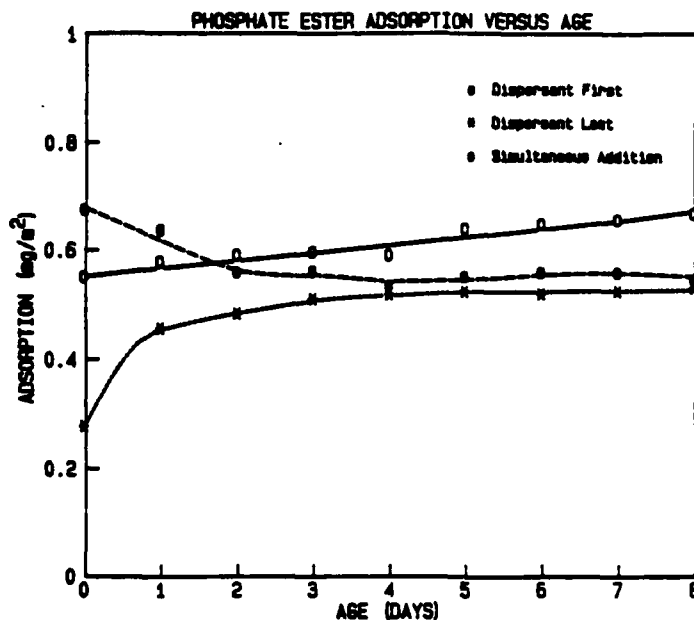


Figure 38. Phosphate ester adsorption versus slurry aging time.

In the dispersant last case, the adsorption behavior is just the opposite of the dispersant first case. Initially a small quantity of phosphate ester is adsorbed, and the amount adsorbed increases with slurry aging time. After approximately four days, an equilibrium surface concentration is reached, the value of which is only slightly less than that in the dispersant first case. These results correlate somewhat with the high shear rate viscosity measurements in Figure 23. This may mean that at high shear rates it is the adsorbed phosphate ester which control the amount of agglomeration. These results, however, do not explain the rheological properties at low shear rates or other properties of the cast tape which vary with order of addition sequence and aging time. Furthermore, if the phosphate ester is an electrostatic stabilizer and the charge on the particles is positive then increased adsorption of the phosphate ester on the surface as we have proposed only decreases the positive zeta potential not increases it. Thus increased adsorption of phosphate ester on the surface should not decrease the viscosity. In order to understand this more thoroughly electrophoresis measurements were made on the tape casting slurry as a function of order of addition.

d. Electrophoretic Mobility

Electrophoretic mobility was measured for supernatants of day one slips prepared by all three component addition sequences. For comparison, a dispersion of solvent, powder and dispersant in the same ratios was also evaluated. Figure 39 shows the zeta potentials calculated from the electrophoretic mobility measurements using the Hukel relation (Equation 1).

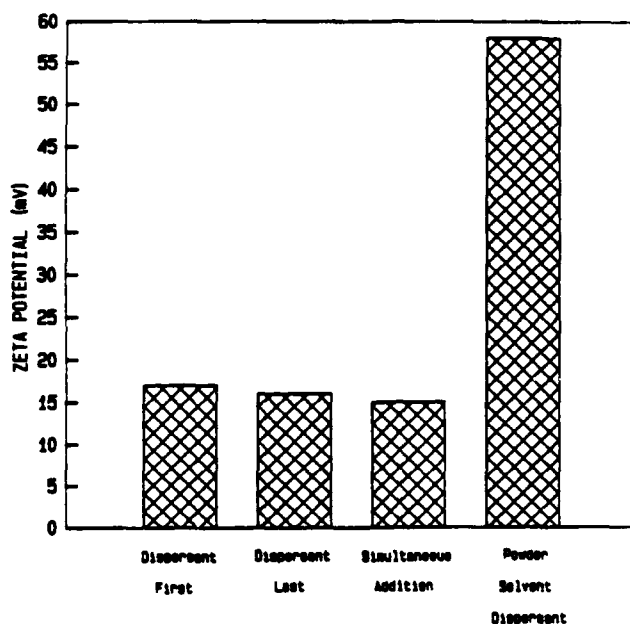


Figure 39. Zeta potential for particles in slips made by all component addition sequences and in the powder-solvent-dispersant systems.

Zeta potential was much lower for the supernatants than for the powder-solvent-dispersant system. This result, however, is likely related to the shifting of the shear plane further out into the double layer as a result of polymer (binder) adsorbing onto the surface. Using the Debye-Huckel equation to estimate the potential profile, shifting the shear plane to about 43 Å should decrease the zeta potential by about a factor of two. This would also decrease the difference in zeta potentials between the powders prepared by different order of addition sequences. The results, however, indicate that zeta potential increase is in the same order as the viscosity increase. Sufficient number of measurements were made to determine the results to be statistically significant.

e. Reaction Between Components of the Tape

To investigate the possibility of a chemical reaction which affects the structure of the acrylic binder, thin films of binder with and without phosphate ester additions were prepared. MEK/ethanol was used as a solvent and acrylic:solvent and acrylic:solvent:phosphate ester ratios were the same as for the tape casting slurry. Figure 40 shows FTIR spectra of an acrylic film, and an acrylic plus phosphate ester film from which the phosphate ester was spectrally subtracted. Any appreciable difference in the spectra would be due to chemical reaction with the phosphate ester. The spectra are clearly very similar, hence there is no spectroscopic indication of permanent structural changes resulting from any proposed chemical interaction in solution.

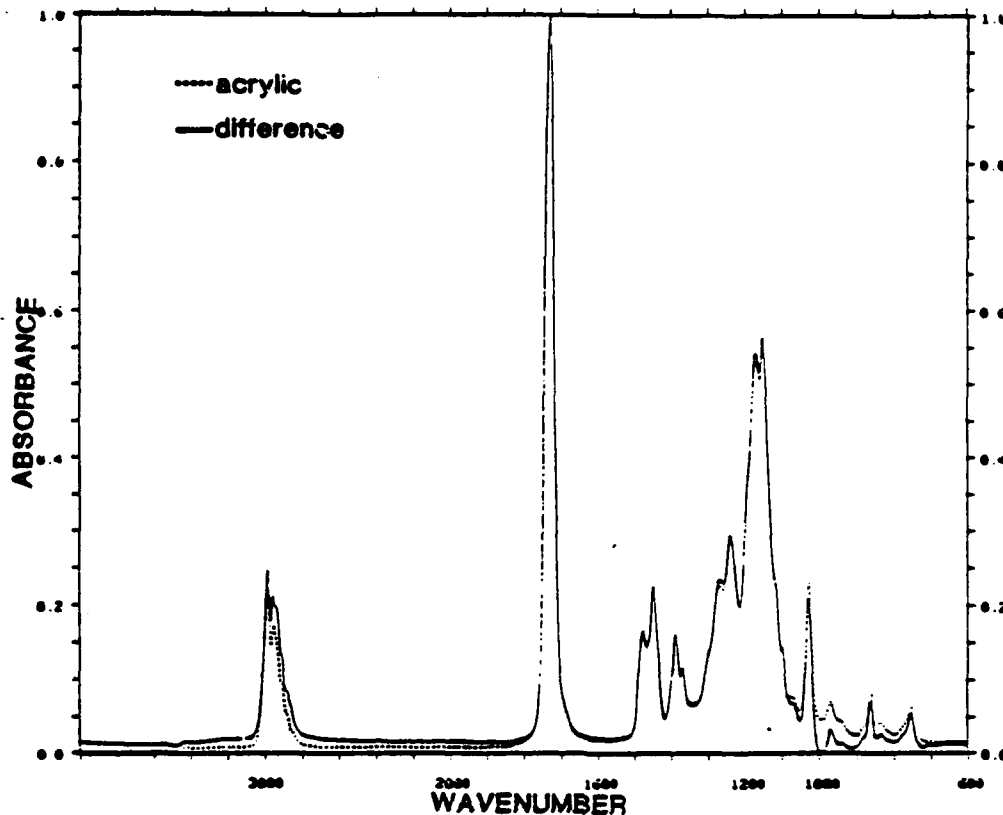


Figure 40. FTIR spectra of cast Acryloid B7-MEK films.

The above result, however, does not rule out a reaction in solution which could greatly affect dispersion properties. To investigate the existence and nature of such a reaction FTIR spectra were obtained for acrylic and acrylic plus phosphate ester solutions in MEK/ethanol. Ratios of components were the same as found in the tape casting composition. Solvents were spectrally subtracted from acrylic and acrylic plus phosphate ester spectra. Subtracting the spectrum of (phosphate ester in MEK/ethanol) - (MEK/ethanol) from the acrylic plus phosphate ester spectrum resulted in a spectrum which could be compared directly to that of the acrylic solution. As Figure 41 shows, there are appreciable differences in the spectra. These include an 8 wavenumber shift of the carbonyl (C=O) band and intensity changes in the C-O stretching region. Therefore in summary, there are spectral indications of a chemical reaction which affects the carbon oxygen bonding of the acrylic binder in solution, but these changes do not apparently carry over to the solid state.

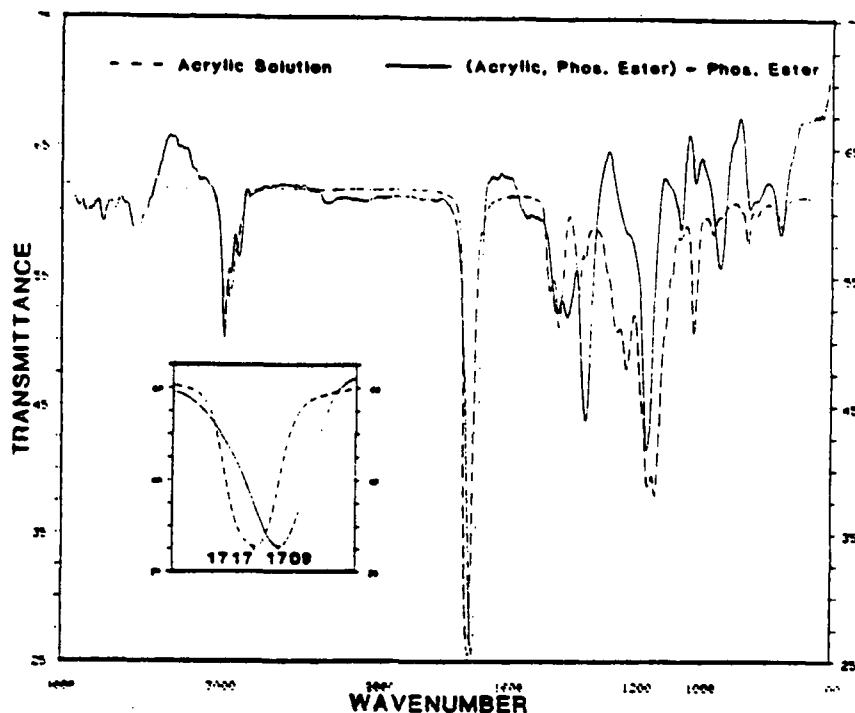


Figure 41. FTIR spectra of Acryloid B7-MEK solutions.

f. Assessment of Dispersibility of Individual Components.

Results in the previous two sections do not clearly establish a mechanism for the order of addition effect. In order to further attempt to understand the effect and also to determine the role of other components besides the dispersant and binder, relative viscosity measurements were made of the slips adding one component at a time as described earlier. In the current study slurries were prepared by adding the desired partial slip composition subjecting it to an ultrasonic probe and measuring viscosity. In a separate experiment the viscosity for the same composition without the powder was measured using a Cannon-Fenske viscometer. Although more properly the viscosity of the supernatant should be measured, the amount adsorbed on the powder was small and did not affect the viscosity of the solution significantly. The results are tabulated again in Table XII.

Table XII. Viscosity of the Solution, Viscosity of the Slip and Relative Viscosity for Several Partial Slip Compositions.

<u>COMPONENTS</u>	<u>VISCOSITY (Cp)</u>		<u>RELATIVE</u>
	<u>SOLUTION</u> <u>VISCOSITY</u>	<u>TOTAL</u> <u>SLIP</u>	<u>VISCOSITY</u>
SDP	0.64	314.9	492.0
SDP, B	27.0	4316.9	159.9
SDP, B, Sa	28.2	2956.8	104.8
SDP, B, Sa, C	31.5	4908.3	155.8
SDP, B, Sa, C, H	30.3	4387.4	144.8
SBP	28.2	14192.8	503.3
SBP, Sa	28.0	13897.2	496.3
SBP, Sa, C	33.0	17149.7	519.7
SBP, Sa, C, H	30.4	12714.4	418.2
SBP, Sa, C, H, D	30.0	5322.3	177.4
SBP	28.2	14192.8	503.3
SBP, D	28.8	6431.1	223.3
SBP, D, Sa	28.2	4730.9	167.7
SBP, D, Sa, C	33.6	5617.9	167.7
SBP, D, Sa, C, H	31.5	4853.0	145.5

KEY: S=MEK/ethanol solvent, P=barium titanate powder, Sa=butyl benzyl phthalate (Santicizer 160), C=polyethylene glycol 400 (Carbowax 400), H=cyclohexanone homogenizer, B=acrylic binder.

In all three sequences adding the acrylic binder greatly increases the overall viscosity, but lowers the relative viscosity, indicating that the binder has a beneficial effect on the suspension stability. The two plasticizers had opposite effects on rheology. Butyl benzyl phthalate decreased both overall viscosity and relative viscosity, while polyethylene glycol 400 increased both. Cyclohexanone decreased both suspension viscosity and relative viscosity.

In order to see more clearly how each component effected the relative viscosity independent of order of addition, the factor by which the last added component changed the relative viscosity when it was added to the slip, ie. the incremental increase (decrease) from one value to the one directly below it in Table XII divided by the relative viscosity of that component. The result is shown in Figure 42 for the three sequences. In this figure a positive value means that that component increased the relative viscosity and a negative value that it decreased the relative viscosity. Each line represents a different sequence of addition. The results indicate that each component has a similar effect on the viscosity independent of order of addition. According to Figure 42 the dispersant and binder have the strongest effect in lowering the relative viscosity of the slip. The other components have little effect, though the PEG slightly raises the relative viscosity in one case.

ORDER OF ADDITION

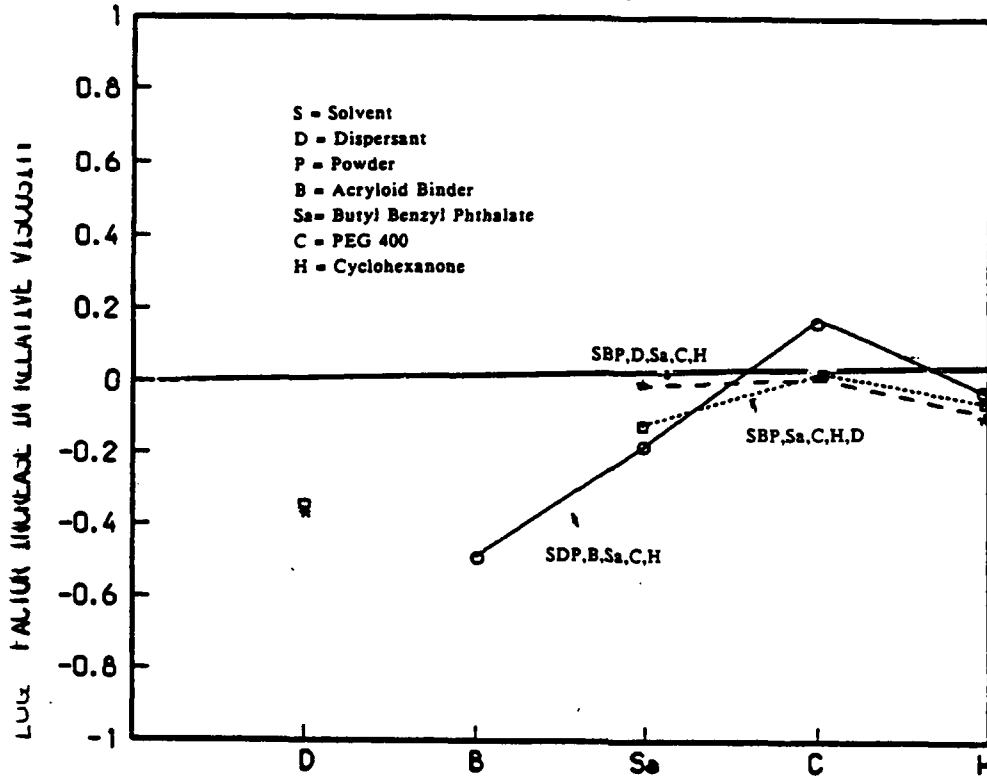


Figure 42. Relative Viscosity Increase for Components. Results are taken from Table XII. The factor increase in relative viscosity as a result of addition of component shown on the abscissa.

None of the above sequences are comparable to the simultaneous addition sequence of the earlier set of experiments which resulted in the most agglomerated slips. In order to determine the component interaction which raised the relative viscosity in the simultaneous sequence, this sequences was investigated in the same manner as those above. In this case each component was added as before, one at a time. Before the powder was added to the partial composition and the rheological measurements were made, the slip was allowed to age one day. Table XIII contains the resulting values.

Table XIII. Viscosity and Relative Viscosity Values Using the Simultaneous Addition Sequence. Before adding powder the solution was aged 24 hours. An old bottle of PEG was used. See Key of Table XII.

COMPONENTS	VISCOSITY (Cp)		RELATIVE VISCOSITY
	FLUID COMPONENTS	TOTAL SUSPENSION	
SD,P	.64	11241±1.96	175.64
SDB,P	28.64±.06	1350.63±212.70	47.16
SDBSa,P	34.03±.49	809.05±36.18	23.77
SDBSaC,P	33.43±.43	1429.17±7.40	42.75
SDBSaCH,P	33.53±.02	1258.77±179.77	37.54

An unexpected result was obtained in Table XIII. The relative viscosity of the simultaneous addition slip after all components were added was lower than for the other sequences shown in Table XII. It was concluded that this resulted from a more careful preparation of these slips using a slightly different procedure in which care was taken to exclude water. Thus it was decided that water greatly affects the results and so another experiment was performed in which the care in avoiding water contamination was studied.

Two series of experiments were performed. A new bottle of PEG was purchased for these sequences. In both series the powder was dried 24 hours and cooled in a desiccator to room temperature, then immediately sealed in a bottle. In the first series a large batch of solvent was prepared and allowed to be exposed to air for 2 hours. This is termed the wet series. In the second series fresh solvent was taken daily from a sealed bottle for each experiment. This was termed the dry series. The results are shown in Table XIV. The increase in relative viscosity is shown in Figure 43 for these two series, along with the one described immediately above. Since the dispersant was always added before other organic components, no data point is associated with the dispersant.

Table XIV. Viscosity and Relative Viscosity Values Using the Simultaneous Addition Sequence, using a new bottle of PEG. Dry: Solvent was taken from a new sealed bottle for each experiment, Wet: Solvent was exposed to the air for 2 hours to allow it to absorb moisture.

<u>COMPONENTS</u>	<u>VISCOSITY (Cp)</u>		<u>RELATIVE VISCOSITY</u>
	<u>FLUID COMPONENTS</u>	<u>TOTAL SUSPENSION</u>	
<u>DRY</u>			
SDBSaC, P	29.6±1.1	999.0±73.2	33.75
SDBSaCH, P	34.4±.9	721.3±59.4	20.97
<u>WET</u>			
SDBSaC, P	35.7±1.6	2070.1±141.8	80.55
SDBSaCH, P	33.8±.5	1872.9±260.5	55.41

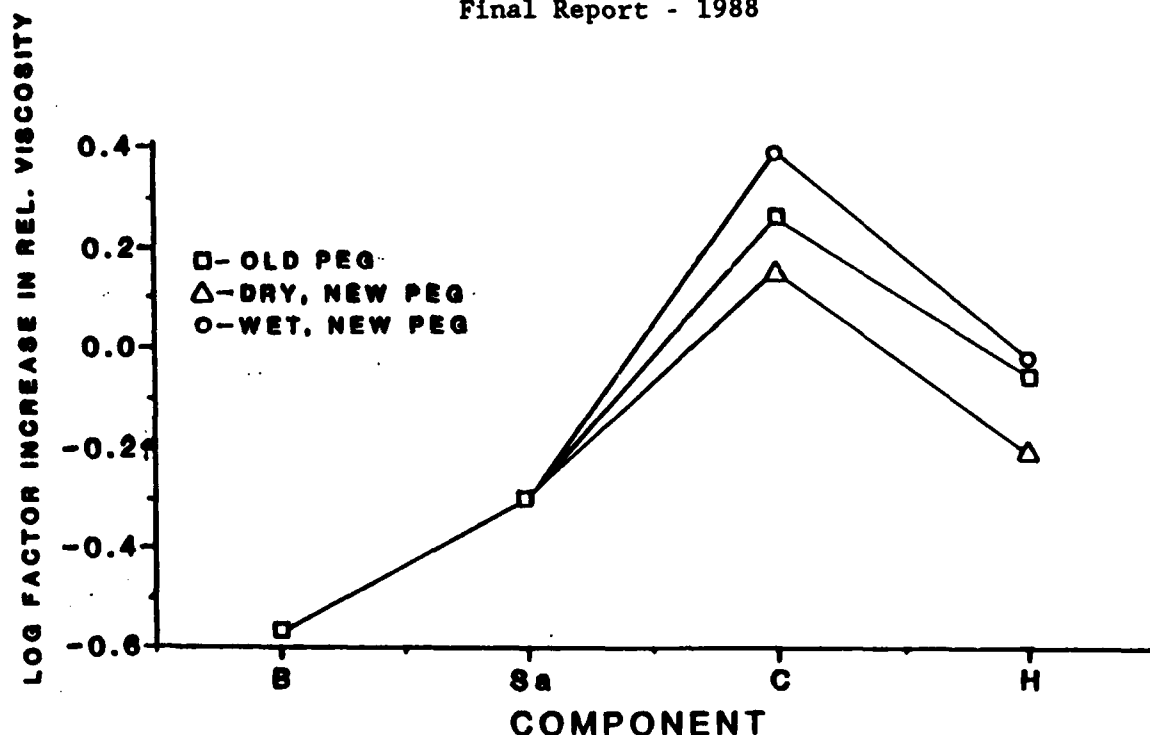


Figure 43. Relative Viscosity Increase for Components. Results taken from Tables XIII and XIV.

Figure 43 shows that the PEG is especially effected by the presence of water. Increased amounts of water in the solvent or in the PEG tends to flocculate the slip. Also water in the solvent has an adverse effect on the slip with the binder. Moreover, water in the PEG affected the way the cyclohexanone changed the relative viscosity. Of the components added PEG is the most hydroscopic. Acrylic binder is also somewhat hydroscopic. This observation we believe will help to understand the roll of water. Furthermore, elimination of these hydroscopic components from the slip may make the slip less susceptible to moisture.

g. The roll of water in the slip and the order of addition Sequence

As a result of the above observations, a model is presented for the roll of water in the slip and how it interacts with the phosphate ester. It was stated earlier that the phosphate ester does not ionize to any appreciable extent as it is introduced into the solvent but when it comes in contact with the polar surfaces of the powder it easily ionizes charging the powder positively. It is proposed that if water of hydration is present around one of the other components of the slip then the phosphate ester may ionize at this site without coming to the surface of the powder. Thus it is not effective in charging the powder particle. One piece of evidence for this is that the zeta potential is smaller in the "hydrated" suspension than in the "dry" suspension. The charge is still positive but the positive zeta potential is decreased. In the extreme of an aqueous suspension in which the phosphate ester completely ionizes before coming to the surface of the powder the charge on the surface is dominated by the anionic phosphate ester and the zeta potential is negative.

It is proposed that the order of addition sequence is related to the above model. If all the organic components are added simultaneously and allowed to age for 24 hours prior to adding the powder, the phosphate ester will undergo considerable ionization as it is in contact with the water. Thus when the powder is finally added, it is unable to charge the particle so fully. This result is confirmed in Figure 39 which shows a smaller zeta potential for the simultaneous addition sequence. When the dispersant is added first it may immediately come to the surface of the particle charging it. If it is added last, it may only slowly come to the surface but during the first 24 hours a considerable amount of the phosphate ester reaches the surface and ionizes. This accounts for the decrease in viscosity during the first 24 hours.

A second observation is that the relative viscosities of the slips are very low when made under dry conditions, even when mixed in the simultaneous addition sequence. This may indicate that the order of addition affect is only present when water is present in the slip. We have attempted to measure the order of addition affect again when only very careful drying conditions were used but have not found consistent results. Under dry conditions very small amounts of water affect the results more. Future studies may include carefully controlled and measured water additions.

Finally PEG may be eliminated or replaced in the slip in order to avoid water contamination.

h. Electrical Conductivity

To determine if any other component ionizes to an appreciable extent, and thus can affect the electrical double-layer, electrical conductivity of solutions containing the other organic components were measured.

Figure 44 plots electrical conductivity versus volume percent addition of the acrylic binder and both plasticizers. As can be seen, all components increase conductivity slightly from the 0.74 micromho/cm value for the MEK/ethanol solvent. However, the increase in all cases is quite small when one considers that one percent phosphate ester results in a conductivity of 8.0 micromho/cm. The highest conductivity is associated with the PEG. This high conductivity is probably associated with water of hydration. From these plots, it is apparent that these components do not ionize to an appreciable extent, making their contribution to electrostatic repulsion minor.

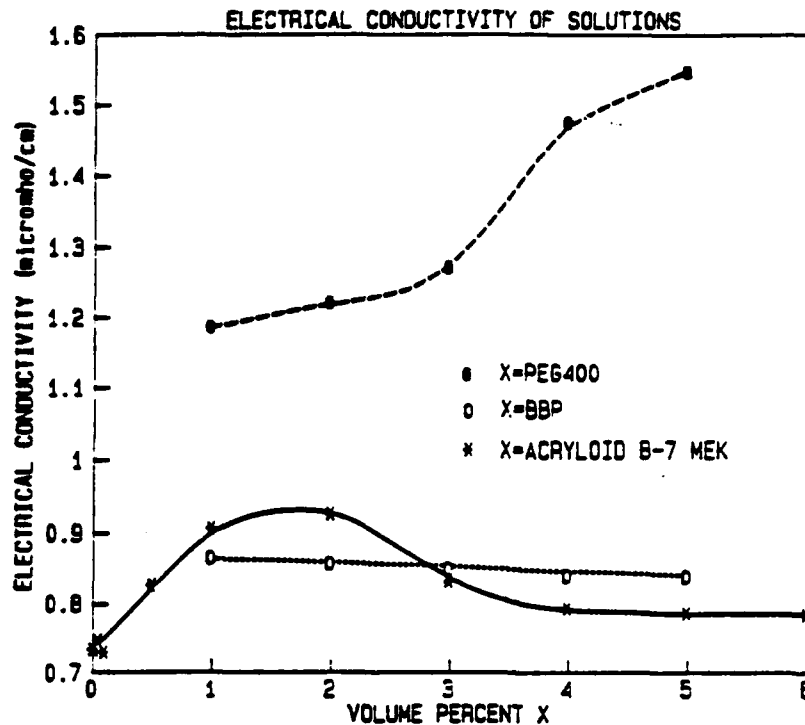


Figure 44. Electrical conductivity of solutions.

E. Casting Behavior and Tensile Strength of Cast BaTiO₃ Tape.

The fabrication of multilayer capacitors or any multilayer ceramic requires a certain degree of green strength in the tape during the process of removing the tapes from the carrier substrate, punching, and the stacking process. Green tensile strength is also an indicator of green tape homogeneity as indicated by the results of Figure 26. Green strength and brittleness of the tape is controlled by binders and plasticizers and particle size and packing.[47] Early studies were conducted to determine the effects of loading rates, drying mode and drying time, on the green tensile strength of barium titanate tape cast tapes[48]. Based on these results the present study was undertaken to determine the effects of each organic component in the slip on the green tape properties. In addition to strength, the viscosity of the slips, the green density and strain to failure were measured.[49]

1. Experimental

Slurry preparation and testing procedures have been described previously. Briefly, the dispersant was added to the solvent followed by the powder. In order to avoid contamination by moisture, powder was kept in a desiccator between use and solvent bottles were sealed between use. The system was subjected to ultrasonic probe agitation for two minutes in order that particles would be separated and weak agglomerates would be broken. This slurry was aged for thirty minutes in order to allow adsorption and stabilization of the dispersant. The remainder of the organic system was added, binder, plasticizers, homogenizer, hand stirring after each addition. The slurry was mechanically stirred for thirty minutes and then forced through a -400 mesh screen in order to remove dried binder and break large agglomerates which may have formed during the addition of the organics. Slips were subsequently deaired over vacuum. Viscosity measurements were made on the concentric cylindrical viscometer. The tapes were cast on smooth glass plates and cut into the standard dog bone shape for tensile testing. In the latter studies two standard loading rates were used, 0.01 sec^{-1} and 0.0005 sec^{-1} . Ten specimens were tested under each condition. sec^{-1} . All tapes were approximately $175 \mu\text{m}$ thick.

Since ceramic forming operations often results in directionally different mechanical properties, the ultimate tensile strength of sample cut longitudinal and transverse to the casting direction was determined. Their respective strengths were $.156 \pm 0.0025 \text{ MPa}$ (22.7 psi) and $.155 \pm 0.0033 \text{ MPa}$ (22.5 psi). indicating no significant directional properties. The standard deviations were on the order of only 2 per cent of the ultimate tensile strength, a very low value. These initial experiments were performed at $.05 \text{ sec}^{-1}$.

2. The effect of the drying method on the strength

The effect of the drying method on the strength of the green tapes was determined on the standard slip composition and is shown in Figure 45. If the tapes were allowed to dry on the glass, the ultimate strength decreased continually with increasing drying time whereas if they were removed from the glass their ultimate strength increased with increasing drying time. In all cases where they were removed from the glass they were allowed to dry first for 1 hour to give them sufficient strength. The decrease in strength when they were allowed to dry on the glass likely arises from the strong bond between the glass and the tape. As the tape dries the top surface of the tape is allowed to shrink but the bottom surface is not and the resulting tensile stresses on the top surface allow cracks to form during drying.

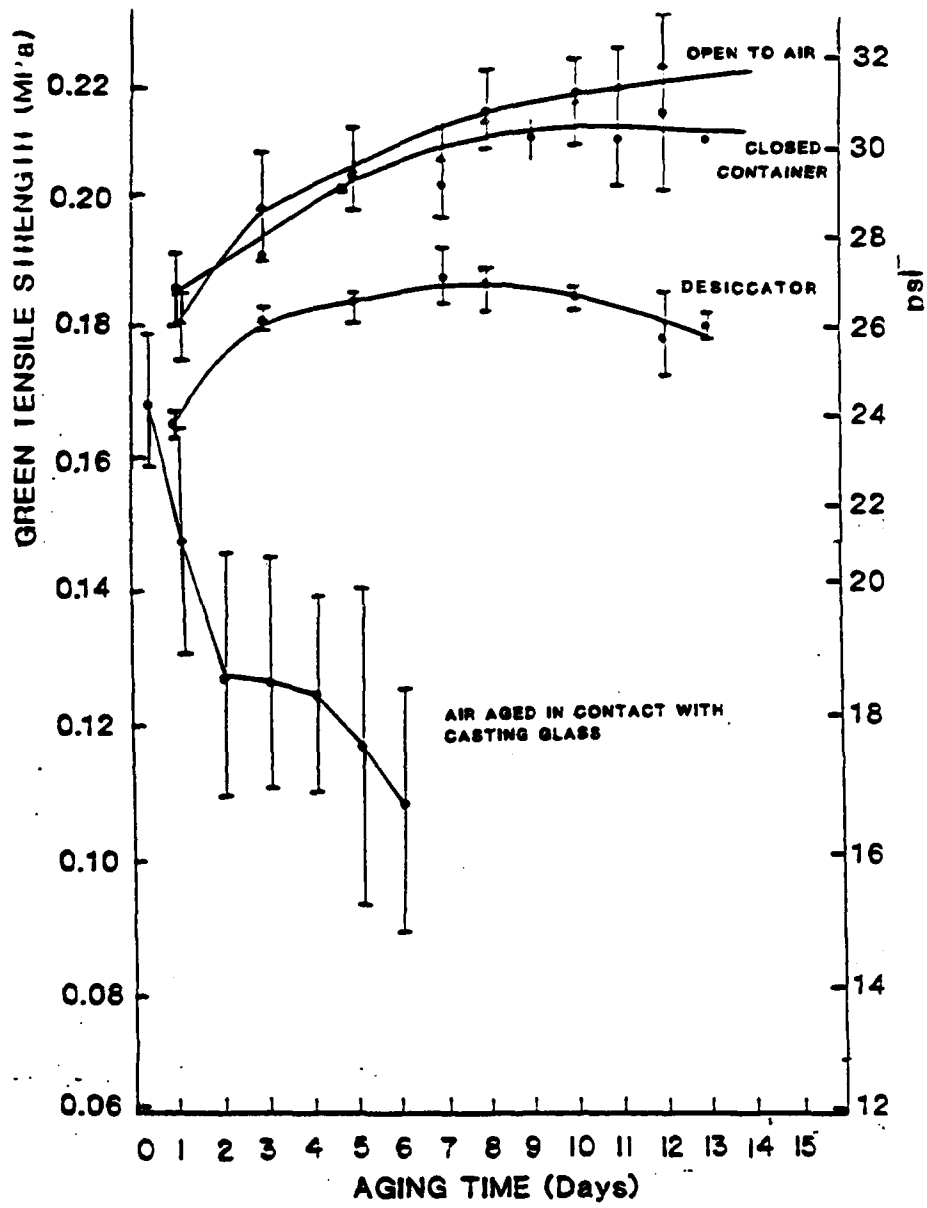
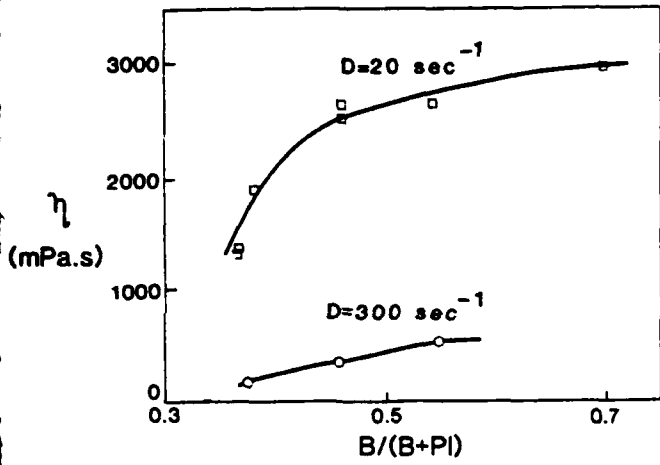


Figure 45. The ultimate tensile strength of green tapes dried under various conditions. The three upper curve relate to tapes which were removed from the glass plate after 1 hour and dried under various conditions.

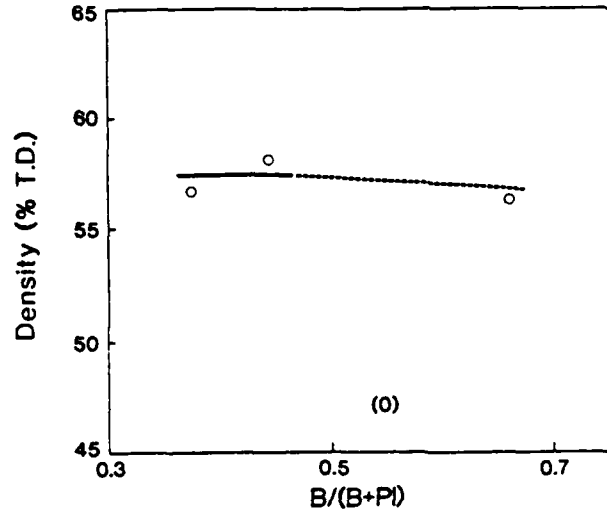
Three different drying conditions were compared on tapes removed from the glass plate 1 hour after casting. In all cases the strength of the cast tapes increased with increasing drying time and the standard deviation was smaller than for tapes dried on the glass plate. Strength of tapes dried in open air increased the fastest with drying time, probably because the solvent is most rapidly eliminated from these samples and the presence of residual solvent lowers the strength. Specimens dried in a closed container were nearly as strong as those dried in open air but the slower solvent removal resulted in lower strengths. The strength of specimens dried in a desiccator containing calcium sulfate, which presumably only removed the water from the atmosphere, increased more slowly and reached a lower maximum strength. It was first proposed that the water acts as a plasticizer and allows a larger ultimate tensile strength to be reached but the width of the stress strain curve is no different than the other samples and so this explanation was abandon. There result is, therefore, not yet explained.

3. Effects of binder to plasticizer ratio.

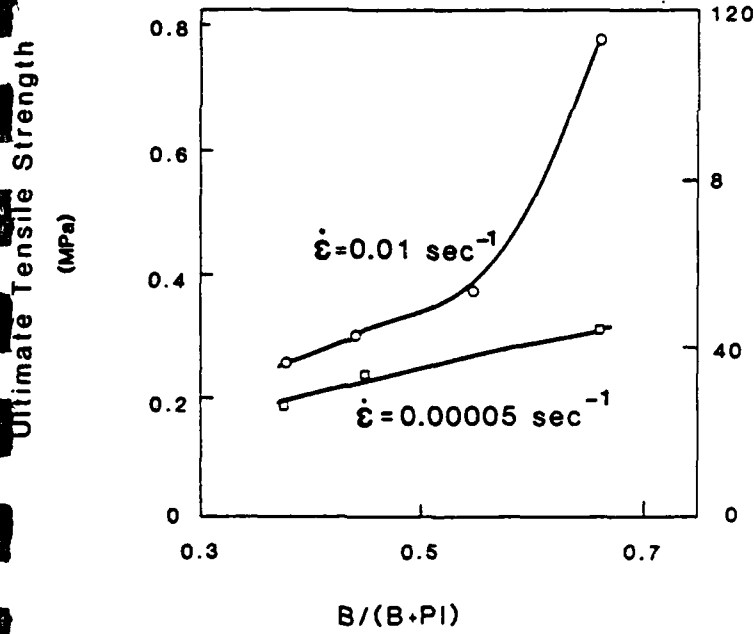
Composition of the slip was varied in several ways to understand the role of the components. An increase in binder to plasticizer ratio resulted in an increase in slurry viscosity, at high and low shear rates, as shown in Figure 46a, little change in powder packing density as shown in Figure 46b, and a large increase in ultimate tensile strength as shown in Figure 46c. The increase in slurry viscosity is expected since the binder is a long chain polymer, whereas the plasticizers are low molecular weight (M.W. 300 to 400). The viscosity versus shear rate curves also show shear thinning, increasing with increasing binder content. As the amount of binder increases the ultimate tensile strength increases sharply. This is in agreement with previous results[47] and is expected based on the differences in molecular weight between the binder and plasticizer.



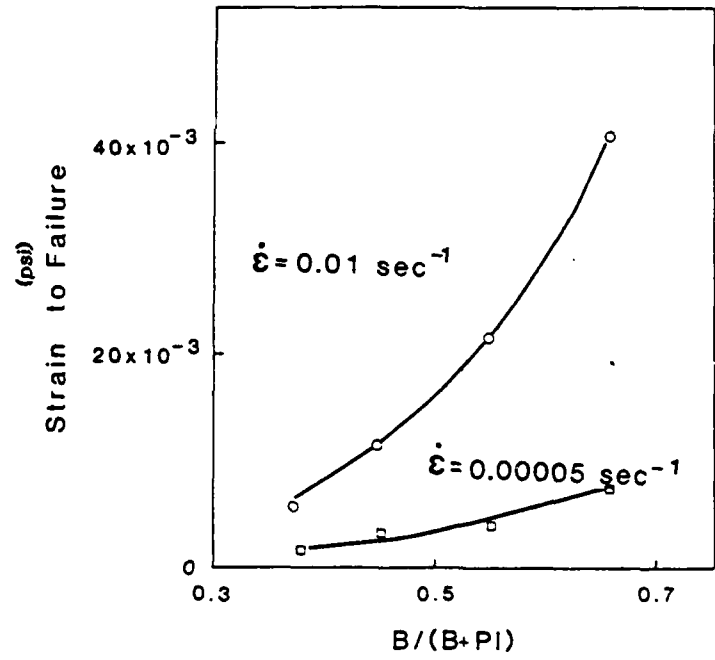
(a)



(b)



(c)



(d)

Figure 46. Effect of the binder to plasticizer ratio on the: (a) viscosity at 10 sec^{-1} and 300 sec^{-1} shear rate, (b) green density, (c) ultimate tensile strength, and (d) strain to failure. The total binder + plasticizer content was kept constant.

Unexpected results were obtained in studying strain to failure versus binder to plasticizer ratio. It is expected that as the amount of plasticizer is increased, the tape would be more flexible and hence strain to failure would increase. The opposite effect has occurred as indicated in Fig. 46d. As binder to plasticizer ratio is increased, the strain to failure increased in the same manner as the ultimate tensile strength. There are two possible explanations for this occurrence. The first is that more than the optimum amount of plasticizer was used. The second is that the plasticizer is not acting as a true plasticizer. A true plasticizer would act in one or both of the following ways: It could break primary bonds forming copolymer with the resin or it could change the conformational state of the polymer. Infrared spectroscopic studies in our laboratory confirm the plasticizer acts in neither of these two ways. The plasticizer, however, is necessary as a release agent, since without it the tape are difficult to remove from the glass substrate without tearing.

4. Effect of each plasticizer

The ratio of the two plasticizers were varied while the total plasticizer content was maintained constant. Increasing the PEG (M.W. 400) at the expense of the butyl benzyl phthalate (BBP) (M.W. 312) gradually increased the viscosity as expected. The most important effect of the plasticizers composition was evident in the properties of the green tape. The green tape containing no PEG was soft and fragile and stuck to the glass plate. In fact, for $\text{PEG}/(\text{BBP}+\text{PEG}) < 0.25$ the tape could not be removed from the glass plate without tearing. By increasing the PEG content tapes became harder and were easily stripped from the glass. Tensile strength measurements could not be made at low PEG content but above $\text{PEG}/(\text{BBP}+\text{PEG}) = 0.50$ the ultimate tensile strength rises rapidly, indicating that PEG is important to the strength of the tapes. The strain to failure passes through a maximum at $\text{PEG}/(\text{BBP} + \text{PEG}) = 0.75$. and thus some BBP causes the tape to be less brittle and so acts as a plasticizer. Results are shown in Figure 47.

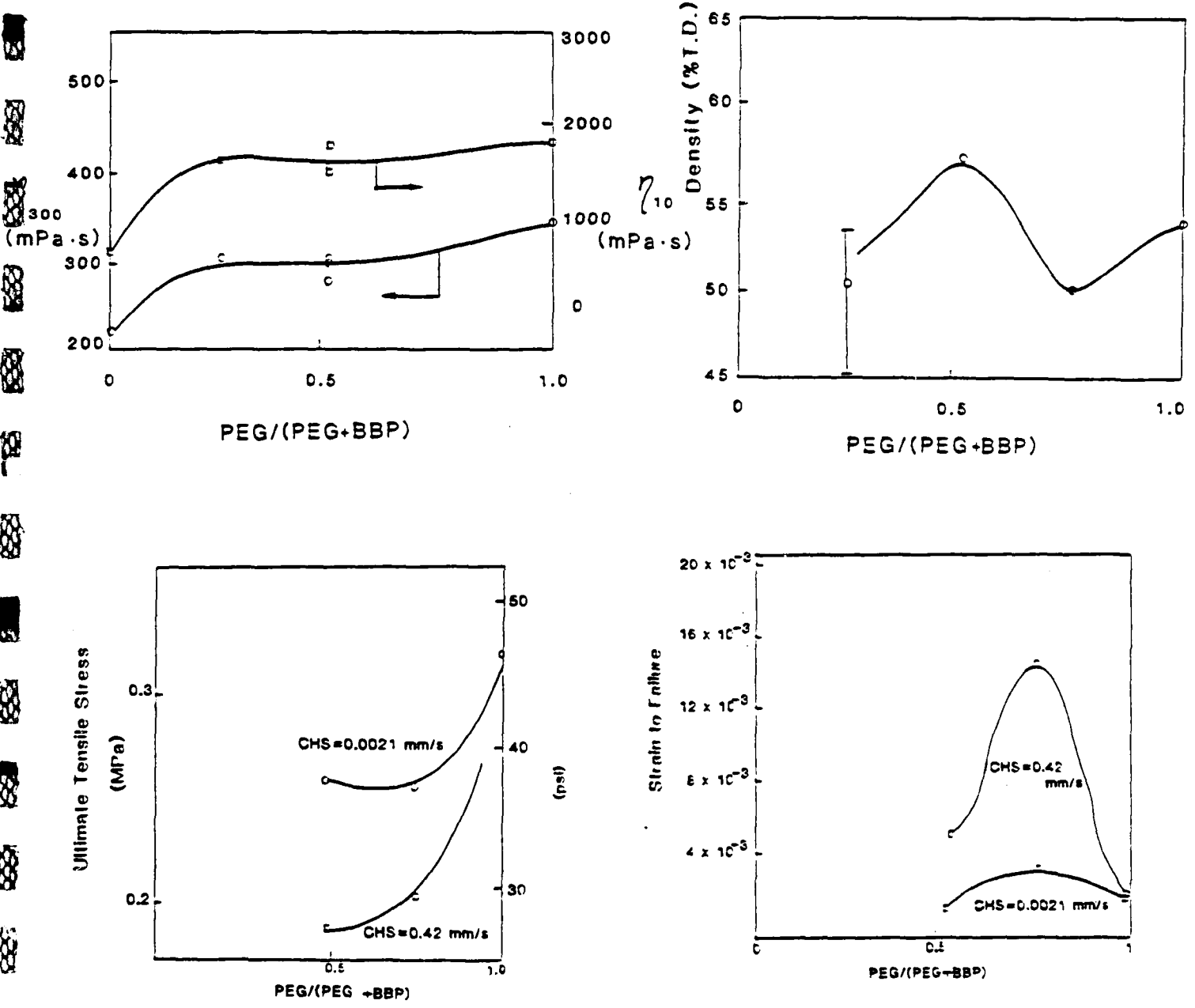
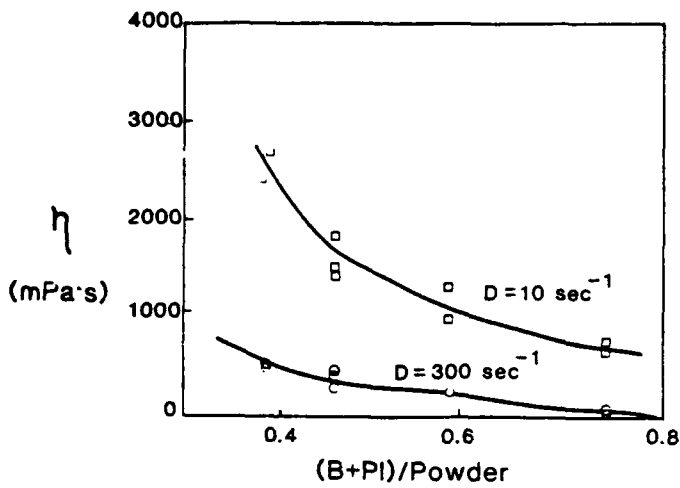


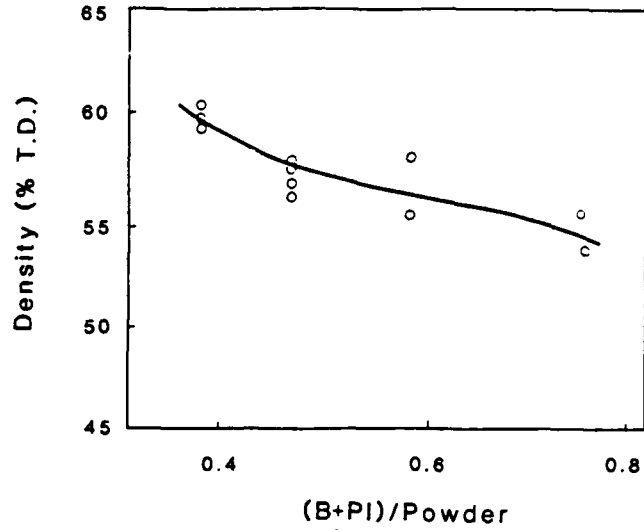
Figure 47. The ratio PEG/Butylbenzyl Phthalate is varied and the following properties measured: (1) slip viscosity, (2) tape green density, (3) ultimate tensile strength and (3) strain to failure.

5. Effects of binder + plasticizer concentration.

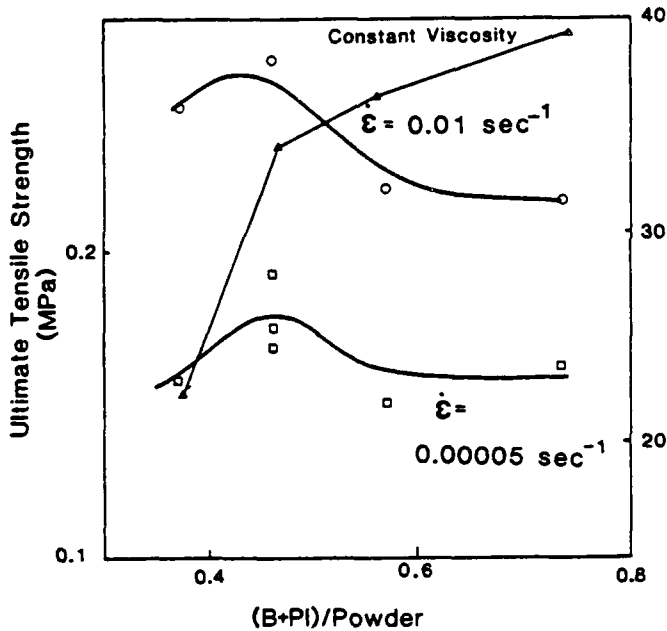
In this series of experiments (binder + plasticizer) powder to ratio was varied keeping the binder to plasticizer ratio constant. Since powder was added at the expense of (binder + plasticizer), this is approximately equivalent to changing the powder loading of the slip. Increasing the (binder + plasticizer) content resulted in a decrease in viscosity, Figure 48a. It also resulted in a decrease in density, Figure 48b, and an increase in strain to failure, Figure 48d. However, the ultimate tensile strength passed through a maximum Figure 48c. It was anticipated that the strength would continue to increase with increasing binder content but as the binder content increased, the tape thickness decreased due to the decrease in powder loading. The thinner tapes tear easier when removing them from the glass and so evidently flaws were produced in the tape when it is removed from the glass, lowering the measured strength. To better test the effect of binder concentration, tapes were prepared with the same thickness by adjusting the viscosity of the slip by adding or subtracting solvent to maintain a constant viscosity slip. This resulted in an almost constant tape thickness independent of powder loading. In this case the ultimate tensile strength increased steadily and did not pass through a maximum. The curve is shown in Figure 48c. For each pair of points of the two curves the composition of the tape is identical prior to testing since any additional solvent evaporates out of the tape. It is primarily with the low viscosity tapes where the ultimate tensile strength differs considerably.



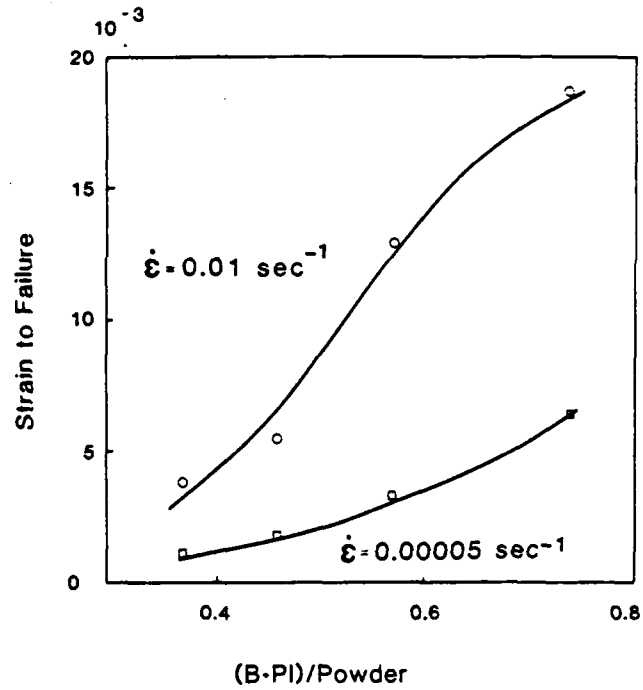
(a)



(b)



(c)



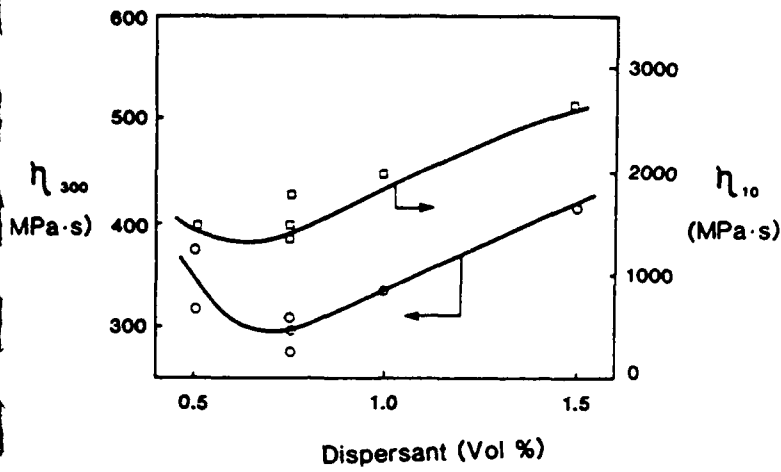
(d)

Figure 48. Effect of binder + plasticizer content on the: (a) viscosity at 10 sec^{-1} and 300 sec^{-1} shear rate, (b) green density, (c) ultimate tensile strength, and (d) strain to failure. The solvent, binder, plasticizer, homogenizer and dispersant concentration were kept constant while the powder content was varied. In (c) "constant viscosity" the solvent content was varied to maintain a constant viscosity independent of binder + plasticizer content.

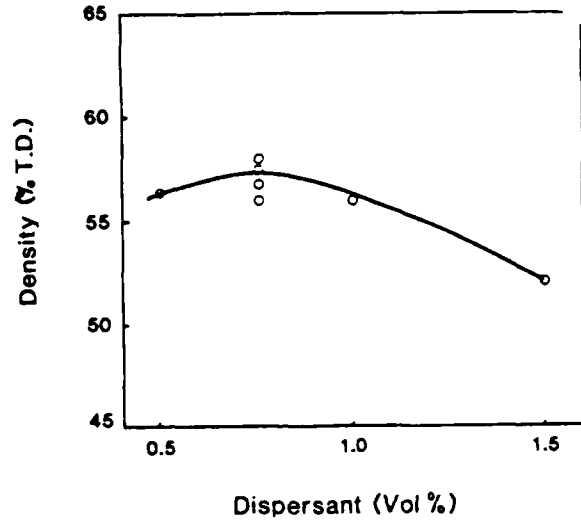
6. Effects of dispersant Content

In this series of experiments the total amount of solvent and dispersant were held constant but the dispersant content was increased at the expense of the solvent.

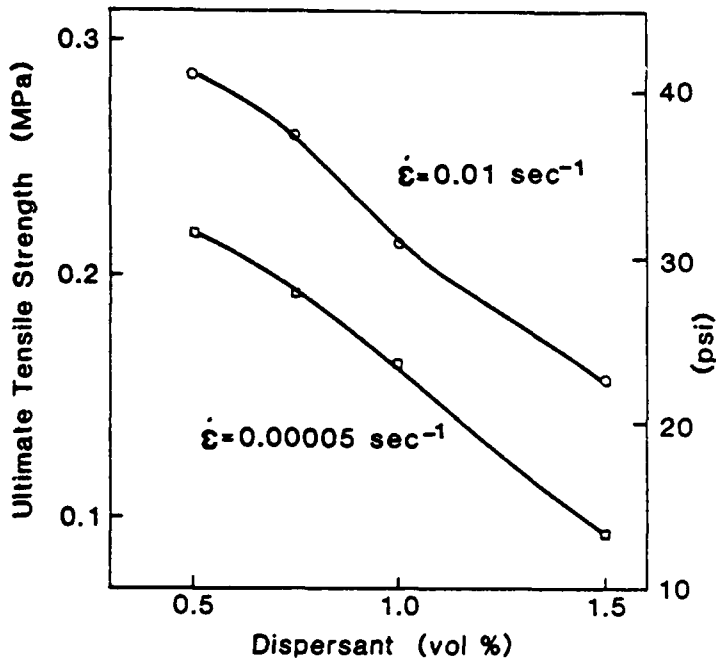
Viscosity data show a minimum at the concentration of 0.75 vol% phosphate ester dispersant as shown in Figure 49a which is in agreement with earlier results. The density of the tapes passes through a maximum at the same dispersant concentration as shown in Figure 49b. On the other hand strength and strain to failure curves shown in Figures 49c and 49d, respectively, did not pass through a maximum or a minimum but decreased continually as the dispersant concentration was increased. It is surprising that the strength and strain to failure also do not maximize as the density maximizes. This suggests that the dispersant weakens the cohesive strength of the binder possibly by preventing the binder from attaching to the particle surface or by reacting with the binder itself.



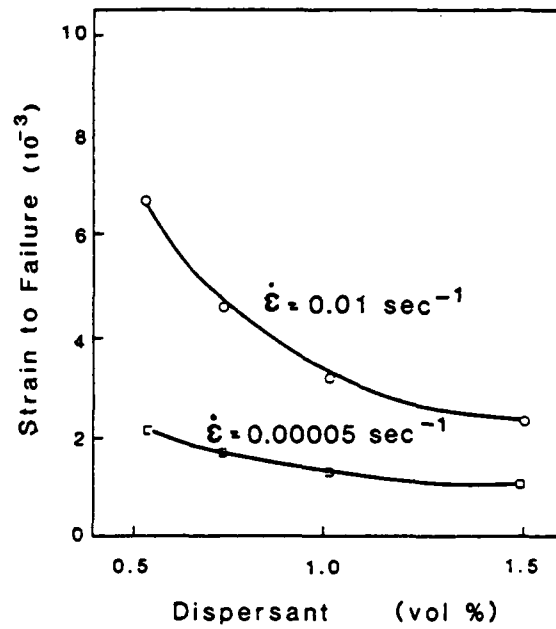
(a)



(b)



(c)

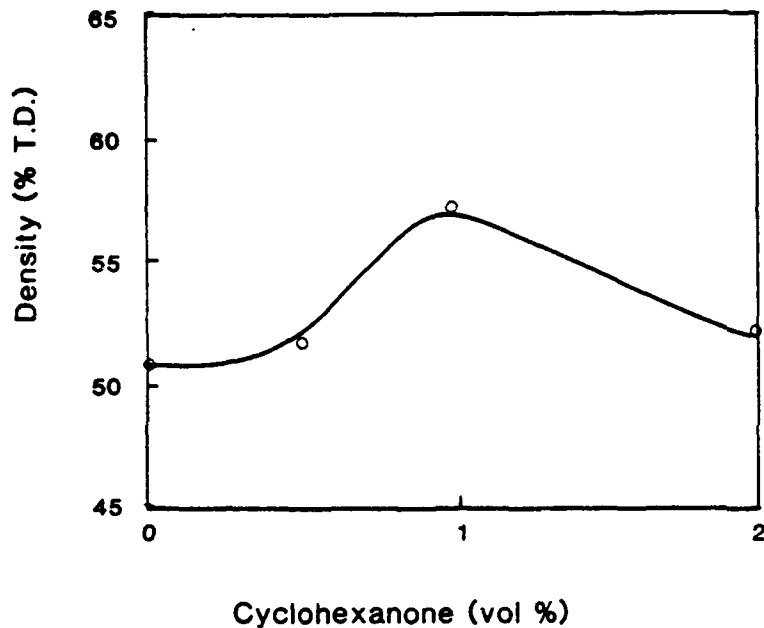


(d)

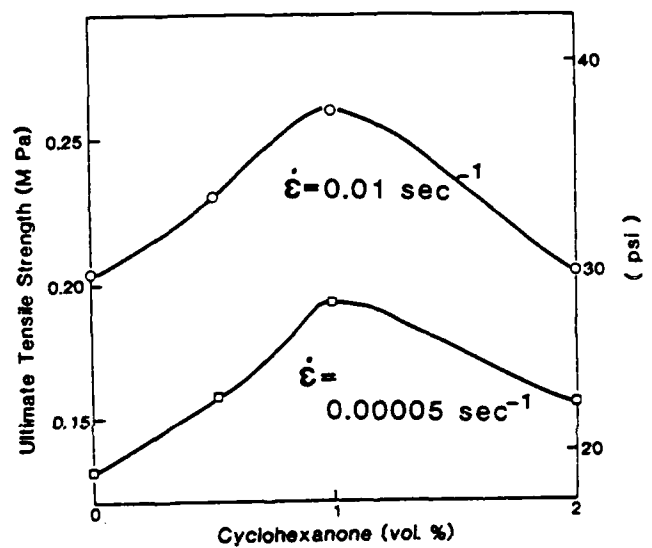
Figure 49. Effect of dispersant concentration on the: (a) viscosity at 10 sec^{-1} and 300 sec^{-1} shear rate, (b) green density, (c) ultimate tensile strength, and (d) strain to failure.

7. Effect of homogenizer content

In this series of experiments the cyclohexanone content was varied as properties were measured. As seen in Figures 50a and 50b it also affect density and strength. Density and ultimate tensile strength pass through a maximum at 1 vol% homogenizer. Viscosity and strain to failure are affected much less. They are approximately constant within experimental error.



(a)



(b)

Figure 50. Effect of homogenizer content on the: (a) green density, and (b) ultimate tensile strength.

CONCLUSION

A typical nonaqueous tape casting system based on a commercial acrylic binder was studied to understand the system in more depth. The following conclusions were drawn:

(1) The best surfactants for dispersing barium titanate in the MEK-ethanol solvent system among those tested was found to be phosphate esters.

(2) The phosphate ester was found to impart a high ζ -potential to the particles and to greatly increase the conductivity of the solution so that a double layer could form. The maximum ζ -potential coincided with the minimum viscosity in two separate studies, varying the phosphate ester concentration and varying the solvent concentration, and so it was concluded that electrostatic stabilization controlled the dispersing properties.

(3) Evidence from conductivity measurements indicated that the phosphate ester adsorbed on the $BaTiO_3$ powder surface prior to ionization in the solution, as suggested by Fowkes.

(4) The sign of the ζ -potential in MEK-ethanol was positive and in water was negative with the addition of the phosphate ester. Impurity water the MEK-ethanol was found to lower the ζ -potential and as a result lead to an unfavorable dispersion.

(5) The state of dispersion of a slip (as measured by relative viscosity) containing the acrylic binder, two plasticizers, the phosphate ester and cyclohexanone was found to be better than that of the solvent, powder and phosphate ester. The only component which adversely affected the relative viscosity was the PEG plasticizer and then especially when water was carried in as an impurity. (Explained on page 1473) →

(6) The order of addition of the organic components strongly affected both the viscosity of the slip and the aging characteristics of the slip. The simultaneous addition of all organics with the solvent and subsequent aging before the powder was added resulted in markedly higher viscosities for the slip. These green density of the tapes, the green tensile strength, the fired density and tensile strength, the surface flatness and the distribution in dielectric strengths could all be correlated to the order of addition and its affect on the rheology.

(7) It was proposed that the order of addition affect was related to the presence of water in the slip which made the phosphate ester less effective in imparting a potential to the powder.

(8) A study of the ratio of plasticizers PEG to butyl benzyl phthalate indicated that the PEG is necessary to give the tape good release from the glass and also more strength but about 25% butyl benzyl phthalate (of the plasticizer) is necessary to decrease the brittleness of the tape.

(9) Decreasing powder content decreases viscosity of the slip as expected but strength passes through a maximum at 35% powder loading. The maximum strength was believed to be related to the thickness of the tape. At constant viscosity strength increases monotonically with increasing binder content.

(10) There is an optimum value of dispersant which gives minimum viscosity and a maximum density. Increasing dispersant beyond this degrades binding action and causes green strength and strain to failure to steadily decrease.

(11) Optimum homogenizer produces a maximum density and strength of tapes at a minimum viscosity.

References

1. R. E. Mistler, D. J. Shanefield and R. B. Runk, "Tape Casting of Ceramics," in Ceramic Processing Before Firing. Edited by G. Y. Onoda and L. L. Hench. Wiley & Sons, New York, 1978.
2. J. C. Williams, "Doctor Blade Process," in Ceramic Fabrication Processes, Edited by Franklin F. Y. Wang, Academic Press, New York, 1976.
3. H. D. Kaiser, F. J. Pakulsi and A. F. Schmeckenbecher, "A Fabrication Technique for Multilayer Ceramic Modules," Solid State Technol., 15[5] 35-40 (May 1972).
4. Y. N. Sun, W. K. Shih, G. W. Scheiffele, M. D. Sacks and J. W. Williams, "Thermal Degradation Mechanisms of Poly(Vinyl Butyral) Binders," to be published in Advances in Ceramics.
5. Y. N. Sun, M. D. Sacks and J. W. Williams, "Pyrolysis Behavior of Poly(methyl Methacrylate), to be published in Advances in Ceramics.
6. E. West, Ceramic Processing Systems, Private Communications.
7. A. Karas, T. Kumagai and W. Roger Cannon, "Casting Behavior and Tensile Strength of Cast BaTiO₃ Tapes as the Organic Composition is Varied," to be published in the Bull. Amer. Ceram. Soc.
8. R. A. Gardner, "High Alumina Content Compositions Containing BaO, MgO, SiO₂ and Sintered Ceramic Articles Made Therefrom," US Patent 3935017 (Jan. 27, 1976).
9. H. R. Usala, "Solvent-Based MLC Binder Studies," Presented at the Annual Meeting of the Amer Ceram Soc., May 1986, Chicago, Ill.
10. F. M. Fowkes, "Donor-Acceptor Interactions at Interfaces," J. Adhesion, 4 155-59 (1972).
11. G.N. Howatt, "Method of Producing High Dielectric High Insulation Ceramic Plates," U.S. Pat. 2,582,993 (1952).
12. G.N. Howatt, R.G. Breckenridge, and J.M. Bronlow, "Fabrication of Thin Ceramic Sheets for Capacitors," Amer. Ceram. Soc., Bull. 30, 237-242 (1947).
13. J.L. Park, "Manufacture of Ceramics," U.S. Pat. 2,966,719 (1961).
14. J.J. Thompson, "Forming Thin Ceramics," Amer. Ceram. Soc., Bull. 42, 480-481 (1963).
15. D.S. Paulley and D.L. Lockwood, "Method for Manufacturing Ceramic Substrates for Electrical Circuits," U.S. Pat. 3,324,212 (1967).
16. M. Bennett, W.K. Boyd, and J.C. Nobile, "Fabrication of Multilayer Ceramic, Microelectronic Structures," U.S. Pat. 3,518,756 (1970).
17. D.J. Shanefield and R.E. Mistler, "The Manufacture of Fine-Grained Alumina Substrates for Thin Films," West. Elec. Eng. 15, 26-31 (1971).

Final Report - 1988

18. D.J. Shanefield and R.E. Mistler, "Fine Grained Alumina Substrates: I, the Manufacturing Process," Amer. Ceram. Soc., Bull. 53, 416-420 (1974).
19. H.W. Stetson and W.J. Gyurk, "Use of Menhaden Oil to Deflocculate Dry Ground Alumina in Manufacture of Substrates," U.S. Pat. 3,780,150 (1973).
20. H.W. Stetson and W.J. Gyurk, "Alumina Substrates," U.S. Pat, 3,698,923 (1972).
21. K. R. Mikeska and W. R. Cannon, "dispersants for Tape Casting Pure Barium Titanate"; pp. 164-83 in Advances in Ceramics. The American Ceramic Society, Columbus, Ohio, 1985.
22. R.E. Mistler, private communication.
23. J.F. Argyle, G.O. Medowski, D.W. Ports, and R.D. Sutch, "Fine-Grain Alumina Bodies," U.S. Pat. 3,819,785 (1974).
24. J.P. Callahan and R.A. Stark, "Apparatus for Producing Ceramic Chip Electrical Components," U.S. Pat. 3,538,571 (1970).
25. H. R. Usala, Personal Communications.
26. P. H. Wiersema, A. L. Loeb, and J. Th. Overbeek, J. Colloid Interface Sci., 22 (1966) 78-99.
27. W. O. O'Brien and L. R. White, J. Chem, Soc., Faraday Trans II, 74 (1978) 1607-1629.
28. J. B. Wachtman, W. Capps, and J. Mandel, "Biaxial Flexure Tests of Ceramic Substrates," J. Mater., 7 [2] 188-94 (1972).
29. ICI Americas Inc. Technical Bulletin.
30. Personal communications with Robert F. Conley.
31. S. K. Friedman, Witco Corp., Organics Div., Paterson, N.J., private communication, 1986.
32. R. Morrison and R. Boyd, Organic Chemistry, 3rd ed., Allyn and Bacon, Inc., Boston, 1973.
33. F. A. Cotton and G. Wilkinson, Advanced Inorganic Chemistry, 4th ed., John Wiley and Sons, Inc., 1980, 474-480.
34. J. Emsley and D. Hall, The Chemistry of Phosphorus, John Wiley and Sons, Inc., N.Y., 1976.
35. G. D. Parfitt and J. Peacock, "Stability of Colloidal Dispersions in Nonaqueous Media", in Surface and Colloid Sci., Vol. 10, E. Matejevic, Ed., Plenum Press, 1978.

36. J. J. Kipling, Adsorption from Solutions of Non-Electrolytes, Academic Press Inc., N.Y., 1965.
37. A. Kitahara, "Nonaqueous Systems," Electrical Phenomena - Fundamental Measurements and Application, Surfactant Science Series, 15, ?
38. F. M. Fowkes, H. Jinnai, M.A. Mostafa, F.W. Anderson, and R.J. Moore, "Mechanism of Electric Charging of Particles in Nonaqueous Liquids", ASC Symposium Series, No. 200, Colloids and Surfaces in Reprographic Technology, M. Hair and M.D. Croucher, Ed. 1982.
39. P. Somasundaran and D. W. Fuerstenau, J. Phys. Chem., 70 (1966) 90.
40. T. Sato, R. Ruch, Stabilization of Colloidal Dispersions by Polymer Adsorption, Marcel Dekker, 1980.
41. F. R. Eirich, "Structure of Macromolecules at Liquid-Solid Interfaces", in Chemistry and Physics of Interfaces, Sidney Ross, Ed., Am. Chem. Soc., Washington, DC, 1963.
42. F. R. Eirich, "The Conformational States of Macromolecules Adsorbed at Solid-Liquid Interfaces", J. Coll. Int. Sci., 58, 1977, 423-436.
43. P. J. Flory, "The Components of Real Polymer Chain", J. Chem. Phys., 17, 1949, 303-310.
44. T. C. Patton, Paint Flow and Pigment Dispersion, John Wiley and Sons, NY, 1964.
45. N. D. P. Smith, S. E. Orchard, A. J. Rhind-Tutt, "The Physics of Brushmarks", J. Oil Colour Chem. Assn., 44, 1961, 618.
46. B. A. Firth and R J. Hunter, "Flow Properties of Coagulated Colloidal Suspensions," J. Coll. Interface Sci., 57 [2] 248-56 (1976).
47. R. A. Gardner and R. W. Nufer, "Properties of Multilayer Ceramic Green Sheets," Solid State Technology, [3] 38-43 (1974).
48. S. Forte, J. R. Morris, and W. R. Cannon, "Strength of Tape Casting Tapes," Bull. Amer. Ceram. Soc., 64 [5] 724 (1985).
49. A. Karas, T. Kumagai, and W. R. Cannon, "Casting Behavior and Tensile Strength of Cast BaTiO₃ Tape as the Organic Composition is Varied," to be published in Bull. Amer. Ceram. Soc.

Publications from this Work

1. Kurt R. Mikeska and W. Roger Cannon, "Dispersants for Tape Casting Pure Barium Titanate", in Advances in Ceramics, Vol. 9, Forming of Ceramics, American Ceramic Society, 1984, pp. 164-183.
2. Susan Forti, John R. Morris and W. Roger Cannon, "The Green Strength of Cast Tapes" Bull. Amer. Ceram. Soc., 64 [5] 724 (1985).
3. Linda Braun, John R. Morris, and W. Roger Cannon, "Binder and Plasticizer Effects on the Viscosity of Tape Casting Slips" Bull. Amer. Ceram. Soc. 64 [5] 727-729 (1985).
4. J. B. Blum and W. R. Cannon, "Tape Casting of Barium Titanate," Electronic Packaging Materials, MRS Symposia Proceedings 40, Edit. E.A. Giess, K-N Tu, D. R. Uhlmann, Pittsburgh, PA. 1985.
5. John R. Morris and W. Roger Cannon, "Rheology and Component Interactions in Tape Casting Slurries," Mat. Res. Soc. Symp. Proc., vol. 60, (1986) pp.135-142,
6. W. R. Cannon, J. R. Morris and W. R. Cannon, "Dispersants for Non-Aqueous Tap Casting," in Advances in Ceramics, vol. 19, Multilayer Ceramic Devices, (Edit. J. B. Blum and W. R. Cannon) Amer. Ceram. Soc. 1986, pp. 161-174 .
7. K. R. Mikeska and W. Roger Cannon, "Non-aqueous Dispersion Properties of Pure BaTiO₃ for Tape Casting," Colloids and Surfaces, 29, 305-321 (1988).
8. Angela Karas, Toshiya Kumagai, and W. Roger Cannon, "Casting Behavior and Tensile Strength of Cast BaTiO₃ Tape as the Organic Composition is Varied," to be published in Bull. Amer. Ceram. Soc..
9. W. Roger Cannon, R. Becker and K. R. Mikeska, " Interactions between Organic Additives Used for Tape Casting, " to be published in Advances in Ceramics.

Presentations from this Work

1. K. Mikeska and W. R. Cannon. "Dispersants for Tape Casting Pure Barium Titanate", 1983 Annual Meeting of the American Society".
2. Linda Braun, Susan Forti, John R. Morris, and W. Roger Cannon. "Strength of Cast Tapes of Barium Titanate using Several Binder-Dispersant Combinations; presented at the 1984 Annual Meeting of the American Ceramic Society.
3. Kurt R. Mikeska and W. Roger Cannon. "Adsorption of Dispersants onto Barium Titanate", presented at the 1984 Annual American Ceramic Society Meeting.
4. K. R. Mikeska and W. R. Cannon. "Dispersion of BaTiO₃ in the MEK-Ethanol System", 58th Colloid and Surface Science Symposium, Amer. Chemical Soc., Pittsburgh, 1984.
5. J. R. Morris and W.R. Cannon, "Powder-Binder-Dispersant Interactions in Nonaqueous Tape Casting Slurries of BaTiO₃, presented at the Fall Meeting of the American Ceramic Society, San Fransisco, CA Nov 1984.

Final Report - 1988

6. J. B. Blum and W. R. Cannon, "Tape Casting of Barium Titanate" Materials Research Society, Boston, Nov. 1984.
7. K. R. Mikeska, D. C. Eng, and W. R. Cannon, "Dispersion Properties of BaTiO₃," Annual Meeting Amer. Ceram. Soc., May. 1985.
8. J.R. Morris and W.R. Cannon, "Affects of Component Addition Sequence on Green and Fired Properties of Barium Titanate Tapes," Annual Meeting Amer. Ceram. Soc., May 1985.
9. J.R. Morris and W.R. Cannon, "Component Interactions in Barium Titanate Tape Casting Slurries," Materials Research Conf., Nov. 1985.
10. W. R. Cannon, "Dispersion and Rheology," Gordon Research Conference on Solid State Ceramics," Plymouth, N.H. Aug. 1985 (invited speaker).
11. W. R. Cannon, J. R. Morris, and K. R. Mikeska, "Dispersants for Nonaqueous Tape-casting," Electronics Meeting of the American Ceramic Society, Nov. 1985 (invited speech).
12. K. R. Mikeska, J. R. Morris and W. R. Cannon, "Surfactants for Tape-casting Barium Titanate in MEK-ethanol," , Spring Meeting of the American Chemical Society, NY. April 1986.
13. K. R. Mikeska and W. R. Cannon, "Dispersion Properties of Barium Titanate in MEK-Ethanol," Annual Meeting of Am. Ceram. Soc., Chicago, Ill. May 1986.
14. J. W. Rydzak, J. R. Morris, Jr. and W. Roger Cannon, "FTIR Applications in Ceramics," " Annual Meeting of Am. Ceram. Soc., Chicago, Ill. May 1986.
15. A. E. Karas, J. R. Morris, Jr., and W. R. Cannon, "Effects of Fraction of Interparticulate Voids Filled on Tensile Strength of Green Tapes," " Annual Meeting of Am. Ceram. Soc., Chicago, Ill. May 1986.
16. J. R. Morris, R. E. Hill, and W. Roger Cannon, "Mechanisms of Interaction Between Dispersant and Other Components in Non-aqueous Tape Casting," Annual Meeting of Am. Ceram. Soc., Chicago, Ill. May 1986.
17. W. R. Cannon, "Tape Casting and Interaction between Dispersant and Binder," Presentation at Dupont Seminar Series on Tape Casting, Mar., 1986.
18. Toshiya Kumagai, Angela Karas and W. Roger Cannon, "Casting Behavior and Tensile Strength of Cast BaTiO₃ Tape as Composition is Varied," Annual Meeting Amer. Ceram. Soc. Pittsburgh, May 1987.
19. R. Becker, K. Mikeska and W. R. Cannon, "The Effect of Water in a Non-aqueous System Applicable to Tape Casting Barium Titanate," Poster Session at Gordon Conference, Plymouth N.H., Aug., 1987.
20. W. R. Cannon, "Organics in Tape Casting: Effect on Viscosity, Density, Strength, and Failure Strain," Electronic Div Amer. Ceram. Soc., Denver, CO, Nov. 1987. (Invited Lecture)
21. W. R. Cannon, "Organics in Tape Casting: Effect on Viscosity, Density, Strength, and Failure Strain," N.J. Div. ISHM, Jan. 1988.



DEPARTMENT OF THE NAVY
OFFICE OF NAVAL RESEARCH
ARLINGTON, VIRGINIA 22217
BASIC DISTRIBUTION LIST

IN REPLY REFER TO

Technical and Summary Reports December 1982

<u>Organization</u>	<u>Codes</u>	<u>Organization</u>	<u>Copies</u>
Defense Documentation Center Cameron Station Alexandria, VA 22314	12	Naval Air Propulsion Test Center Trenton, NJ 08628 ATTN: Library	1
Office of Naval Research Department of the Navy 800 N. Quincy Street Arlington, VA 22217 Attn: Code 431	3	Naval Construction Battalion Civil Engineering Laboratory Port Hueneme, CA 93043 ATTN: Materials Division	1
Naval Research Laboratory Washington, DC 20375 ATTN: Codes 6000 6300 2627	1 1 1	Naval Electronics Laboratory San Diego, CA 92152 ATTN: Electron Materials Sciences Division	1
Naval Air Development Center Code 606 Warminster, PA 18974 ATTN: Dr. J. DeLuccia	1	Naval Missile Center Materials Consultant Code 3312-1 Point Mugu, CA 92041	1
Commanding Officer Naval Surface Weapons Center White Oak Laboratory Silver Spring, MD 20910 ATTN: Library	1	Commander David W. Taylor Naval Ship Research and Development Center Bethesda, MD 20084	1
Naval Oceans Systems Center San Diego, CA 92132 ATTN: Library	1	Naval Underwater System Center Newport, RI 02840 ATTN: Library	1
Naval Postgraduate School Monterey, CA 93940 ATTN: Mechanical Engineering Department	1	Naval Weapons Center China Lake, CA 93555 ATTN: Library	1
Naval Air Systems Command Washington, DC 20360 ATTN: Code 31A Code 5304B	1 1	NASA Lewis Research Center 21000 Brookpark Road Cleveland, OH 44135 ATTN: Library	1
Naval Sea System Command Washington, DC 20362 ATTN: Code 05R	1	National Bureau of Standards Washington, DC 20234 ATTN: Metals Science and Standards Division Ceramics Glass and Solid State Science Division Fracture and Deformation Div.	1 1 1

AD-A193 063

DEFLOCCULANTS FOR TAPE CASTING BARIUM TITANATE
DIELECTRICS(U) RUTGERS - THE STATE UNIV NEW BRUNSWICK N
J DEPT OF CERAMICS W R CANNON FEB 88 N00014-82-K-0313

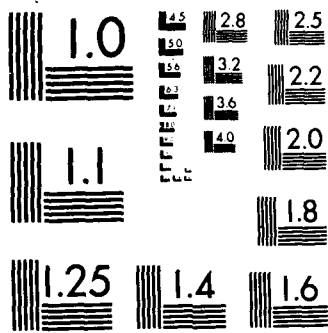
2/2

UNCLASSIFIED

F/G 11/9

NL





MICROCOPY RESOLUTION TEST CHART
NATIONAL BUREAU OF STANDARDS-1963-A

January 1984

NEW MULTILAYER CAPACITOR PROGRAM LIST

Professor Harlan U. Anderson
University of Missouri-Rolla
107 Fulton Hall
Rolla, MO 65401

Professor R. Vest
Purdue University
West Lafayette, IN 47907

Dr. John B. Blum
Rutgers University
College of Engineering
P.O. Box 909
Piscataway, NJ 08859

Dr. J. V. Biggers
Pennsylvania State University
Materials Research Laboratory
University Park, PA 16802

Professor R. Buchanan
University of Illinois
Department of Ceramic Engineering
Urbana, IL 61801

Professor Larry Burton
Virginia Polytechnic Institute
and State University
Blacksburg, VA 24061

Professor Roger Cannon
Rutgers University
College of Engineering
P.O. Box 909
Piscataway, NJ 08859

Prof. Donald M. Smyth
Lehigh University
Materials Research Laboratory
Coxe Laboratory 32
Bethlehem, PA 18015

Dr. N. Eror
Oregon Graduate Center
19600 N. W. Walker Road
Beaverton, OR 97006

Dr. K. D. McHenry
Honeywell Ceramics Center
5121 Winnetka ave., N.
New Hope, MN 55428

Professor D. W. Readey
Department of Ceramic Engineering
1314 Kinnear Road
Columbus, OH 43212

Dr. Lew Hoffman
Hoffman Associates
301 Broadway (US 1) Suite 206A
P.O. 10492
Riviera Beach, FL 33404

Dr. Gordon R. Love
Corporate Research, Development
and Engineering
Sprague Electric Co.
North Adams, Mass 01247

Roger T. Dirstine
Ceramics Research
Unitrode Corporation
580 Pleasant St.
Watertown, Mass 02172

Dr. Sidney J. Stein
Electro-Science Laboratories
2211 Sherman Ave
Pennsauken, NJ 08110

John C. Constantine
Electronic Materials Systems
Englehard Industries Division
1 West Central Ave.
E. Newark, NJ 07029

(Continue of Multilayer Capacitor Program List)

John Piper
Union Carbide Corporation
Electronics Division-Components Dept.
P.O. Box 5928
Greenville, SC 29606

Dr. Kim Ritchie
Vice President
Corporate Research Laboratory
AVX Corporation
P.O. Box 867
Myrtle Beach, SC 29577

Tack J. Whang
Technical Center
Ferro Corporation
7500 E. Pleasant Valley Road
Independence, OH 44131

Advanced Research Projects
Materials Science Director
1400 Wilson Boulevard
Arlington, VA 22209

Dr. Gene Haertling
Motorola Corporation
3434 Vassar, NE
Albuquerque, NM 87107

W.B. Harrison
Honeywell Ceramics Center
5121 Winnetka Ave. N.
New Hope, MN 55428

Prof. L. E. Cross
The Pennsylvania State University
Materials Research Laboratory
University Park, PA 16802

Dr. P.L. Smith
Naval Research Laboratory
Code 6361
Washington, DC 20375

Professor R. Roy
The Pennsylvania State University
Materials Research Laboratory
University Park, PA 16802

Dr. R. Rice
Naval Research Laboratory
Code 6360
Washington, DC 20375

Dr. G. Ewell
MS6-D163
Hughes Aircraft Company
Centinela & Teale Streets
Culver City, CA 90230

Dr. George W. Taylor
Princeton Resources, Inc.
P.O. Box 211
Princeton, NJ 08540

Dr. J. Smith
GTE Sylvania
100 Endicott Street
Danvers, MA 01923

Professor R. Buchanan
Department of Ceramic Engineering
University of Illinois
Urbana, Ill 61801

Dr. Wallace A. Smith
North American Philips Laboratories
345 Scarborough Road
Briarcliff Manor, NY 10510

Professor B. A. Auld
Stanford University
W.W. Hansen Laboratories of Physics
Stanford, CA 94306

Mr. G. Goodman, Manager
Corporation of Applied Research
Group
Globe-Union Inc.
5757 North Green Bay Avenue
Milwaukee, WI 53201

Director
Applied Research Lab
The Pennsylvania State Univ.
University Park, PA 16802

::
RE/431/84/46

(Continue of Multilayer Capacitor Program List)

Army Research Office
Box CM, Duke Station
Attn: Met. & Ceram. Div.
Durham, NC 27706

National Bureau of Standards
Inorganic Mats. Division
Washington, DC 20234

Dr. R. R. Neurgaonkar
Rockwell International Science Center
1049 Camino Dos Rios
P.O. Box 1085
Thousand Oaks, CA 91360

Darnall P. Burks
Sprague Electric Company
P. O. Box 5327
Wichita Falls, TX 76307

Mr. J.D. Walton
Engineering Experiment Station
Georgia Institute of Technology
Atlanta, GA 30332

Roger T. Dirstine
Unitrode Corporation
580 Pleasant Street
Watertown, MASS 02172

Dr. T. C. Dean
TAM Ceramics, Inc.
Box C
Bridge Station
Niagara Falls, NY 14305

Dr. Kim Ritchie
AVX Corporation
P. O. Box 867
Myrtle Beach, SC 29577

Mr. Paul Baker
Bourns Inc.
693 West 1700 So. Street
Logan, UTAH 84321

Dr. David Cronin
Trans-Tech
5520 Adamstown Rd.
Adamstown, MD 21710

END

DATE

FILMED

9-88

DTIC